



## Deliverable 2.4



## Deliverable data

<b>Deliverable No</b>	2.4
<b>Deliverable Title</b>	Analysis of routing and traffic data
<b>Work Package no: title</b>	WP2 : Initial Data Collection, Collation, Analysis and Management (Task 2.4 : Analysis of routing and traffic data)

<b>Dissemination level</b>	Confidential	<b>Deliverable type</b>	Report
<b>Lead beneficiary</b>	AALTO		
<b>Responsible author</b>	Eur.Ing Spyros Hirdaris PhD - Assoc. Professor, AALTO, FI		
<b>Co-authors</b>	AALTO : Mingyang Zhang, Jakub Montewka NAPA : Teemu Manderbacka		
<b>Date of delivery</b>	31-11-2019		
<b>Approved</b>	<b>Name (partner)</b>	<b>Date [DD-MM-YYYY]</b>	
Peer reviewer 1	Pentti Kujala, AALTO	25-11-2019	
Peer reviewer 2	Henning Luhmann, MW	27-11-2019	

## Document history

Version	Date	Description
V.01	25-11-2019	FLARE Extreme Scenarios and Scenario Modelling (1 <sup>st</sup> Draft for comments by reviewers)
V.02	27-11-2019	FLARE Extreme Scenarios and Scenario Modelling

*The research leading to these results has received funding from the European Union Horizon 2020 Program under grant agreement N. 814753.*

*This report reflects only the author's view. INEA is not responsible for any use that may be made of the information it contains.*

The information contained in this report is subject to change without notice and should not be construed as a commitment by any members of the FLARE Consortium. In the event of any software or algorithms being described in this report, the FLARE Consortium assumes no responsibility for the use or inability to use any of its software or algorithms. The information is provided without any warranty of any kind and the FLARE Consortium expressly disclaims all implied warranties, including but not limited to the implied warranties of merchantability and fitness for a particular use.

*This document may not be copied, reproduced, or modified in whole or in part for any purpose without written permission from the FLARE Consortium. In addition, to such written permission to copy, acknowledgement of the authors of the document and all applicable portions of the copyright notice must be clearly referenced. All rights reserved.*

## TABLE OF CONTENTS

<b>TABLE OF CONTENTS</b> .....	<b>3</b>
<b>List of Symbols and Abbreviations</b> .....	<b>5</b>
<b>List of Figures – Report</b> .....	<b>6</b>
<b>List of Figures – Annexes</b> .....	<b>7</b>
<b>List of Tables – Report</b> .....	<b>8</b>
<b>List of Tables – Annexes</b> .....	<b>8</b>
<b>EXECUTIVE SUMMARY</b> .....	<b>9</b>
<b>1. AIMS AND SCOPE</b> .....	<b>12</b>
<b>2. DATA DESCRIPTION</b> .....	<b>12</b>
2.1 Introduction .....	12
2.2 Weather data .....	14
2.3 Bathymetry data .....	18
<b>3. VESSELS AND OPERATIONAL AREAS</b> .....	<b>19</b>
3.1 Vessel specifications .....	19
3.2 Operational areas .....	19
<b>4. BIG DATA ANALYTICS</b> .....	<b>22</b>
4.1 Data interpolation methods .....	22
4.2 Modelling of collision encounters .....	24
4.3 Modelling of grounding encounters .....	29
<b>5. KEY RESULTS</b> .....	<b>33</b>
5.1 Trends from global weather data .....	35
5.2 Trends from sample ship weather data .....	45
5.3 Demonstration of collision encounters .....	46
5.4 Demonstration of grounding encounters .....	54
5.5 Discussion .....	60
<b>6. CONCLUSIONS</b> .....	<b>62</b>
<b>7. REFERENCES</b> .....	<b>62</b>
<b>ANNEX A</b> .....	<b>67</b>



Guidelines on AIS pre-processing method .....	67
<b>ANNEX B - Supplementary Material.....</b>	<b>70</b>
Collision Scenarios for other ship Groups in the Gulf of Finland .....	70
Weather data distributions – passenger ships.....	75
Weather data distributions – RoPax ships .....	81
Weather data statistics in 8 Areas .....	84
Grounding data for scenario 2 .....	89
<b>Public summary .....</b>	<b>91</b>



## List of Symbols and Abbreviations

*Unless otherwise stated in the main text of this report the meaning of the symbols used are outlined in the following list. Mathematical symbols are directly explained in the main text of the report.*

<b>AIS</b>	Automatic Identification System
<b>DCPA</b>	Distance at Closest Point of Approach
<b>DoA</b>	Description of Action
<b>EC</b>	European Commission
<b>EC</b>	European Union
<b>ETA</b>	Estimated Time of Arrival
<b>GEBCO</b>	General Bathymetric Chart of the Oceans
<b>IALA</b>	International Association of Marine Aids to Navigation and Lighthouse Authorities
<b>IHO</b>	International Hydrographic Organization
<b>IMO</b>	International Maritime Organization
<b>IOC</b>	Intergovernmental Oceanographic Commission
<b>MMSI</b>	Maritime Mobile Service Identity
<b>NCEP</b>	National Centres for Environmental Prediction
<b>NOAA</b>	National Oceanic and Atmospheric Administration
<b>PMT</b>	Project Management Team
<b>QA</b>	Quality Assurance
<b>ROT</b>	Rate of Turn
<b>SG</b>	Steering Group
<b>TCPA</b>	Time at Closest Point of Approach
<b>UKC</b>	Under keel Clearance
<b>UTC</b>	Universal Time Coordinated
<b>VCRO</b>	Vessel Conflict Ranking Operator
<b>WP</b>	Work Package



## List of Figures – Report

Figure 1. A comparison of global sea weather forecast accuracies. Now-cast accuracies are indicated by zero day forecast. Root Mean Square (RMS) errors of forecasted significant wave height (upper), wind speed (middle), and wave peak period (lower) (Bidlot, 2017).....	16
Figure 2. The mapping location of weather data (Red traffic patterns show the trajectories of passenger ships with weather data; blue traffic patterns show the trajectories of RoPax ships with weather data; Yellow boxed areas represent 50 areas of interest based on BMT, 1990 global wave statistics; Blue boxed areas represent 8 areas of interest under FLARE project).....	17
Figure 3. Sample areas and bathymetry data visualization. ....	18
Figure 4. Summary of selected operational areas.....	19
Figure 5. Passenger ship and RoPax ships trajectories: Gulf of Finland (Red line: Passenger ship -106 ships; Blue line: RoPax ship - 38 ships). ....	20
Figure 6. Passenger ship and RoPax ships trajectories: English Channel (Red line: Passenger ship (146 ships); Blue line: RoPax ships - 57 ships). ....	21
Figure 7. Passenger ship and RoPax ships trajectories: Gibraltar straight (Red line: Passenger ship (178 ships); Blue line: RoPax ship - 67 ships). ....	21
Figure 8. Interpolation method of weather data as per Haranen et al. (2017). ....	23
Figure 9. The framework of weather interpolation method. ....	23
Figure 10. Overview of the collision encounter detection method. ....	24
Figure 11. AIS spatio-temporal sample.....	25
Figure 12. The coordinate system of striking and struck ships. ....	27
Figure 13. The distance of striking and struck ships. ....	27
Figure 14. The distance and dynamics of striking and struck ships. ....	28
Figure 15. COLREGs encounter types (Huang et al., 2019).....	28
Figure 16. Collision scenarios relative striking positions. ....	29
Figure 17. The minimum distance between ships and shallow waters. ....	31
Figure 18. Grounding scenarios detection method. ....	31
Figure 19. Relationship between Water depth, Ship Draught and UKC (Zhao et al., 2018). ....	32
Figure 20. The relationship between the shallow water and the spatial AIS data of a selected ship.....	32
Figure 21. The determined isobaths based on the selected bathymetry data, considering the safe water depth of selected ships. ....	33
Figure 22. The ship trajectories of the selected ship for year 2019; the colour bar denotes vessel speed in knots. ....	34
Figure 23. Wave Height (m) cumulative distributions for all Passenger ships in 8 areas over different seasons. ....	36
Figure 24. Wave Height (m) cumulative distributions for all RoPax ships in 8 areas over different seasons. ....	37
Figure 25a. Wave direction with respect to ship heading in spring and summer seasons. ....	39

Figure 26. The wave scatter diagrams in the Gulf of Finland.....	41
Figure 27. Wave or Wind direction with respect to ship is heading each season in the Gulf of Finland. ...	42
Figure 28. Speed distribution in real wave height and period each season. ....	43
Figure 29. Speed visualization of Ropax ships in the Gulf of Finland in various seasons.....	43
Figure 30. Seasonal speed distributions of Ropax ships in the Gulf of Finland. ....	44
Figure 31. Weather parameters cumulative distributions for the 3-year operations (covering the three-year operational history of the sample ship).....	45
Figure 32. Encounter angles distribution (covering the three-year operational history of the sample ship). ....	46
Figure 33. The minimum distance could between two ships. ....	47
Figure 34. The locations of the mentioned encounter scenarios. ....	48
Figure 35. The number of ship types of the striking ship. ....	48
Figure 36. Types of striking ships of 6 groups. ....	49
Figure 37. The speed distributions of the struck ship. ....	50
Figure 38. The speed distributions of the striking ships of group 2.....	50
Figure 39. The mass of the struck ship for each voyage.....	51
Figure 40. The mass of the striking ships of group 2.....	51
Figure 41. The distribution of collision angles. ....	52
Figure 42. The distribution of relative bearing angles. ....	52
Figure 43. The distribution of the distance between two ships. ....	53
Figure 44. The bathymetry map with the recorded ship trajectories delivered from AIS data. ....	54
Figure 45. The relationship between isobaths and ship trajectories.....	55
Figure 46. The typical grounding scenarios in the Gulf of Finland.....	56
Figure 47. The distribution of the draught of the selected ship. ....	57
Figure 48. The distribution of the mass of the selected ship. ....	57
Figure 49. The speed distribution of the selected ship encountered for power grounding. ....	58
Figure 50. The distance distribution of the selected ship to the shallow water (forward to shallow waters) for power grounding. ....	58
Figure 51. The speed distribution of the selected ship encountered for drift grounding.....	59
Figure 52. The distance distribution of the selected ship to the shallow water (lateral to shallow waters) for drift grounding. ....	59

## List of Figures – Annexes

Figure B. 1. The collision encounter analysis for Group 1.....	70
Figure B. 2. The collision encounter analysis for Group 2.....	71

Figure B. 3. The collision encounter analysis for Group 4.....	72
Figure B. 4. The collision encounter analysis for Group 5.....	73
Figure B. 5. The collision encounter analysis for Group 6.....	74
Figure B. 6 - A. Key Weather parameters cumulative distributions for Passenger ships. ....	75
Figure B. 7. - A Wave or Wind direction with respect to ship is heading each season. ....	78
Figure B. 8. -A Key Weather parameters cumulative distributions for RoPax ships. ....	81
Figure B. 9. The speed distribution of the selected ship encountered during power grounding.....	89
Figure B. 10. The distance distribution of the selected ship to the shallow water (Forward to shallow waters) during power grounding. ....	89
Figure B. 11. The speed distribution of the selected ship encountered during drift grounding .....	90
Figure B. 12. The distance distribution of the selected ship to the shallow water (lateral to shallow waters) during drift grounding. ....	90

## List of Tables – Report

Table 1. Summary and Classification of Type A - AIS data formats. ....	14
Table 2. Information on 8 key areas selected for global weather data. ....	17
Table 3. Statistics of all passenger ships and RoPax ship form AIS information. ....	20
Table 4. The ship specification of the sample Ro-Pax ship.....	34
Table 5. The summary of the wave height in 8 areas (Wave height) .....	38
Table 6. The encountered potential collision events of the selected ships.....	47
Table 7. The groups of the striking ship types.....	49

## List of Tables – Annexes

Table B. 1. Wave height variations – Passenger ships.....	84
Table B. 2. Current speed variations – Passenger ships. ....	85
Table B. 3. Wind speed variations – Passenger ships. ....	86
Table B. 4. Wave period variations – Passenger ships.....	87
Table B. 5. Swell height variations – Passenger ships.....	88





## EXECUTIVE SUMMARY

- Problem definition: It is believed that in terms of assessing serious flooding accident response, hydro-meteorological observations and the area of operation may have a significant impact on the probability of encountering accidents as well as the survivability and consequences after flooding. It is essential to conclude on whether this statement is of relevance for the case of large passenger and Ro-Pax ships. Accordingly, this report contributes toward understanding operational risks associated with passenger and Ro-Pax vessel encounters by collecting and analysing big data from wave statistics, ship routing and traffic patterns for use by WP3.1, WP4 and WP6.

- Technical Approach: The report presents state of the art methods for the collection and analysis of big data analytics by combining trends from global hydro-meteorological conditions and encounters of relevance to passenger and Ro-Pax ships over 3 years (2017 – 2019). With reference to vessel encounters that may lead to grounding or collisions special emphasis has been attributed to three key risk areas of operation namely Gulf of Finland, English Channel and Gibraltar Straight. Weather mapping accounted for global environmental conditions such as sea states, currents, wind and swell for which real operational data were made available by commercial providers at 180 min intervals and 1.25° grid resolution in 8 areas of operation worldwide (North Atlantic, Caribbean Sea, Mediterranean Sea, Baltic Sea, North Sea, South East Asia, Northeast Pacific, and South Pacific). Vessel positioning data were made available by AIS (Automatic Identification System) messages within 2 minutes interval sampling from all the cruise and Ro-Pax vessels of interest in the three risk areas. GEBCO bathymetry data and weather data were interpolated for each AIS data point location and time. The information was statistically analysed and expert judgment conclusions were provided.

- Short description of the work plan main activities :

- ✓ Identification of key risk areas of operation
- ✓ Collection and analysis of hydro-meteorological, AIS, GEBCO data
- ✓ Development of procedures for big data analytics
- ✓ Identification of key patterns from hydro-meteorological conditions world wide
- ✓ Mapping of hydro-meteorological patterns to vessel encounters
- ✓ Demonstration of key results for a Ro-Pax vessel operating in the Gulf of Finland



• Key Conclusions: It was concluded that big data analytics may lead to improved recommendations in terms of the impact of the hydro-meteorological conditions on passenger or Ro-Pax vessel encounters. These recommendations could be used for the development of grounding and collision probabilistic risk models (see WP3.1, WP2.5); design of experiments (see WP4); development of an improved survivability factor and/or vulnerability criteria (see WP6.1) and last but not least improved operational decision making. For the keen reader data analytics procedures are outlined in Section 4 and detailed discussion points are highlighted in Sections 5.3 – 5.5 of this report. Key observations are summarised as follows :

- ✓ Systematic manipulation of large data volumes (e.g. AIS, weather and bathymetry data) for different traffic areas may be very challenging. For example, 3 year data (2017-2019) in the Gulf of Finland contain about 40 billion records of dynamic AIS data. Therefore, the technical approach stipulated in this report focused on (1) development of methods for big data analytics; (2) identification of trends on the impact of global hydro-meteorological areas of relevance over three years (2017 – 2019); (3) detailed understanding of Ro-Pax vessel operations for the representative area of Gulf of Finland for one year (2019). This approach may be considered adequate in terms of validating possible scenarios.
- ✓ For 99% of the time passenger ships navigate in less than 6.4 m significant wave heights, in swell heights of less than 5.7 m, in wind speed conditions that are less than 24.8 m/s over ground and in currents that are less 1.7 m/s over-ground. However, the combination of these conditions do not reflect hydro-meteorological data encountered in one area of operation over the same time of the year. They rather reflect the span of overall extreme events.
- ✓ Globally, the average sailing speed of passenger ships is higher than Ro-Pax ships.
- ✓ The area of operation is interlinked with geography (e.g. bathymetry conditions), hydro-meteorological conditions and traffic patterns that together or separately could influence accidents. Review of available data for the three key risk areas of operation has shown that ships navigate at their highest average speed in Gibraltar straight, very few passenger ships sail in the Gulf of Finland in winter and the variations of ship speed are not so markedly significant over different seasons or day/night time navigation. On the other hand, the Gulf of Finland and the English Channel demonstrate more representative traffic grounding and collision encounters.
- ✓ Differences in the geographical shape, weather, bathymetry and local shipping regulations may lead to different encounter scenarios that do not necessarily reflect



global operational trends in open seas. Depending on the ship type, location, time of the year the encounter situation should be looked at closely. For example :

- In the Gulf of Finland, 72.5 % of the collision encounter scenarios are crossing and most of the striking locations are positioned laterally to the struck ships. On the other hand, in the English Channel, 63.1% of the collision encounter scenarios are crossing and 57.6% relate to head-on or overtaking encounters. For these cases striking locations are in way of the bow/ stern of the struck ship.
- Detailed analysis of Ro-Pax ship operations in the Gulf of Finland over the year 2019 demonstrated that :
  - For collision encounters: the speed of the struck ship is between 22 and 26 knots and the speed of the striking ship may largely vary from 8 to 23 knots depending on their type (e.g. 8 -14 knots for tankers ; 14 -23 knots for passenger ships). For 62% of the collision encounter scenarios the mass of the struck ship is between  $2.7 \cdot 10^4$  and  $2.8 \cdot 10^4$  tonnes and the collision angles vary considerably between  $[200^\circ - 260^\circ]$  depending on the ship type (e.g.  $[90^\circ - 120^\circ]$  for tanker ships;  $[210^\circ - 260^\circ]$  for passenger ships). For the same sample of encounters the mass of striking ships varies between  $1.0 \cdot 10^4$  and  $4.0 \cdot 10^4$  tonnes (e.g.  $[1.0 \cdot 10^4 - 2.5 \cdot 10^4]$  tonnes for passenger ships;  $[1.5 \cdot 10^4 - 4.0 \cdot 10^4]$  tonnes for tankers).
  - For grounding encounters: the speed of ships varies depending on the type of grounding scenario (i.e. drift or power grounding in open seas or close to port). For example, the speed of ships that encountered power grounding may vary between 13 and 23 knots depending on the area (e.g. 21-23 knots in open seas versus 13 – 15 knots in port). On the other hand drifting grounding speeds may be between 19 - 23 knots in open seas and 15 - 17 knots in a port. The distance of a ship to shallow waters depends on ship speed and the area of operation with open seas grounding being prone to longer distances than port grounding. For example, the distance may vary between 2 and 3.5 Km for power grounding and 1 – 2 km for drift grounding in open seas while the corresponding numbers are 350– 550 m and 150 - 300m for power and drift grounding in a port respectively.



## 1. AIMS AND SCOPE

The aim of this task was to collect representative operational information for the passenger ships (cruise liners and Ro-Pax vessels) used in FLARE project. This was done to:

- Understand the hydro-meteorological conditions under which passenger ships operate;
- Identify potential grounding /collision scenarios based on traffic density records available.

To this end, weather and ship movement data have been collected for a range of passenger ships steaming worldwide, and a group of Ro-Pax ships navigating in three risk areas (Gulf of Finland, English Channel, Gibraltar straight) from 2017 - 2019. Weather mapping accounted for environmental conditions such as sea states, currents, wind and swell for which real data were made available by commercial providers at 180 min intervals and 1.25° grid resolution. Vessel positioning data were made available by AIS (Automatic Identification System) messages within 2 minutes interval sampling from all the cruise and Ro-Pax vessels of interest in the three risk areas. General Bathymetric Chart of the Oceans (GEBCO) data and weather data were interpolated for each AIS data point location and time. The information was statistically analysed.

## 2. DATA DESCRIPTION

### 2.1 Introduction

Since 2004, all passenger ships and ships over 300 GT have been fitted with AIS transponders (see IALA, 2004 and IMO 2014). Satellites have been systematically used since 2008 to collect improved quality data from AIS transceivers installed on ships worldwide (Yang D. et al., 2019). With the improvement in quality and accessibility of AIS data over the last few years maritime research expanded toward understanding big data analytics (e.g. Arguedas et al., 2018; Wang et al., 2017; Pallotta et al., 2014). Recent research studies discuss marine safety (Hansen et al., 2013; li et al., 2018; kim et al., 2017; Zhou et al., 2019) and sustainability (e.g. Winther et al., 2014; Kivekäs et al., 2014; Longépé et al., 2015; Campana et al., 2017; Anderson et al., 2017; Watson et al., 2015; Aase et al., 2015; Goerlandt et al., 2017). In terms of traffic analysis the focus has been mostly on grounding and collision analysis (e.g. Montewka et al., 2010; Goerlandt and Kujala, 2014; Goerlandt et al., 2010; Qu et al., 2011; Montewka et al., 2014), near-miss detections (Zhang et al., 2017) and collision avoidance especially considering recent interest in autonomous shipping operations (Szlupczynski et al., 2018). Based on big data analytics



passenger ship motion patterns and traffic behaviours could be constructively analysed using advanced data mining techniques. The aim of such studies is to systematically evaluate how trends of traffic behaviours may influence probabilities of collision and grounding events. AIS data may be useful to analyse traffic densities (Sidibé and Shu, 2017; Zhao et al. 2014). However, errors and inaccuracies associated with data manipulation or poor analysis techniques may lead to drifting of dynamic data (Tu et al. 2018) and hence erroneous results. According to IALA (2016) AIS data may be classified as :

- **Type A** based on data from AIS transceivers that can generate 11 data fields containing static, dynamic and voyage-related information (e.g. IMO number, ship draught, destination, Estimated Time of Arrival, navigation status, etc.). Big Data analytics of such kind contain information on ship movement automatically transmitted every 2–10s based on ship sailing speed and every 3 min while a ship is anchored. The time interval of static data and voyage-related information is 6min, regardless to their navigational status.
- **Type B** based on data from AIS transceivers that can generate 6 data fields. In this case the IMO number, ship draught, destination, ETA (Estimated Time of Arrival), ROT (rate of turn), and navigation status are omitted.

A detailed summary / classification of AIS data formats is presented in Table 1. The AIS data used in this project have been of **Type A** and were acquired from various AIS data providers (FleetMon - <https://www.fleetmon.com/> ; MarineTraffic - <https://www.marinetraffic.com> ).

Table 1. Summary and Classification of Type A - AIS data formats.

Type	Data field	Description
<b>Static</b>	AIS identity and location	Maritime Mobile Service ID (MMSI) and location of the system's antenna on board
	Ship identity	Ship name, IMO number, type, and call sign of the ship
	Ship size	Length and width of the ship
<b>Dynamic</b>	Ship position	Latitude and longitude (up to 0.0001 min accuracy)
	Speed	Ranging from 0 knots to 102 knots (0.1knot resolution)
	Rate of Turn	Right or left (ranging from 0 to 720° per minute)
	Course	Shipping course, heading, and bearing of the ship
	Timestamp	The second field of the UTC time when the subject data packet was generated
	Navigation status	Includes at anchor\under way using engine(s) \not under command\others
<b>Voyage</b>	Destination, ETA	Destination port and the estimated time of arrival of the ship
	Draught	Ranges from 0.1 m to 25.5 m

## 2.2 Weather data

Collecting data that reflect real weather conditions may be challenging. This is because weather data measured onboard ships are confidential, despite technology advancements data from state of the art hardware (e.g. sensor technology, anemometers etc.) is not always reliable and in any case full scale measurements may require the installation and use of expensive systems that are not commonly installed. Specialist issues associated with data of relevance to different ship segments pose additional difficulties. For example, for passenger ships risk mitigation associated with passenger comfort and safety are key; hence in practice passenger ship operations are at first planned for good weather windows and weather routing accounting for different scenarios is applied. The results presented in this report are based on statistical weather data for 8 sea areas (see BMT, 1990). The wave statistic areas considered were: North Atlantic, Caribbean Sea, Mediterranean Sea, Baltic Sea, North Sea, South East Asia, Northeast Pacific, and South Pacific (see Figure 2 and Table 2). This approach allowed for comparison of global weather data with the statistics derived from the actual weather conditions passenger ships encountered during their actual operation over a period of 3 years

(2017-2019). Weather data were obtained from various organisations<sup>1</sup>. Data analytics looked into processing swell and wind waves as well as wind and sea currents. In specific wave conditions were based on the WAVEWATCH III (WW3) model developed by USA NOAA<sup>2</sup>. Swell and wind wave components were presented by three parameters namely: (a) significant wave height; (b) wave zero-crossing period, and (c) wave direction. Wave conditions were made available every 180 minutes at spatial resolution of 1.25° (Hulkkonen et al., 2019). From the now-casts, the wave heights were obtained within 0.3 meter of uncertainty (globally) and based on operational experience wave periods were estimated within a couple of seconds (e.g. see Manderbacka, 2019 and Bidlot, 2017). The accuracies of main sea weather forecast providers and models were compared by JCOMM (Joint Technical Commission for Oceanography and Marine Meteorology) against data collected on weather buoys using Root Mean Square (RMS) error estimators, see Figure 1. Models compared were ECM (ECMWF – European Centre for Medium-Range Weather Forecasts), MOF (MetOffice), FNM (FNMOC – Fleet Numerical Meteorology and Oceanography Center), NCP (NCEP - National Centers for Environmental Prediction), MSC (Meteorological Service of Canada), MTF (MeteoFrance), DWD (Deutscher Wetterdienst), BoM (Bureau of Meteorology), SHM (SHOM - Service hydrographique et océanographique de la Marine, Naval Hydrographic and Oceanographic Service), JMA (Japan Meteorological Agency), KMA (Korea Meteorological Administration). Accordingly, data were interpolated in way of each ship's position (see section 5.1). Overall a sample of 89 passenger ships and 100 RoPax ships was considered (see Figure 2).

---

<sup>1</sup> TideTech - <https://www.tidetech.org/>; US NOAA (United States National Oceanic and Atmospheric Administration) - <https://www.noaa.gov/>; Mercator Ocean - <https://www.mercator-ocean.fr>

<sup>2</sup> see <https://polar.ncep.noaa.gov/waves/wavewatch/>



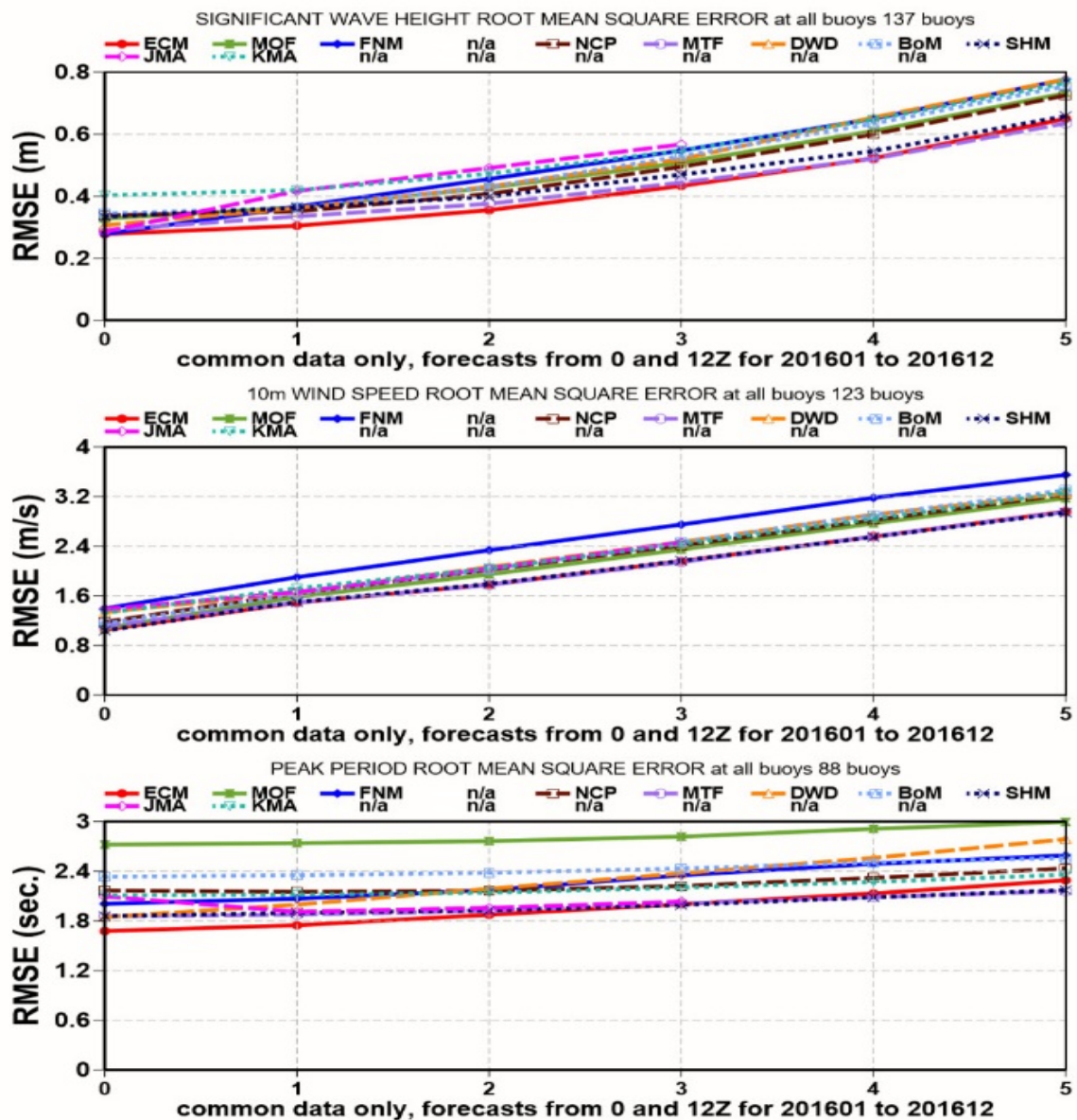


Figure 1. A comparison of global sea weather forecast accuracies. Now-cast accuracies are indicated by zero day forecast. Root Mean Square (RMS) errors of forecasted significant wave height (upper), wind speed (middle), and wave peak period (lower) (Bidlot, 2017).



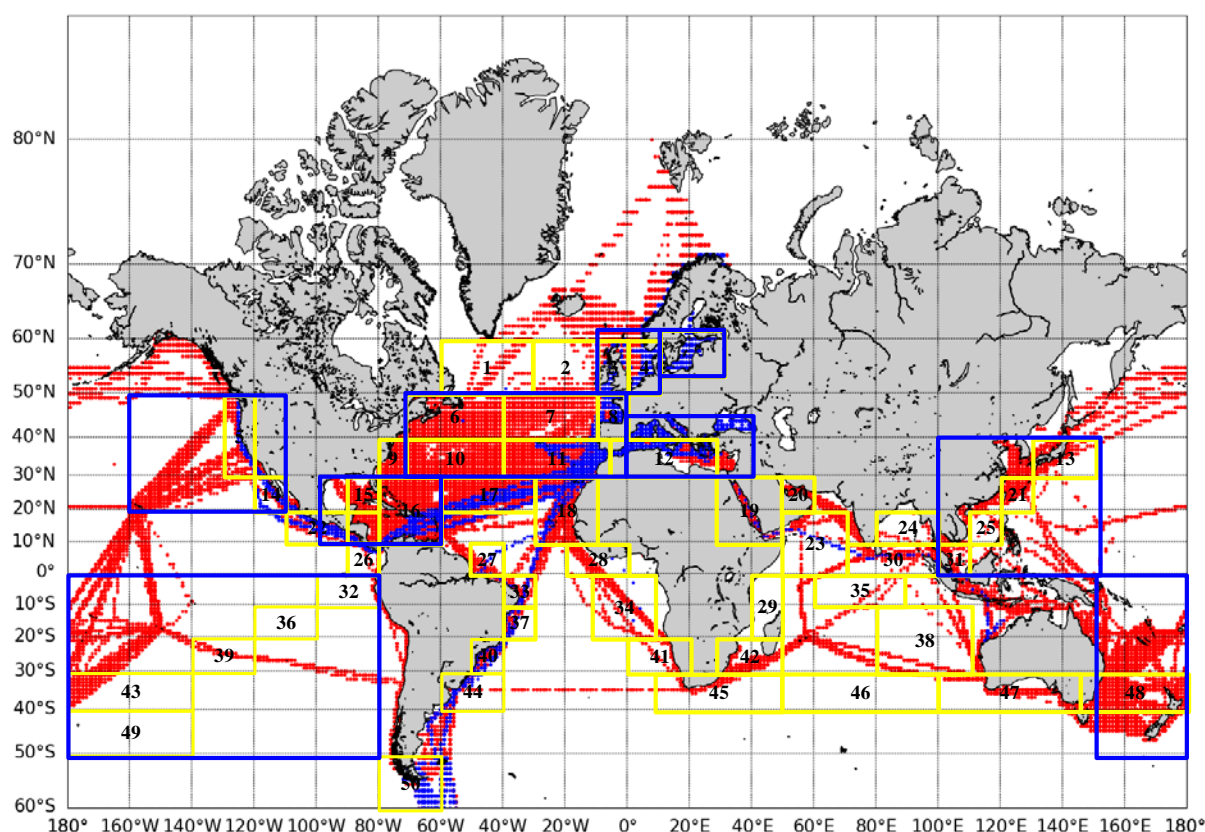


Figure 2. The mapping location of weather data (Red traffic patterns show the trajectories of passenger ships with weather data; blue traffic patterns show the trajectories of RoPax ships with weather data; Yellow boxed areas represent 50 areas of interest based on BMT, 1990 global wave statistics; Blue boxed areas represent 8 areas of interest under FLARE project).

Table 2. Information on 8 key areas selected for global weather data.

Areas	Latitude range	Longitude range	Sub-areas in BMT
North Atlantic	30° N and 50° N	0° and 70° W	6/7/8/10/11
Caribbean Sea	10° N and 30° N	60° W and 100 w°	15/16
Mediterranean Sea	30° N and 45° N	0° E and 40 E°	12
Baltic Sea	53° N and 63° N	10° E and 30 E°	None
North Sea	50° N and 63° N	10° W and 10 E°	3/4
South East Asia	0° N and 40° N	100° E and 150 E°	13/21/25/31
Northeast Pacific	20° N and 50° N	110° W and 160 w°	5
South Pacific	0° and 50° S	150° E and 80 w°	32/36/39/43/48/49

## 2.3 Bathymetry data

Bathymetry data for the sea areas ships encountered during their operations made use of publicly available records (ship position histories and water depth data) offered by GEBCO (General Bathymetric Chart of the Oceans)<sup>3</sup> in the three key risk areas of operation (Gibraltar Strait, Gulf of Finland and English Channel). These bathymetry data were interpolated in way of each vessel's position (see sections 4.2 and 5.1) with the aim to understand the operational conditions under which passenger ships operate near shallow waters. A sample model of bathymetry data is shown in Figure 3.

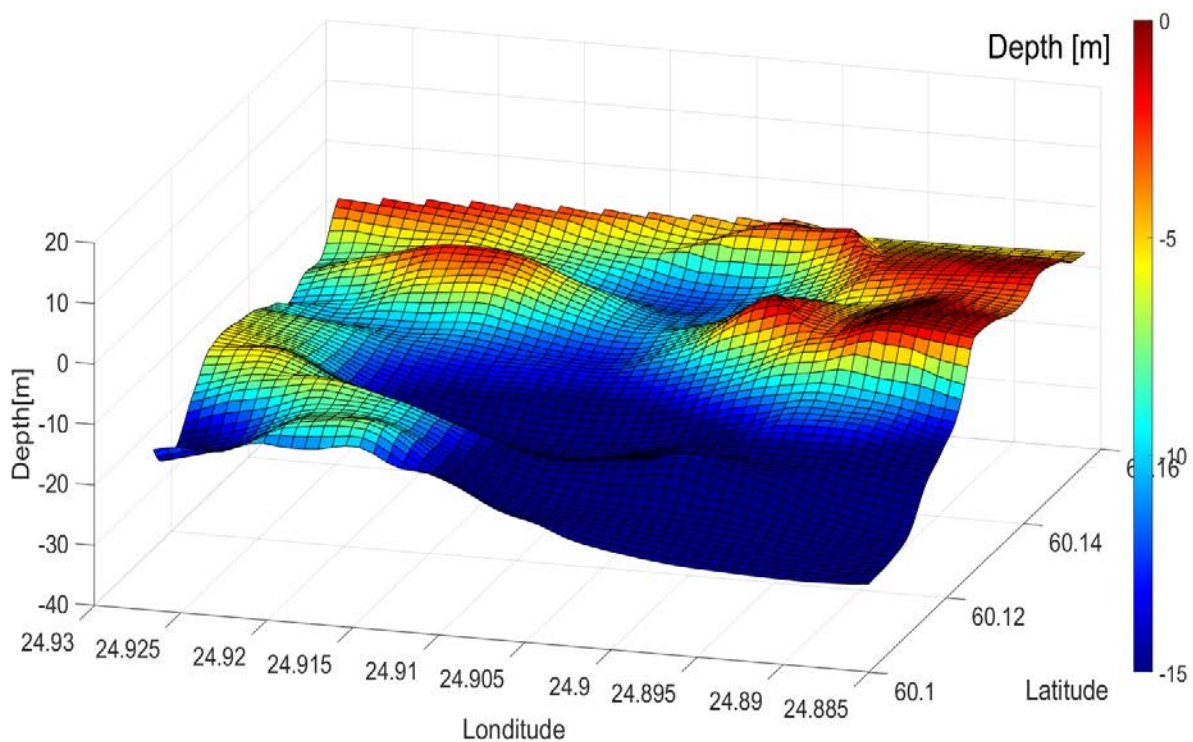


Figure 3. Sample areas and bathymetry data visualization.

<sup>3</sup> GEBCO is part of the International Hydrographic Organization (IHO) and the Intergovernmental Oceanographic Commission (IOC) (of UNESCO) <https://www.gebco.net>.

### 3. VESSELS AND OPERATIONAL AREAS

#### 3.1 Vessel specifications

As per requirements of WP2.1 a number of sample of large passenger ship and RoPax ships (Gross tonnage > 10,000 GT; Length > 120m) were extracted to analyse the route information and traffic density.

#### 3.2 Operational areas

Following discussions with ship operators AIS data were collected for three key risk areas namely (a) Gulf of Finland; (b) English Channel and (c) Gibraltar straight (see Figure 4). In all these areas, ships navigate within reach of 15 to 40 nautical miles from the terrestrial antennas. Notably, in all these areas ships experience high density navigation patterns and occasionally challenging coastal bathymetry; hence data records may be considered topical in terms of both collision and/or grounding accidents. The AIS data records presented in Table 1 were collected for the passenger ship sample shown in Table 3 over a 3 year period (2017 – 2019). Technical review indicated that the quality of AIS data is better close to shore, i.e. within reach of 15 to 40 nautical miles from terrestrial antennas. This is because satellite receivers obtain global coverage of the ship positions and it is more common to have data gaps, i.e. missing received signals from ships that navigate in dense areas. Traffic patterns are summarized in Figures 5 – 7.

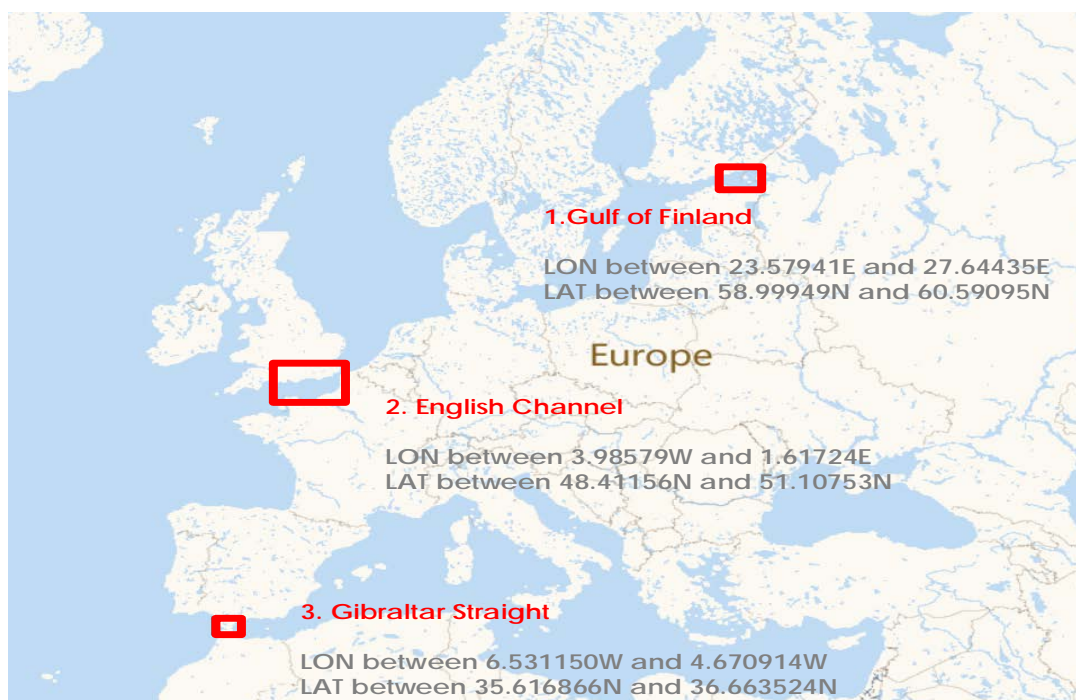


Figure 4. Summary of selected operational areas.

Table 3. Statistics of all passenger ships and RoPax ship form AIS information.

Area	RoPax ships	Passenger ships
Gulf of Finland	38	106
English Channel	57	146
Gibraltar straight	67	178

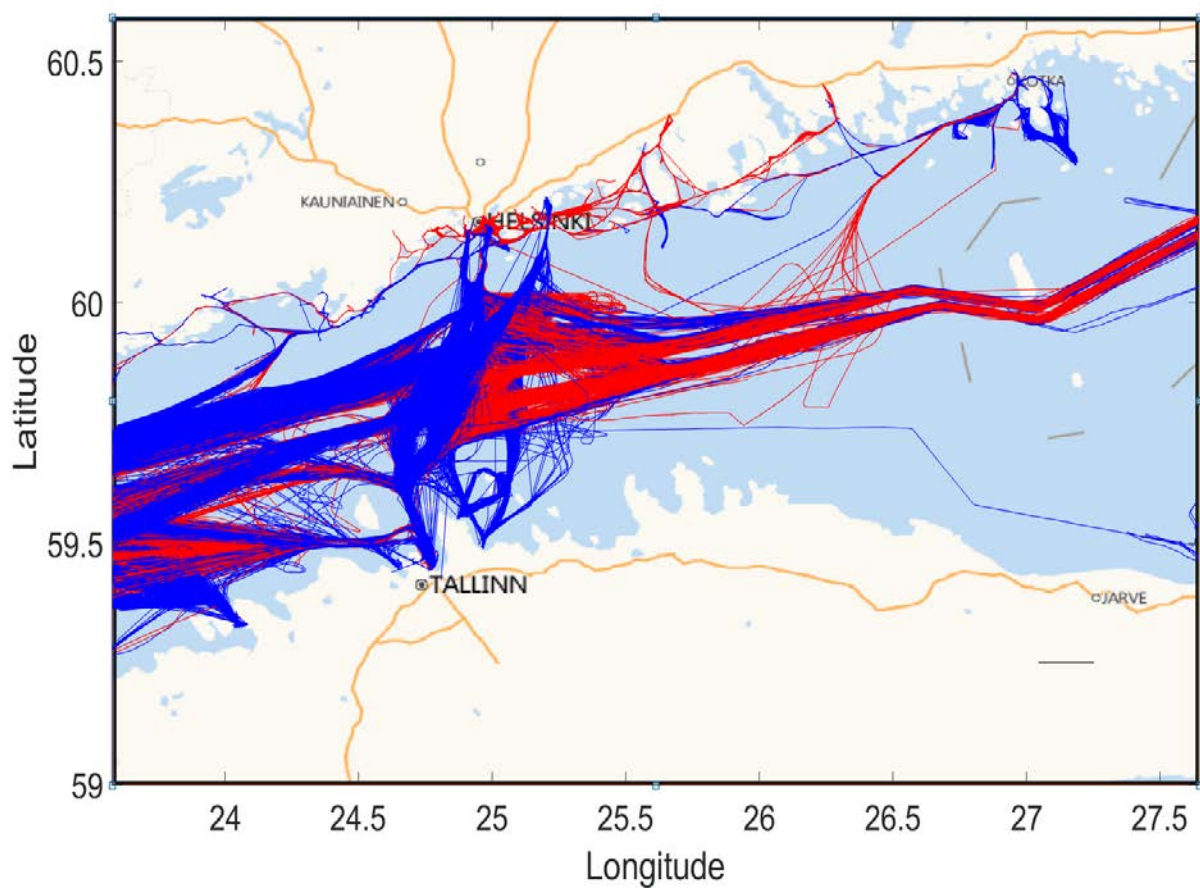


Figure 5. Passenger ship and RoPax ships trajectories: Gulf of Finland (Red line: Passenger ship - 106 ships; Blue line: RoPax ship - 38 ships).



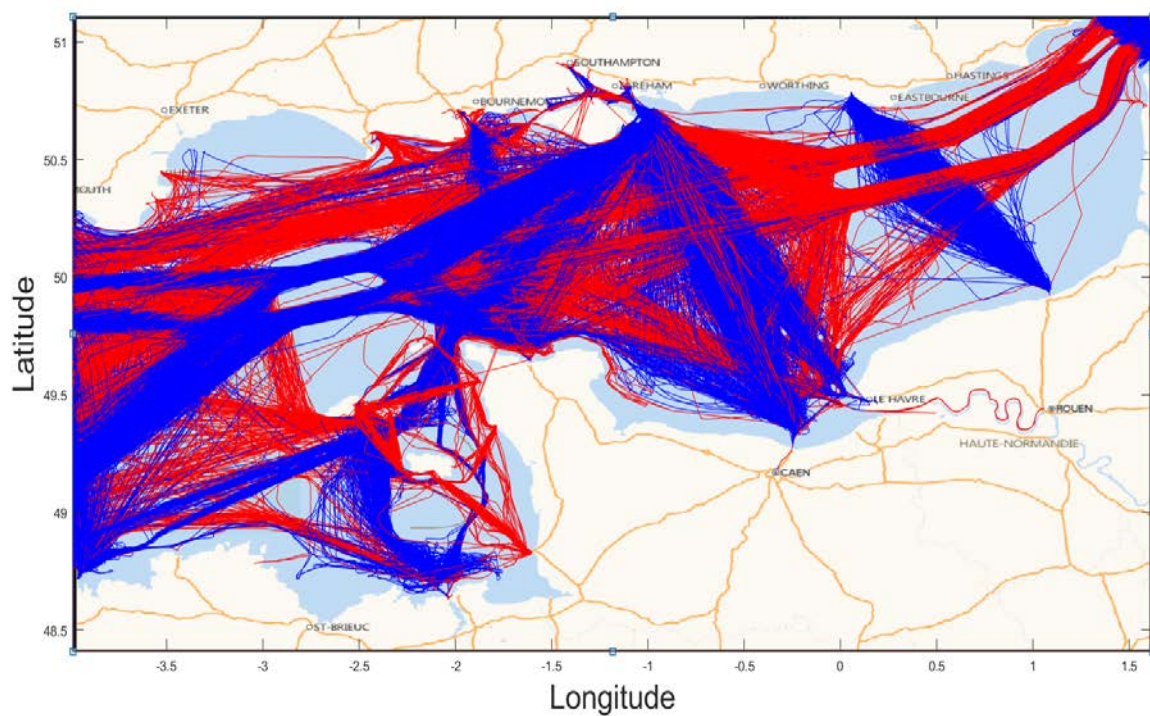


Figure 6. Passenger ship and RoPax ships trajectories: English Channel (Red line: Passenger ship (146 ships); Blue line: RoPax ships - 57 ships).

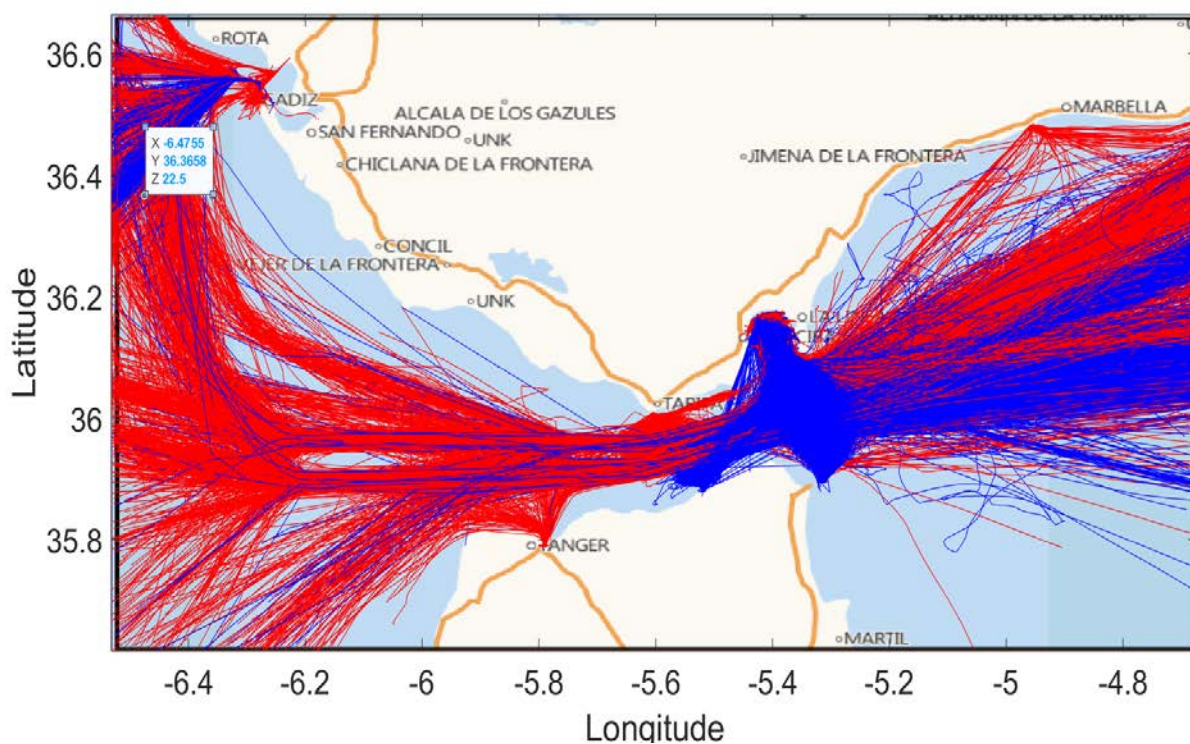


Figure 7. Passenger ship and RoPax ships trajectories: Gibraltar straight (Red line: Passenger ship (178 ships); Blue line: RoPax ship - 67 ships).

## 4. BIG DATA ANALYTICS

This section outlines the principles and methods used for the manipulation of big data records made available in this project.

### 4.1 Data interpolation methods

In framing up the weather data history records for each ship both ship location and global ocean now-cast records were considered. The former were obtained from the Automatic Identification System (AIS) messages. The weather now-cast data, covering all sea areas globally, were downloaded from the records made available by the providers outlined in section 2.2. In specific, weather records included data in the following format:

- 180 min intervals at 1.25 degrees resolution
- Wind speed and direction from US NOAA - <https://www.noaa.gov/>
- Wave height, period and direction from tidetech, which uses Wave Watch 3 model.
- Tidal current, water level from Tidetech - <https://www.tidetech.org/>
- Ocean current from Mercator Ocean<sup>4</sup> - <https://www.mercator-ocean.fr>

In turn, a weather interpolation method was used to link the weather AIS data with hydro-meteorological conditions in 8 areas of operation. Since the bathymetry data is dependent on the location, bilinear and/or trilinear interpolation methods were applied as appropriate (see Figures 8, 9 and Haranen, 2017). The big data analytics methodology developed is demonstrated in Figure 9 and comprised of the following three steps :

- **Step i** – The positions with respect to timestamp of all ships having length >125 m and Gross tonnage > 10,000 were extracted from worldwide AIS database.
- **Step ii** – Weather data available from TideTech, US NOAA and Meractor Ocean (see section 3.2), were extracted. These data included information of ship trajectories, dates and times.
- **Step iii** – An interpolation procedure was used to find the link between operational and hydro-meteorological conditions under which ships operate.

Using these data the joint probability distributions of ship speed with respect to wave height and wave period as well as the wave direction with respect to ship's heading were obtained.

---

<sup>4</sup> For the purposes of this project it was decided not to use ocean current data. Yet available records were used for future use.

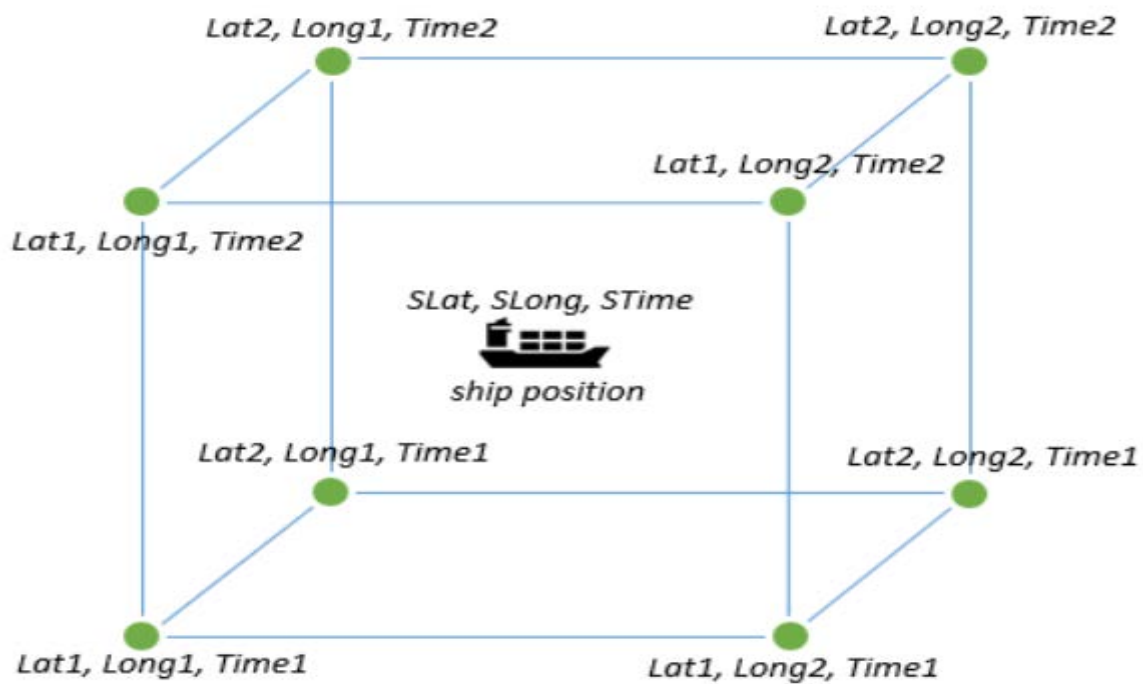


Figure 8. Interpolation method of weather data as per Haranen et al. (2017).

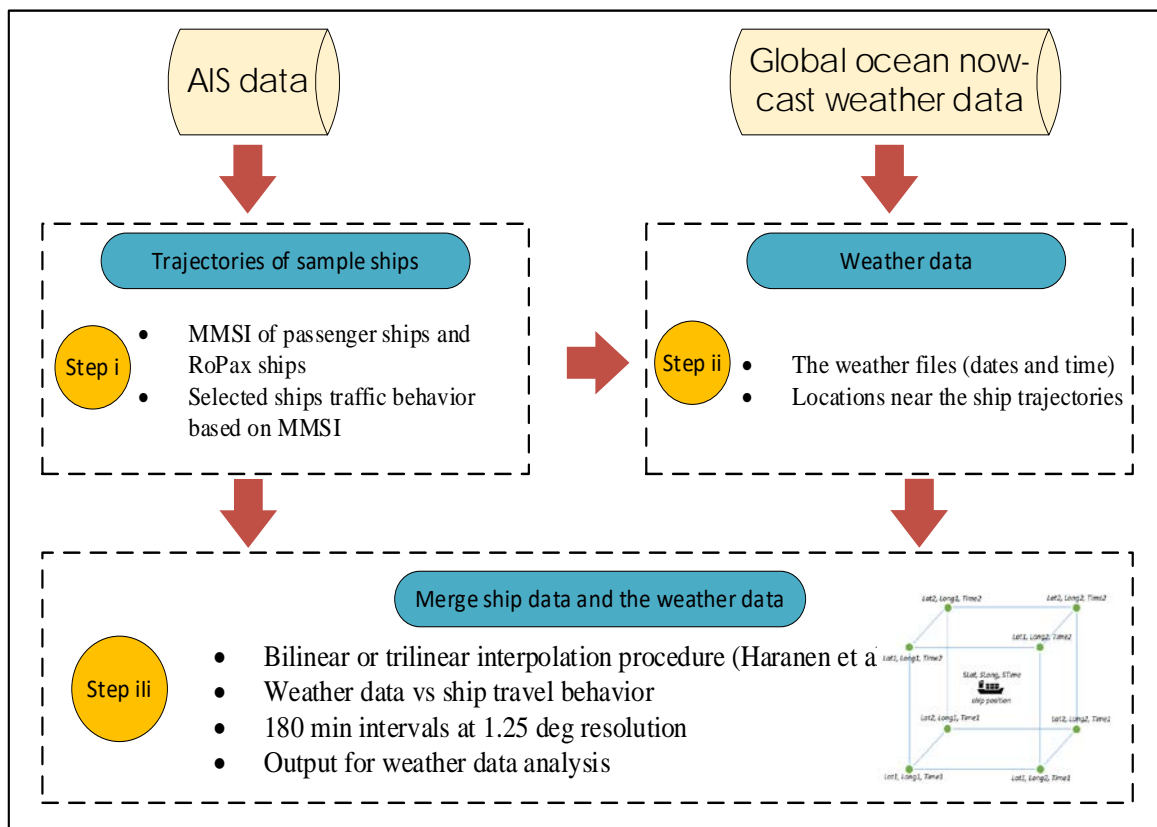


Figure 9. The framework of weather interpolation method.

## 4.2 Modelling of collision encounters

To understand the potential of collision encounters a model using AIS traffic data was developed (see Figure 10). This model considered factors associated with ship distance, relative speed, bearing angle, heading, rate of turn, courses, etc.

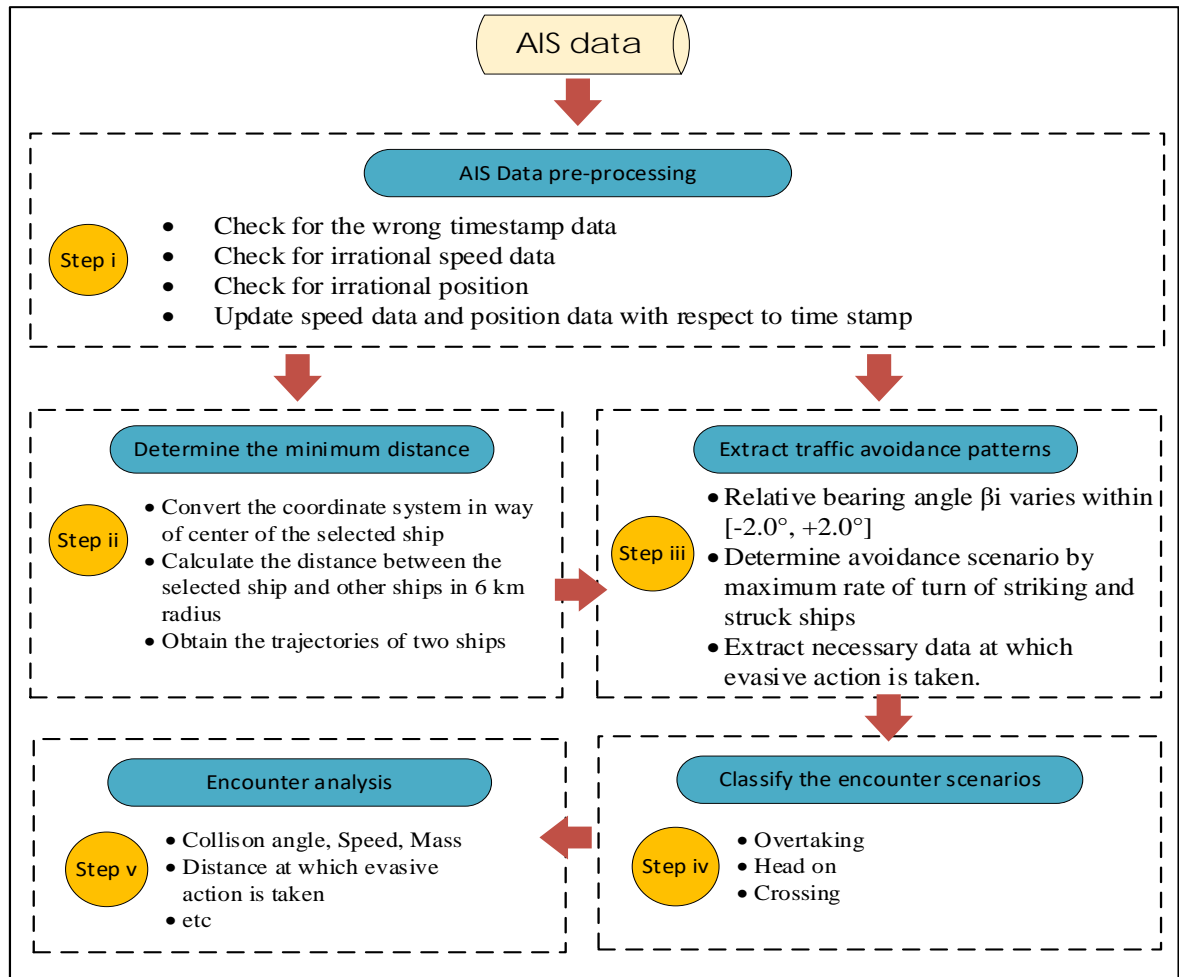


Figure 10. Overview of the collision encounter detection method.

The key steps of the method used to model collision encounters using big data analytics are summarised in five steps as follows:

- Step i – AIS data pre-processing** (for the scientific background of the methods used see Annex A). This process detected and cleaned-up erroneous data records following the classification of data streams for a ship's traffic pattern (these are usually MMSI number sequences using appropriate time stamps referred to as "*the tracks*"). In this way information for each ship was made easily available (see Figure 11).



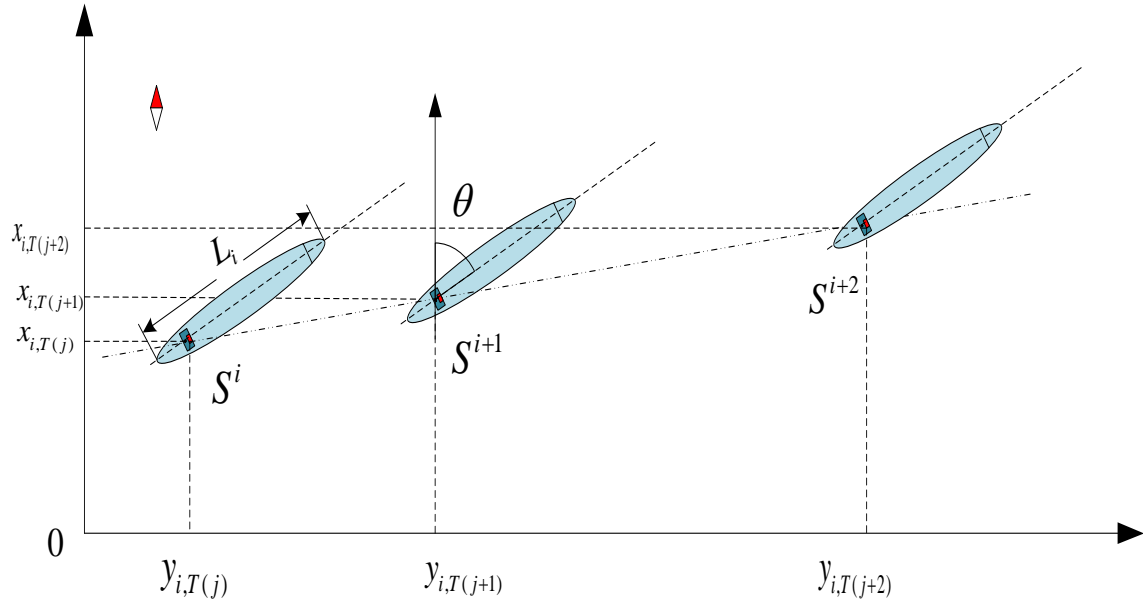


Figure 11. AIS spatio-temporal sample.

- **Step ii – Determine the minimum distance between two ships.** In this step the coordinate system was converted (Figure 12), and the distance between the striking and struck ships for a targeted geographical area were evaluated. Based on common observation ranges of ship born radars in open sea areas it is usually reasonable to consider the collision risk of ships within 6 km and for time intervals of the order of 720s (see Figure 13). The distances between struck and striking ships were calculated based on the following equations<sup>5</sup> :

$$\beta_i = \arccos\left(\frac{y_j - y_i}{\sqrt{(x_j - x_i)^2 + (y_j - y_i)^2}}\right) - \theta_i \quad (1)$$

$$\beta_j = \theta_j - \theta_i - \beta_i - \pi \quad (2)$$

<sup>5</sup> Equations (3), (4) show that ship dimensional lengths may be used to evaluate critical distance lengths between struck and striking ships. For the striking ship (see Equation 3) the reference point corresponds to 3/5 of a ship's length; the corresponding striking ship point corresponds to 4/5 of a ship's length (see Equation 4). If ship types change or other the reference of the AIS position on-board is adopted, Equations (3)-(4) would need to be adapted accordingly.

$$l_i = \frac{3}{5} L_i \cos(\beta_i) \quad (3)$$

$$l_j = \frac{4}{5} L_j \cos(\theta_j - \theta_i - \beta_i - \pi) \quad (4)$$

$$l_{ij} = Dis_{ij} - l_i - l_j \quad (5)$$

where  $\beta_i$  is the angle between encountered ships of heading;  $\theta_i$  is the course of the encountered ships;  $(x_i, y_i)$  and  $(x_j, y_j)$  are the locations of two encountered ships;  $l_{ij}$  is the relative distance between the encountered ships and  $Dis_{ij}$  is the relative distance between the reference of AIS positions of two ships. The coefficients of the Equations (3)-(4) are defined based on AIS data (Kang et al., 2019).

- **Step iii – Idealization of the collision avoidance behavior.** As part of this step relative bearing angles were calculated based on stored traffic data within 6 km radius. In such cases if the relative bearing angle  $\beta_i$  varies within  $[-2.0^\circ$  to  $+2.0^\circ]$  within the observation time of 720 s, the encounter scenario is considered relevant. The traffic data of struck and striking ships are stored in space and time (See  $T_i$  in Figure 14). This model does not account for parameters associated with evasive actions prior to collision. Instead, evasive manoeuvres are simplistically defined based on the maximum rate of turn of striking ships during an encounter scenario.
- **Step iv – Classification of encounter types.** As part of this step encounter types have been determined according to COLREGs convention (Johansen et al., 2016) based on the relative speed, position, heading, bearing, and course (see Figure 15).
- **Step v – Encounter scenario analysis.** As part of this step the encounter scenarios at which evasive action is taken were analysed to calculate striking and struck ship's speed, collision angle, type of striking ship, relative striking location, the mass of striking ship, distance at which evasive action is taken. Based on the AIS data at which evasive action is taken, the mass can be roughly inferred from the ship size and ship specification, which may be related to the consequences of a collision (Montewka et al., 2014). As shown in Figure 16 the collision and possible relative striking positions are classified as : (a) *Front-side*, (b) *Head - head*, (c) *frontal*, (d) *Front-side*, (e) *Rear-end*. Consequently, the anticipated relative collision location along a ship's hull was estimated.

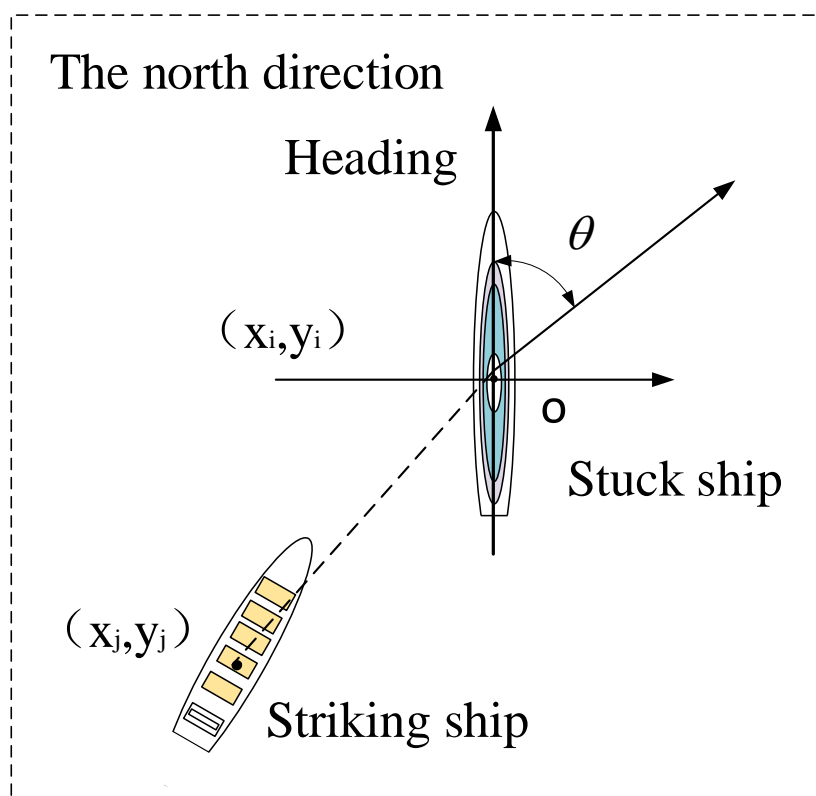


Figure 12. The coordinate system of striking and struck ships.

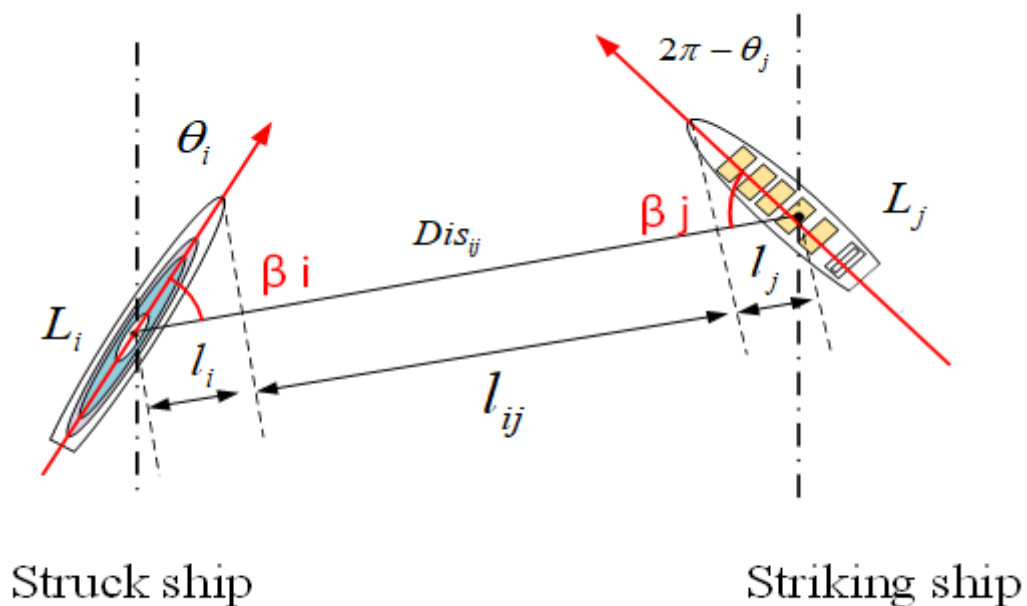


Figure 13. The distance of striking and struck ships.

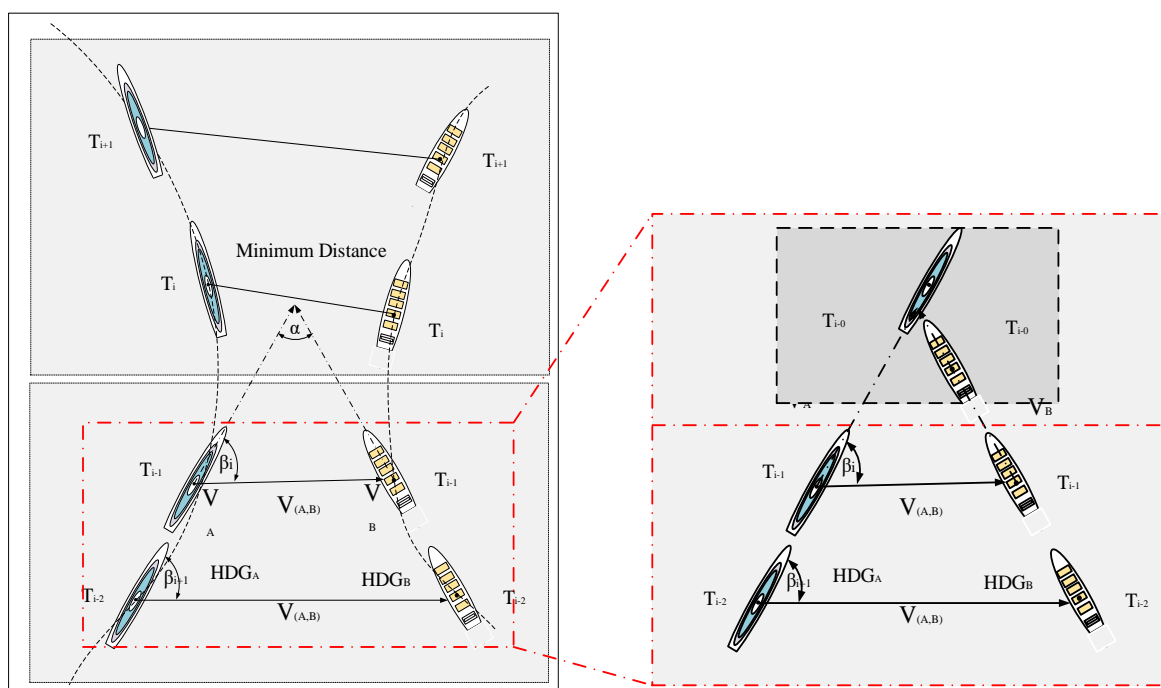


Figure 14. The distance and dynamics of striking and struck ships.

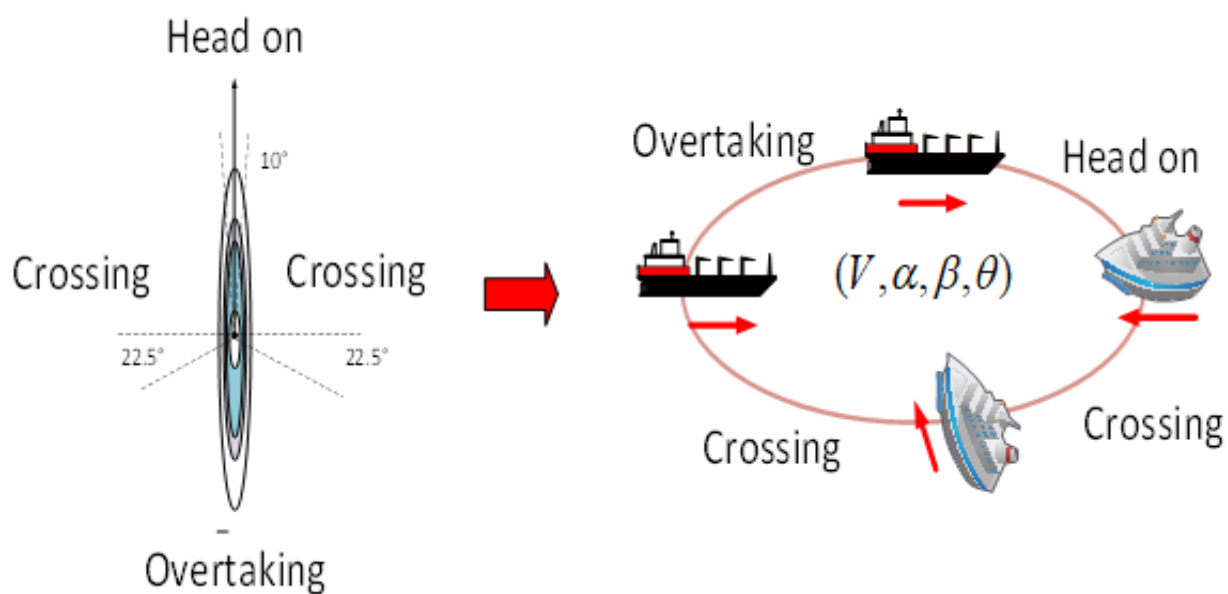


Figure 15. COLREGs encounter types (Huang et al., 2019).

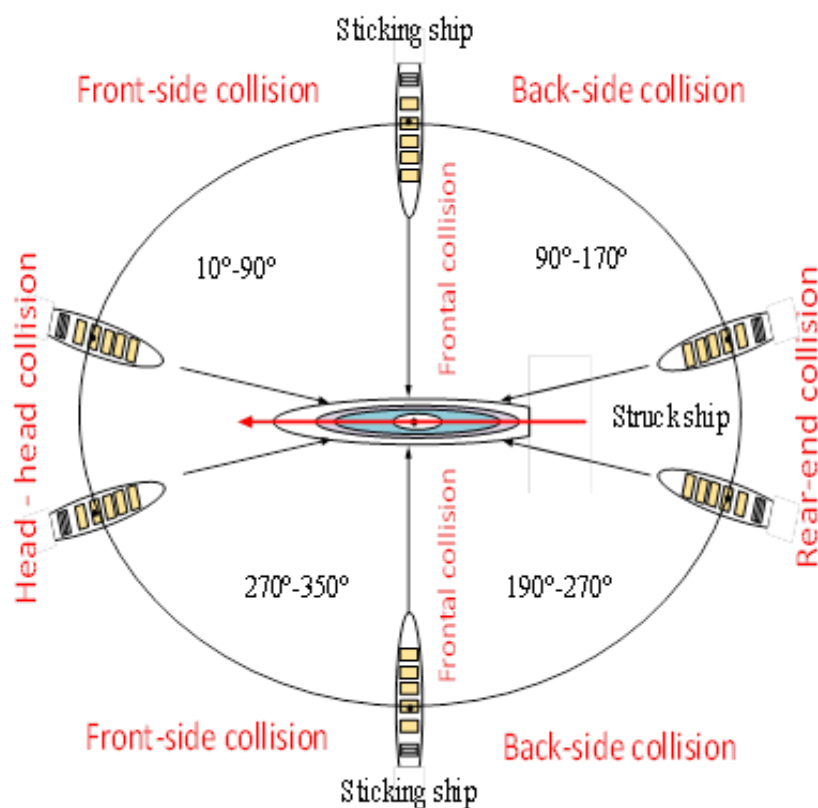


Figure 16. Collision scenarios relative striking positions.

### 4.3 Modelling of grounding encounters

A model utilising AIS traffic data and GEBCO data in shallow waters (forward to and lateral shallow waters) was developed for power and drifting grounding (see Figures 17,18). The model content and structure are based on expert judgement and on this basis the account for relative speed, bearing angle, heading, Rate of turn and vessel course. The big data analytics methodology developed comprises of the following five steps :

- **Step i** – AIS data pre-processing (identical to step I of section 5.2).
- **Steps ii and iii** – Extraction and classification of bathymetry data as per voyage trajectories using GEBCO (or equivalent) database. As part of this step bathymetry data charts were used to identify shallow waters near to ship trajectories for each voyage. At first instance, safe water depths for the operation of the selected ships were based on their draught and UKC (under keel clearance) for each voyage (see in Figure 19).

- **Step iv – Calculation of the min. distance to grounding point.** At first instance data from shallow water observations within 6 Km conventional radar range were collected and the ship coordinate system was converted in relation to the direction and positioning of the grounding target (see Figure 20). Consequently, the positioning of a ship in shallow waters prior to a grounding encounter was estimated based also on her dimensions (3/5 ship lengths for passenger vessels). The distance to grounding  $Dis_F$  was calculated as <sup>6</sup>:

$$Dis_i = Dis_F - l_i \quad (7)$$

and the minimum distance to lateral shallow waters  $Dis_L$  after the grounding avoidance action was evaluated according to the equation :

$$DisM_L = Min.(Dis_L) \quad (8)$$

Bathymetry data were cross-checked for water depths below the originally safe water depths and accordingly isobaths were calculated (see Figure 21)<sup>7</sup>.

- **Step v – Encounter scenario analysis.** AIS, GEBCO, mass and speed data as well as ramming angles in way of grounding were used to conclude on power and drifting scenarios.

---

<sup>6</sup> This is the minimum distance during which the grounding avoidance action may be taken (i.e. the minimum distance in relation to the original AIS position during which ship heading may change before the bump in way of shallow water takes place).

<sup>7</sup> Safe Water is considered shallow when its depth is less than the ship draught plus under keel clearance which was considered to correspond to 20% of a ship's draft in this project task.

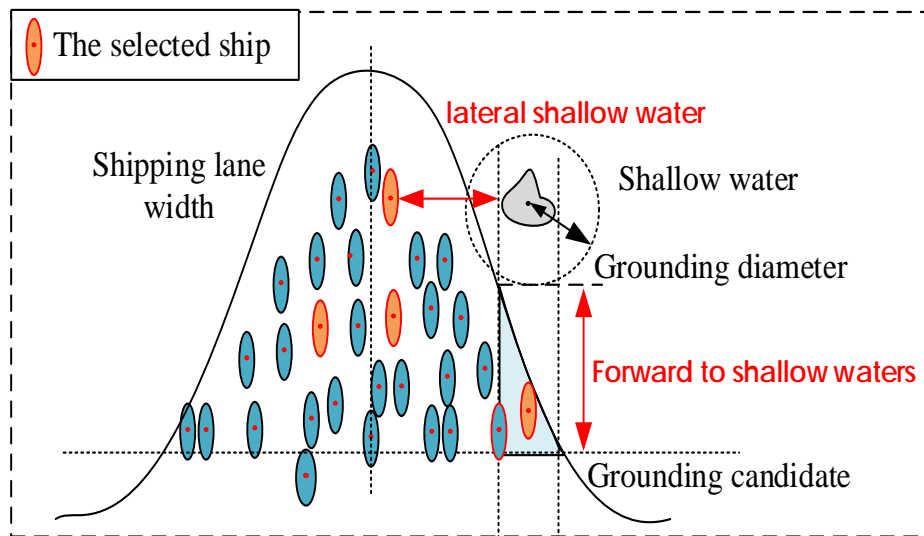


Figure 17. The minimum distance between ships and shallow waters.

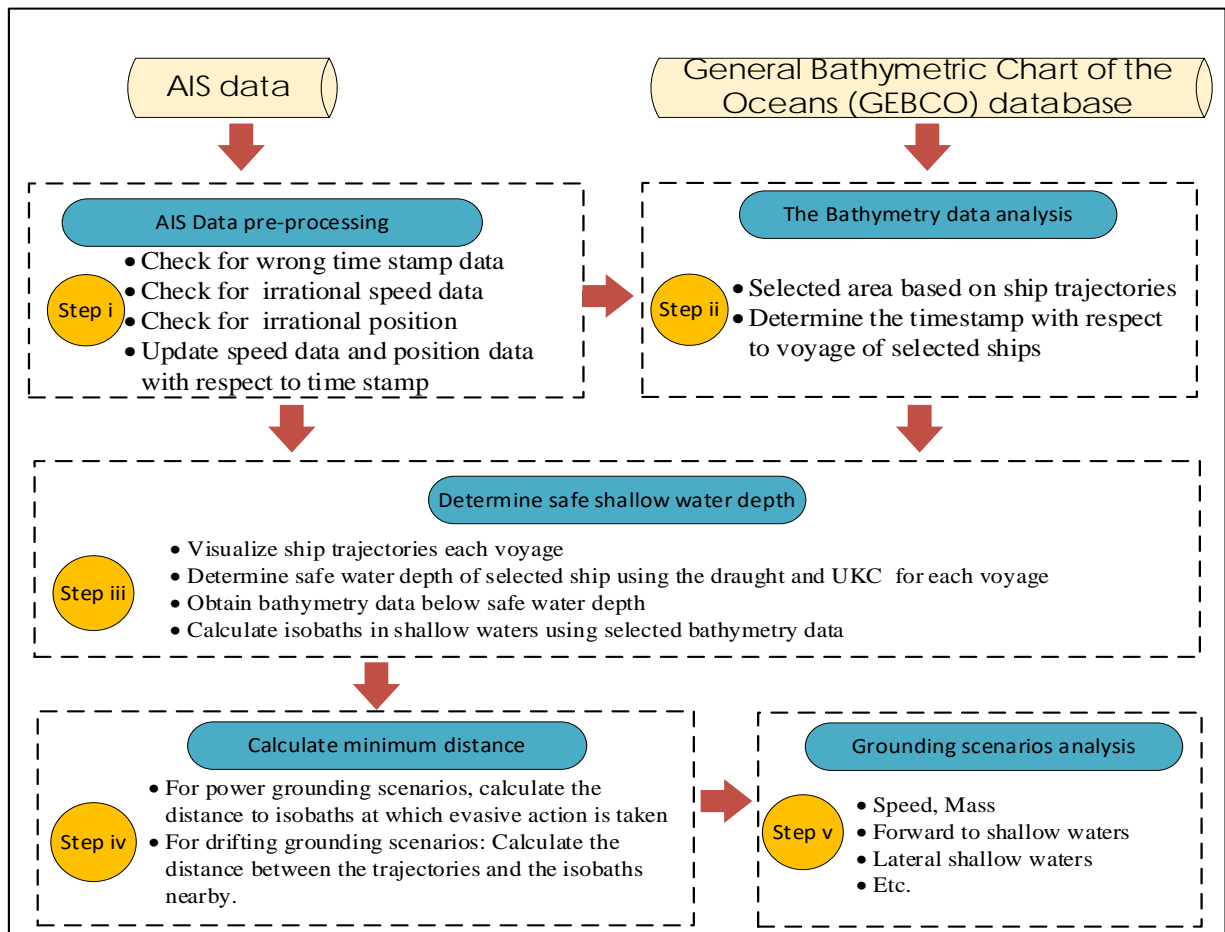


Figure 18. Grounding scenarios detection method.

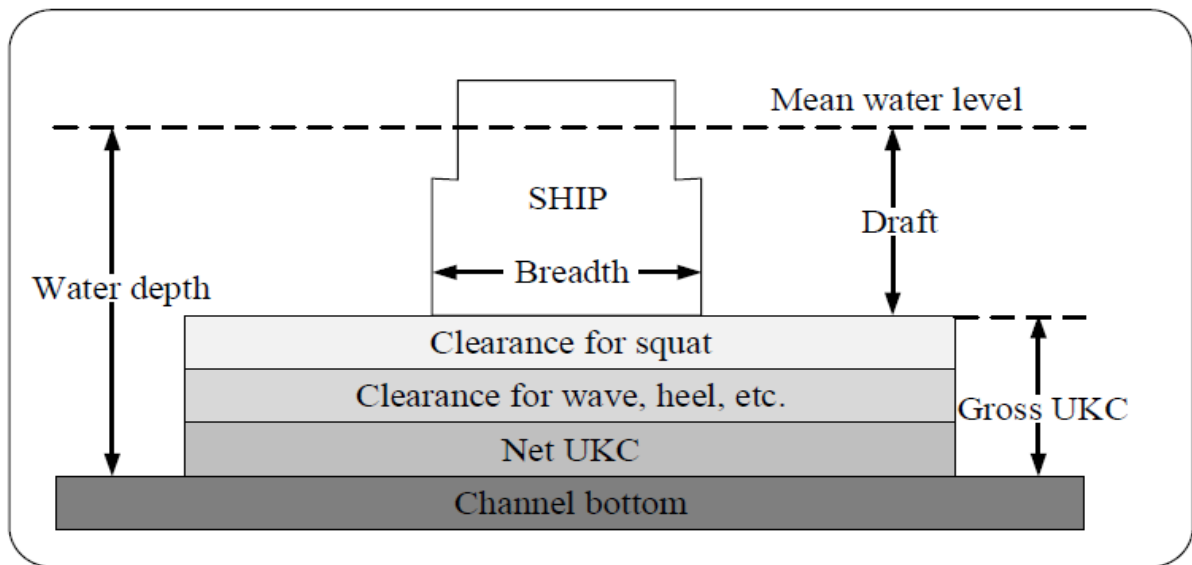


Figure 19. Relationship between Water depth, Ship Draught and UKC (Zhao et al., 2018).

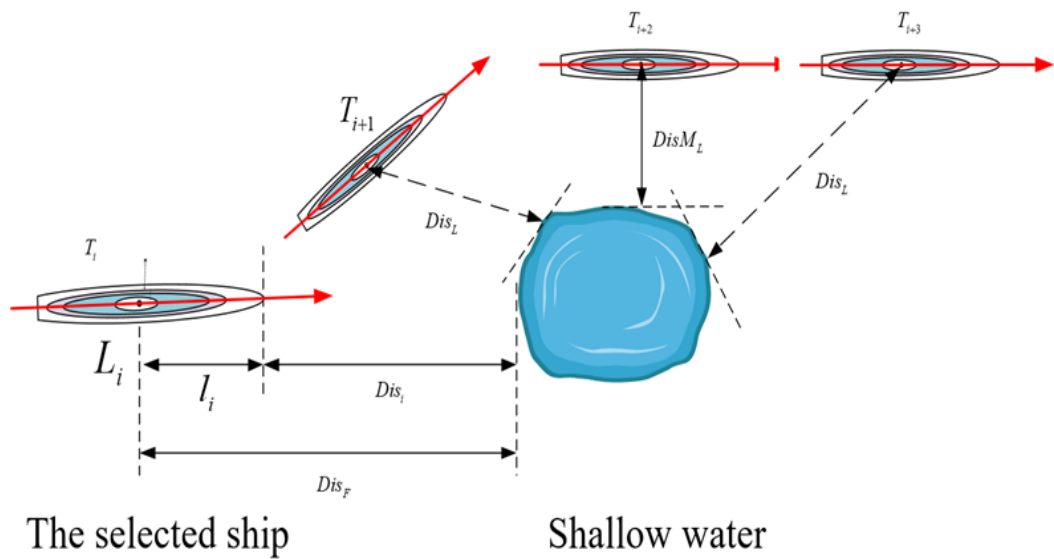


Figure 20. The relationship between the shallow water and the spatial AIS data of a selected ship.



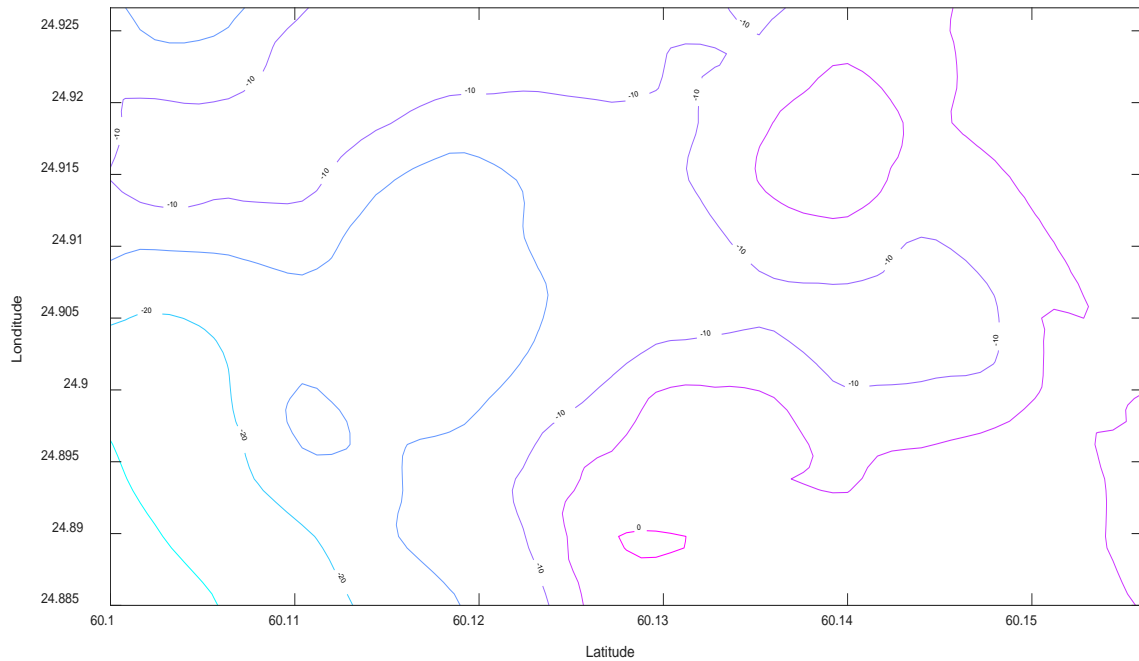


Figure 21. The determined isobaths based on the selected bathymetry data, considering the safe water depth of selected ships.

## 5. KEY RESULTS

Systematic manipulation of large data volumes (e.g. AIS, weather and bathymetry data) for different traffic areas may be challenging. For example, 3 year data (2017-2019) in the Gulf of Finland contain about 40 billion records of dynamic AIS data. This section presents key results with the aim to establish trends of relevance to the occurrence of significant wave heights and the relationship of ship heading to wave parameters for all Ro-Pax and large passenger vessels used in this project (Table 2) navigating in the 8 areas of operation outlined in Figure 2 over a three year period (2017-2019). Then weather and traffic data for a Ro-Pax ship operating between Helsinki and Tallinn (see Figure 22 and Table 4) were used to evaluate critical collision and grounding encounters for year 2019 only. The later is considered adequate in terms of validating possible scenarios. Big data analytics followed the state of art methods described in Section 4.

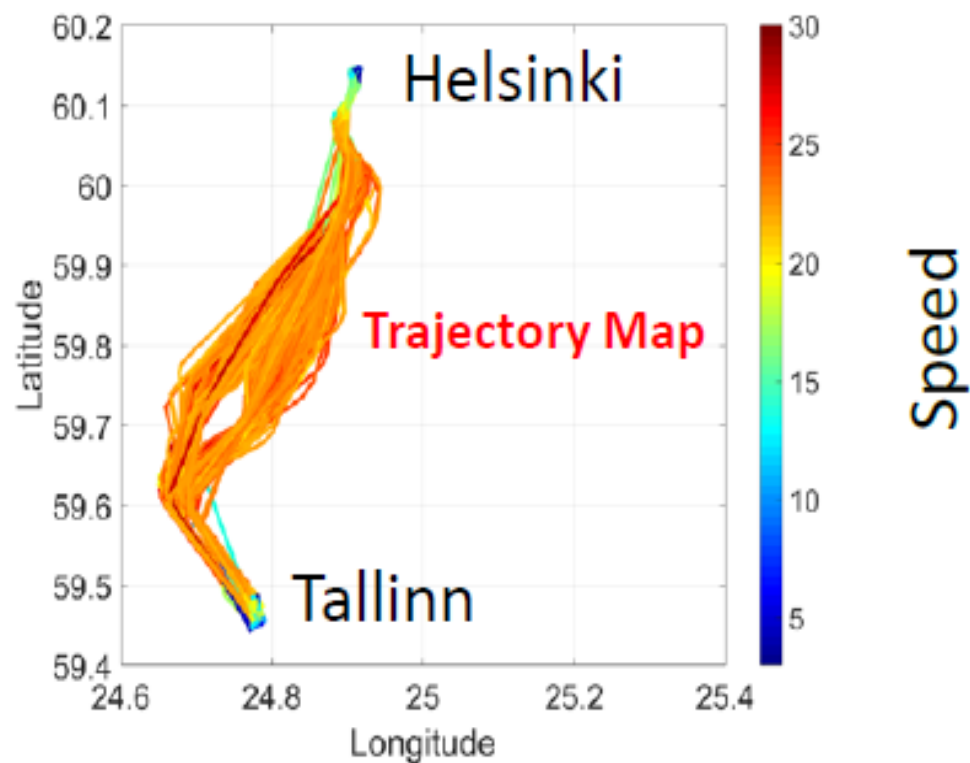



Figure 22. The ship trajectories of the selected ship for year 2019; the colour bar denotes vessel speed in knots.

Table 4. The ship specification of the sample Ro-Pax ship.

Principal Particulars	IMO No. 276829000	
Length	212 m	
Breath	30.6 m	
Average draught	6.9 m	
Gross Tonnage	49 134. 0 t	

## 5.1 Trends from global weather data

Weather data records were interpolated at each position of every ship Operational histories from 110 largest RoPax and Passenger ships was used (see Section 4). Then, swell and wind wave components were combined to form the significant wave height as :

$$H_{wave} = \sqrt{(H_{Swell})^2 + (H_{Windwave})^2} \quad (9)$$

Combined wave height histories were used to produce cumulative distributions for each of the 8 areas over 4 seasons<sup>8</sup> from 2017-2019 (see Figures 23, 24, Table 5 for key results and ANNEX B for more detailed records). The following conclusions were drawn:

- In all sea areas and for all seasons 99% of the time ships navigate in wave heights smaller than 6.4 m.
- For most of the time passenger ships have been navigating in less than 3 m significant wave heights, except for the winter months where they navigate in the North Atlantic.
- During spring, wave heights are small in the northern areas except for the northern Pacific. On the other hand ships navigating in the southern hemisphere during spring experience wave heights up to 4 m.
- During summer season operations the lowest wave heights were observed.
- Wave height seasonal variations are not that significant. Exception to this are the wave heights experienced by passenger ships in the northern hemisphere during autumn where the 3.5 m significant wave heights evident are lower to BMT (1990).
- Smaller wave heights in comparison with BMT data are most probably due to the planned itineraries and weather routing. This deviation may also be due to limited data records available for this area and could be investigated further in the future.
- Winter season experiences the highest wave height in all areas except in the Southern Hemisphere and Caribbean Sea.

Figures 25 a, b demonstrate the relationship between wave directions and ship headings for all ships operating over different seasons throughout the available operational history records (i.e. 2017 – 2019). These results combined with the wave height distributions shown in Figures 23, 24 and Table 5 could be used to simulate realistic environmental conditions of relevance to serious

---

<sup>8</sup> Data were divided into 4 seasons along this specification BMT (1990) Global Wave statistics (Spring : Mar-Apr ; Summer: Jun-Aug; Autumn: Sep-Nov; Winter : Dec-Feb).

flooding events (see section 5.5) . All results for Passenger and Ro-Pax ships are presented in ANNEX B.

To find the link between operational and hydro-meteorological conditions under which the Ro-Pax ships (Table 3) operate in Gulf of Finland, ship travel behaviors were in further analysed in various weather conditions for 38 ships that operated 66.1% of their total time (i.e. 27,301.46 days from 2017 – 2019) in this area. Figure 26 represents in the form of a scatter diagram wave heights and periods in various intervals (0.5 m for wave height and 0.5 min for wave period). In turn Figure 27 plots the relationship between wave and wind directions versus ship headings for each season and finally, Figures 28 – 30 show the seasonal speed distributions. In specific, Figure 28 classifies ship speeds based on wave spreads that correspond to real operational conditions and Figure 29 extrapolates these results to various seasons. Probability density functions of seasonal speed variations for all RoPax ships operating in Gulf of Finland are shown in Figure 30.

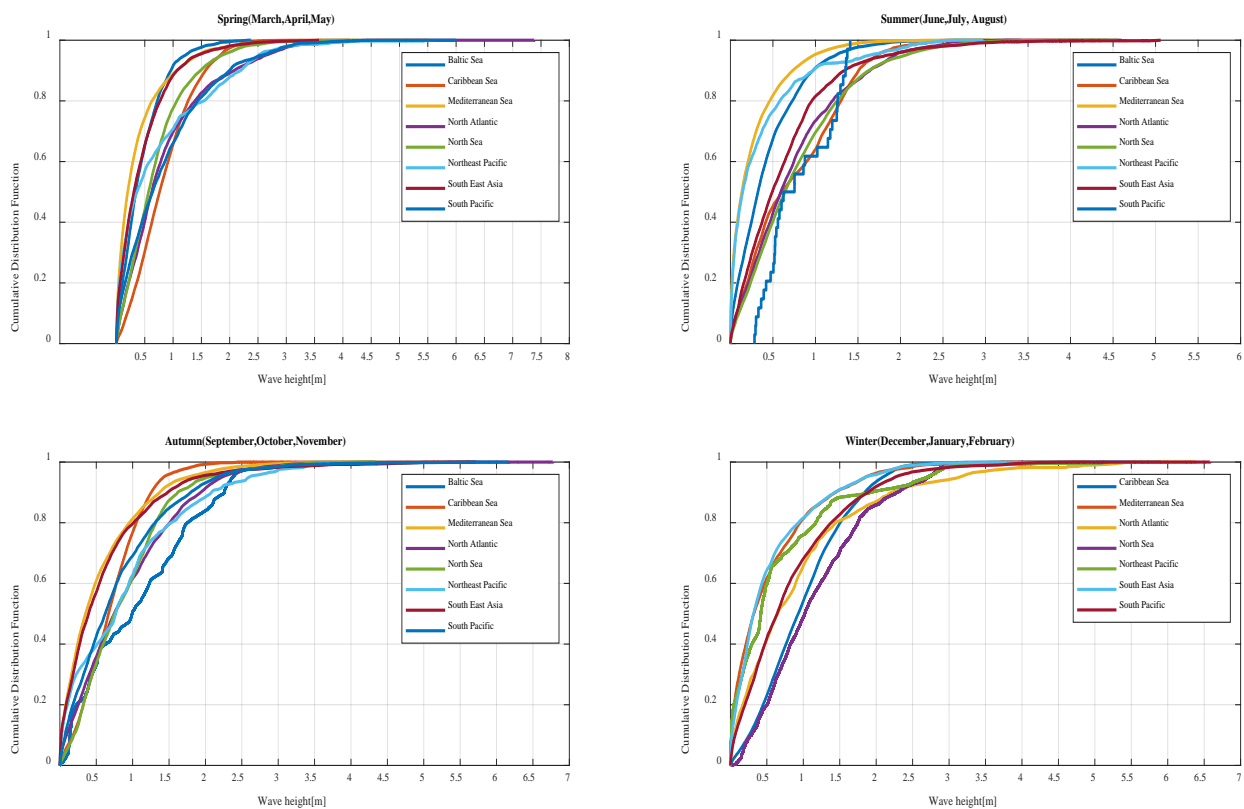


Figure 23. Wave Height (m) cumulative distributions for all Passenger ships in 8 areas over different seasons.

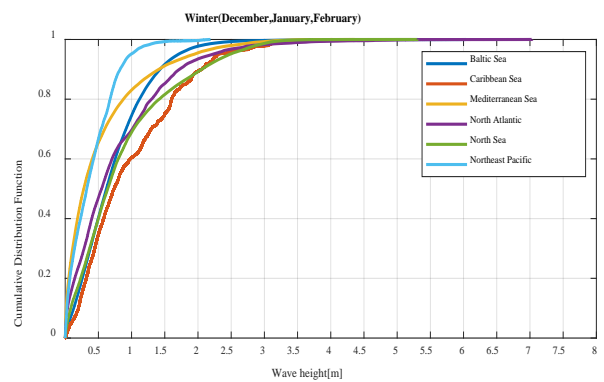
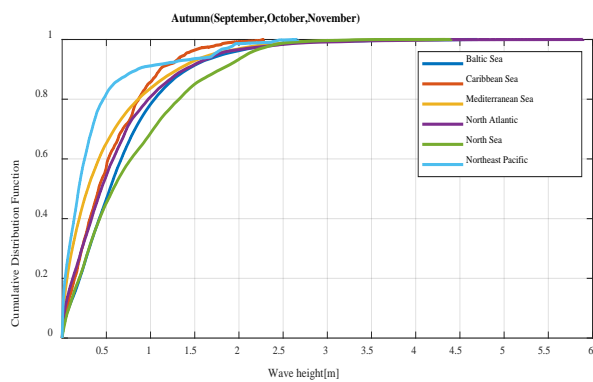
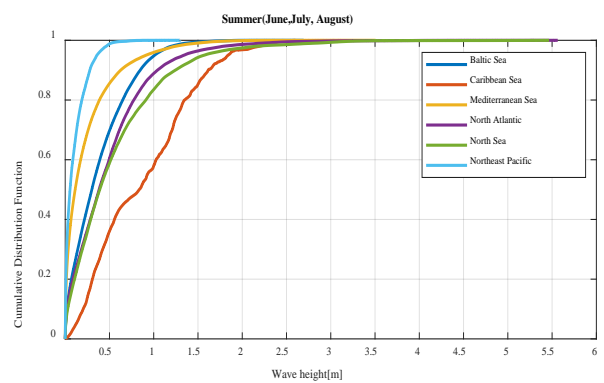
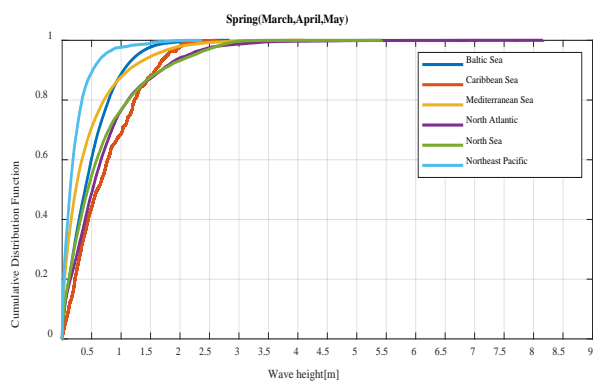


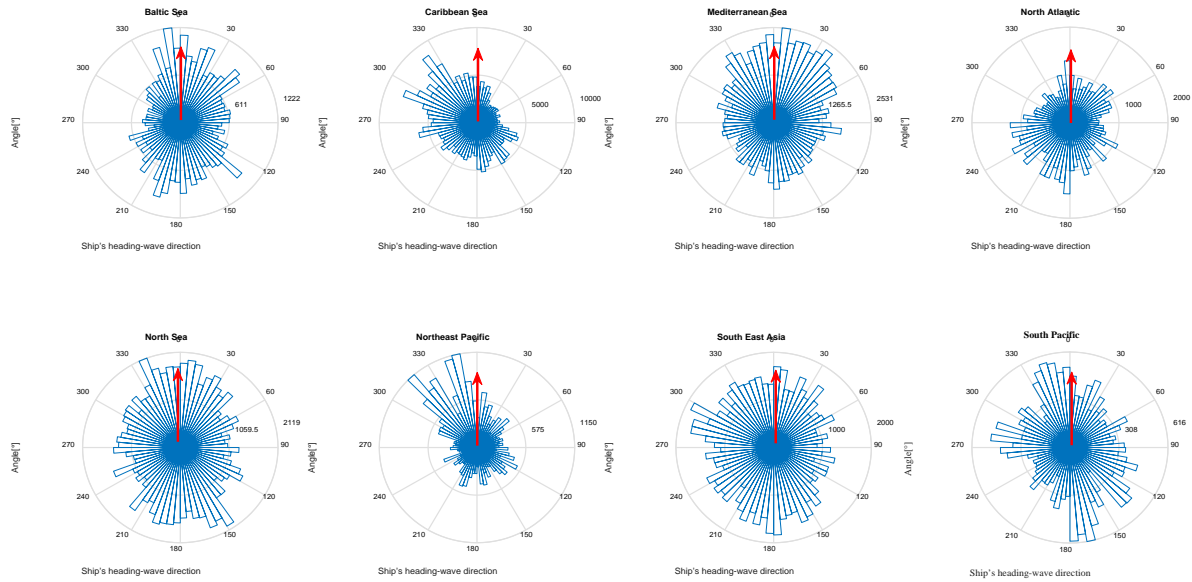
Figure 24. Wave Height (m) cumulative distributions for all RoPax ships in 8 areas over different seasons.

Wave height (m)	Areas	Spring				Summer				Autumn				Winter				Percent (%)
		25%	50%	75%	99%	25%	50%	75%	99%	25%	50%	75%	99%	25%	50%	75%	99%	
	Baltic Sea	0.1485	0.341	0.644	2.318	0.125	0.324	0.625	3.241	0.384	0.991	1.662	2.899			None		78.98%
	Caribbean Sea	0.4284	0.761	1.162	3.59	0.246	0.605	1.204	2.77	0.382	0.668	0.970	3.137	0.530	0.930	1.382	4.054	65.34%
	Mediterranean Sea	0.055	0.198	0.514	4.601	0.027	0.133	0.369	2.657	0.118	0.353	0.801	5.646	0.081	0.321	0.825	4.747	69.64%
	North Atlantic	0.2862	0.623	1.179	5.45	0.273	0.592	1.048	3.286	0.325	0.744	1.342	6.291	0.238	0.648	1.238	6.371	82.94%
	North Sea	0.2707	0.566	0.939	4.248	0.300	0.641	1.127	4.509	0.384	0.750	1.222	4.328	0.582	1.02	1.63	4.014	73.52%
	Northeast Pacific	0.080	0.362	1.125	5.65	0.033	0.144	0.458	2.979	0.155	0.768	1.291	4.986	0.112	0.418	0.937	5.2	74.384%
	South East Asia	0.100	0.306	0.662	3.577	0.207	0.492	0.866	5.057	0.135	0.394	0.834	5.699	0.120	0.316	0.747	5.339	72.18%
	South Pacific	0.218	0.638	1.239	6.003	0.506	0.624	0.735	1.409	0.250	0.623	1.157	6.011	0.272	0.640	1.209	6.248	76.57%

Note: The percent denotes the total ships spend hours (weather data records) of the total operational time (total time ships in this area) in each area.

Table 5. The summary of the wave height in 8 areas (Wave height)

### Spring(March, April, May)



### Summer(June, July, August)

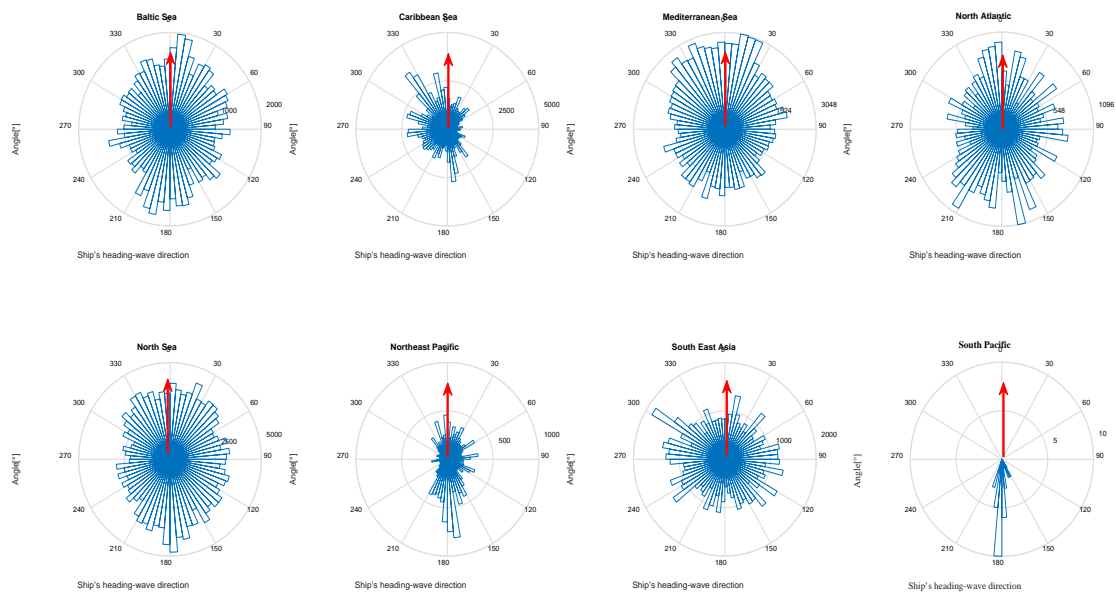
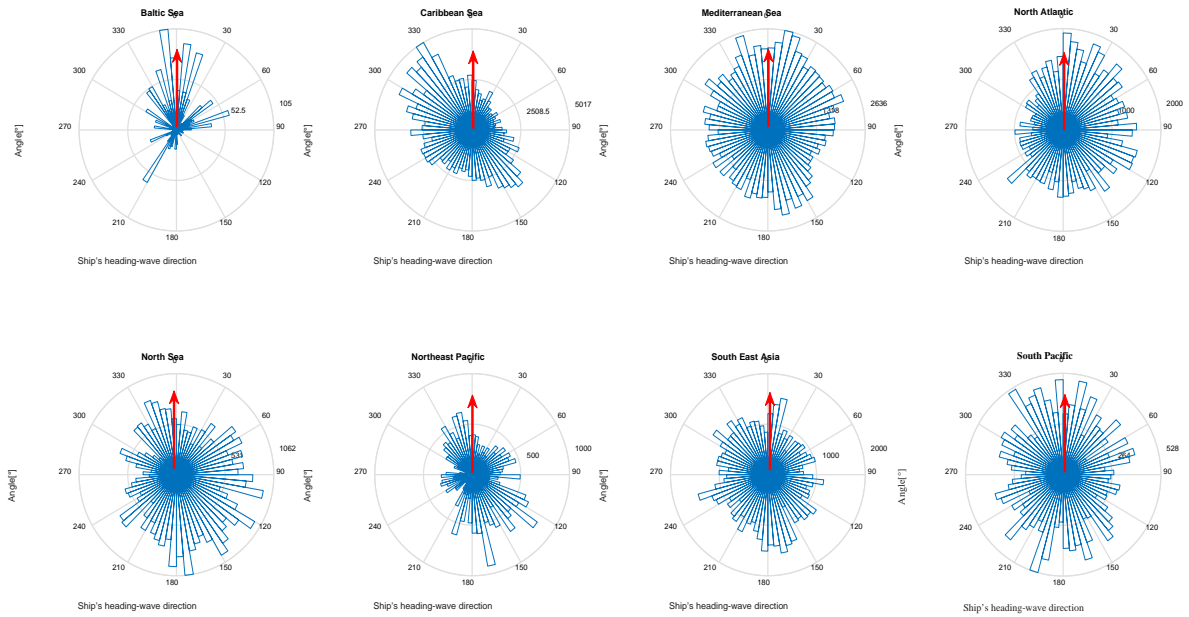


Figure 25a. Wave direction with respect to ship heading in spring and summer seasons.

Autumn(September,October,November)



Winter(December,January,February)

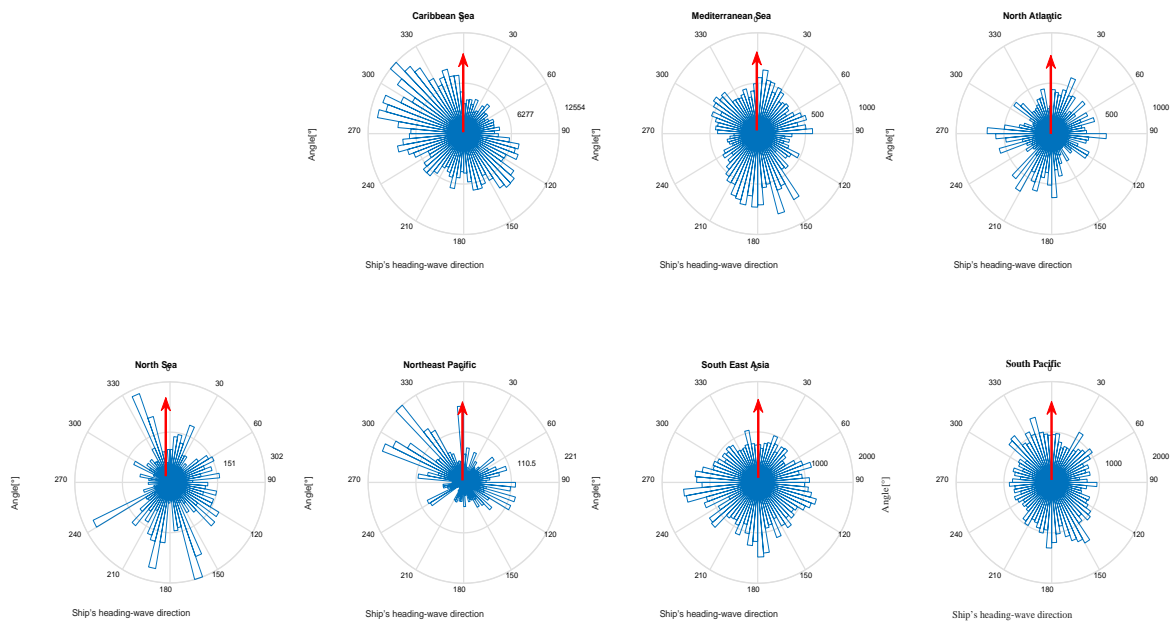


Figure 25b. Wave direction with respect to ship headings for autumn and winter seasons.



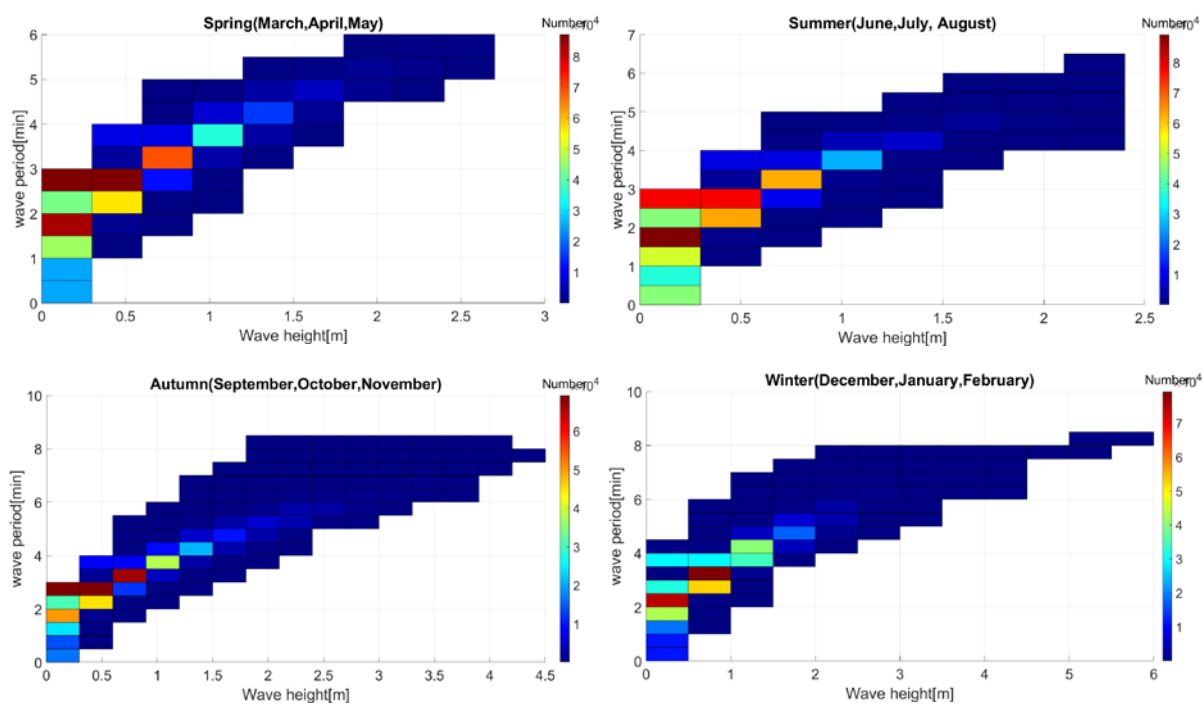
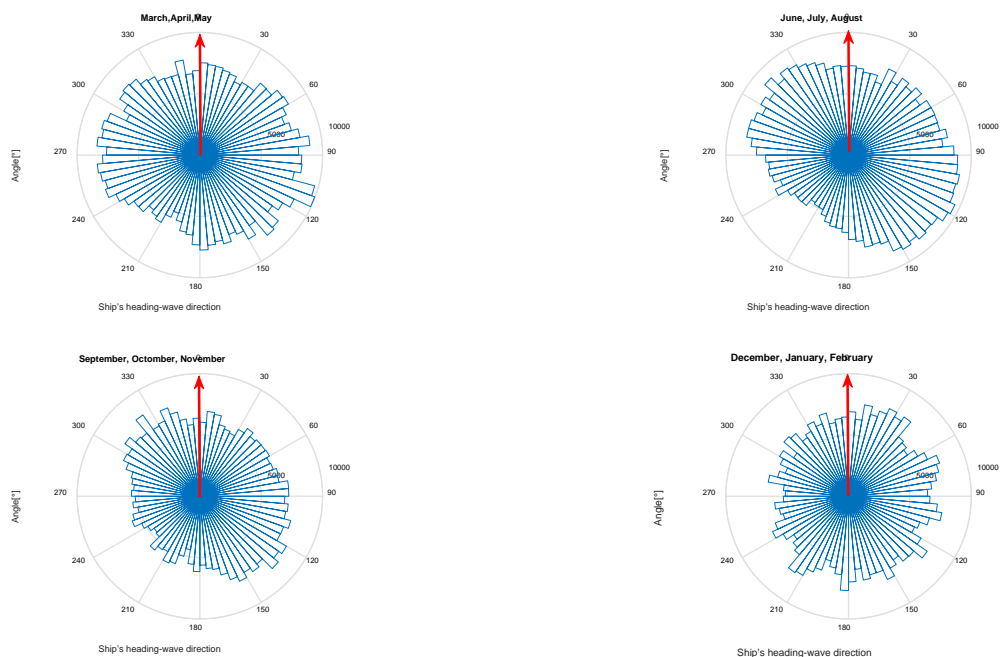
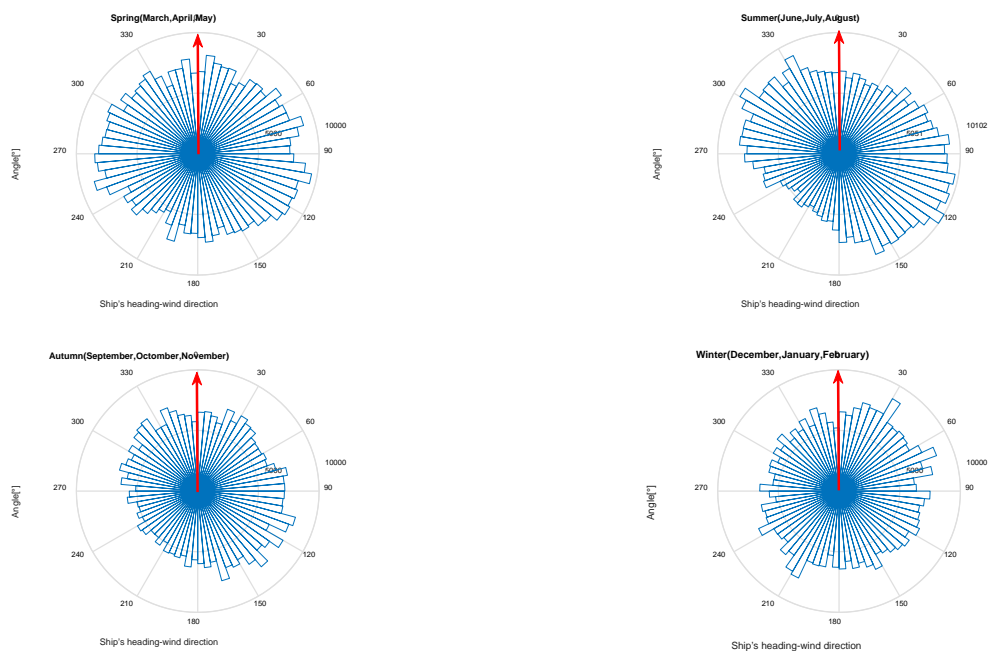


Figure 26. The wave scatter diagrams in the Gulf of Finland.



(A: Wave direction with respect to ship is heading in the Gulf of Finland)



(B: Wind direction with respect to ship is heading in the Gulf of Finland)

Figure 27. Wave or Wind direction with respect to ship is heading each season in the Gulf of Finland.

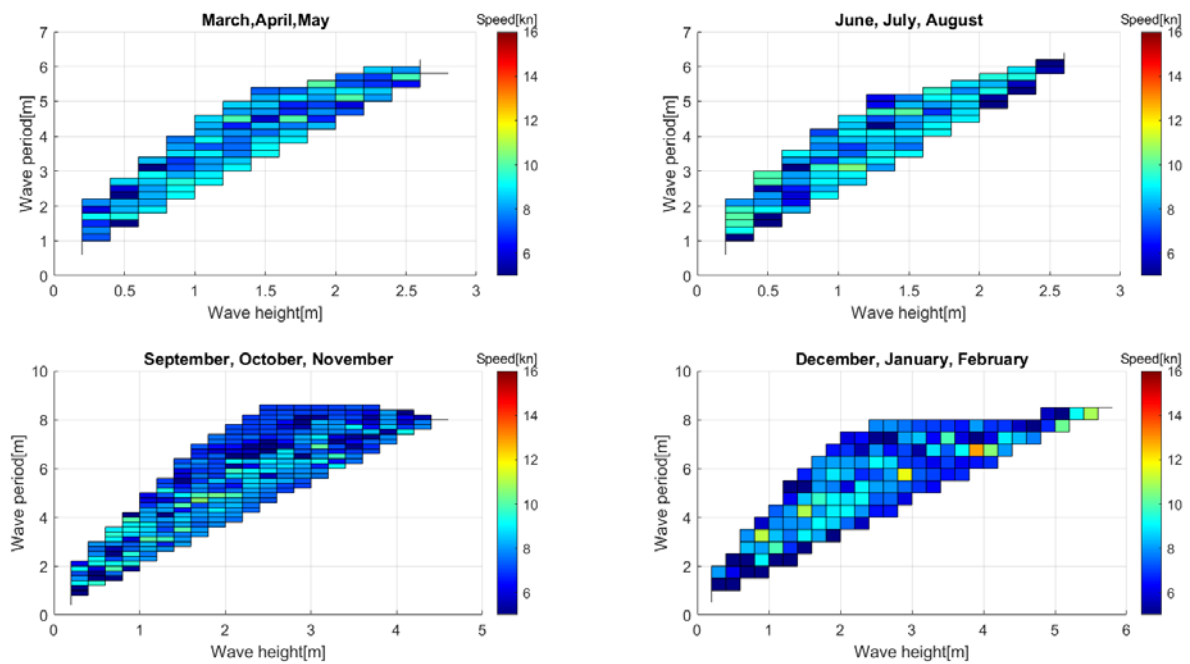


Figure 28. Speed distribution in real wave height and period each season.

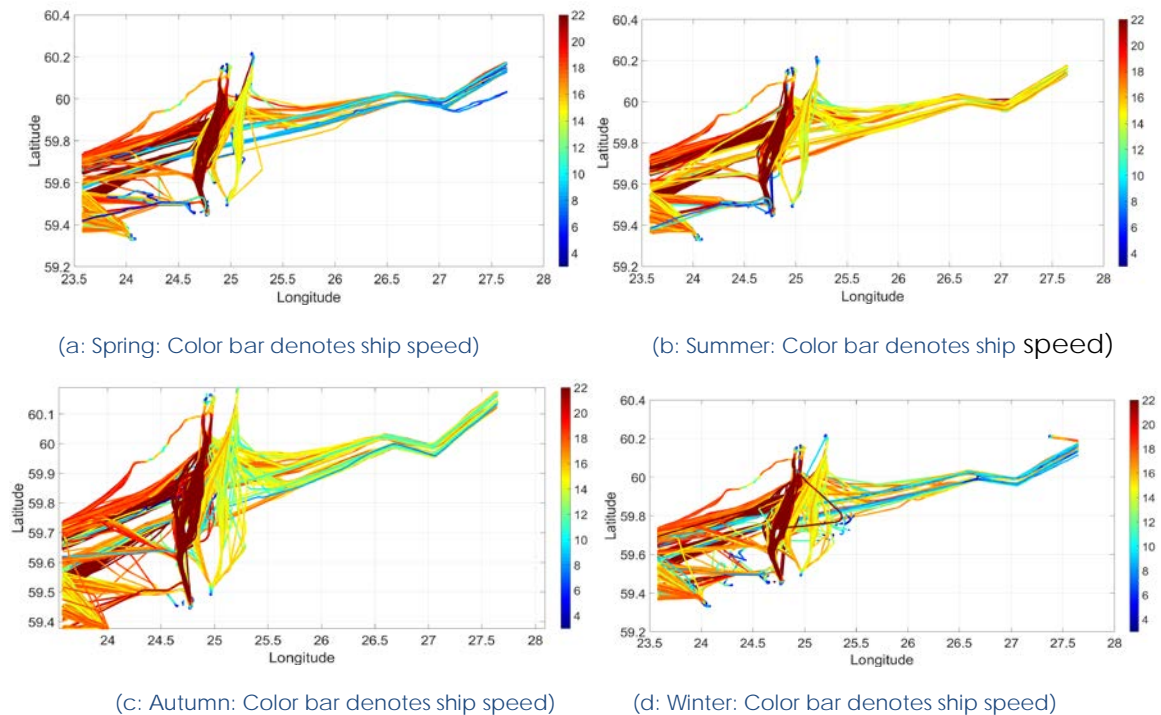


Figure 29. Speed visualization of Ropax ships in the Gulf of Finland in various seasons.

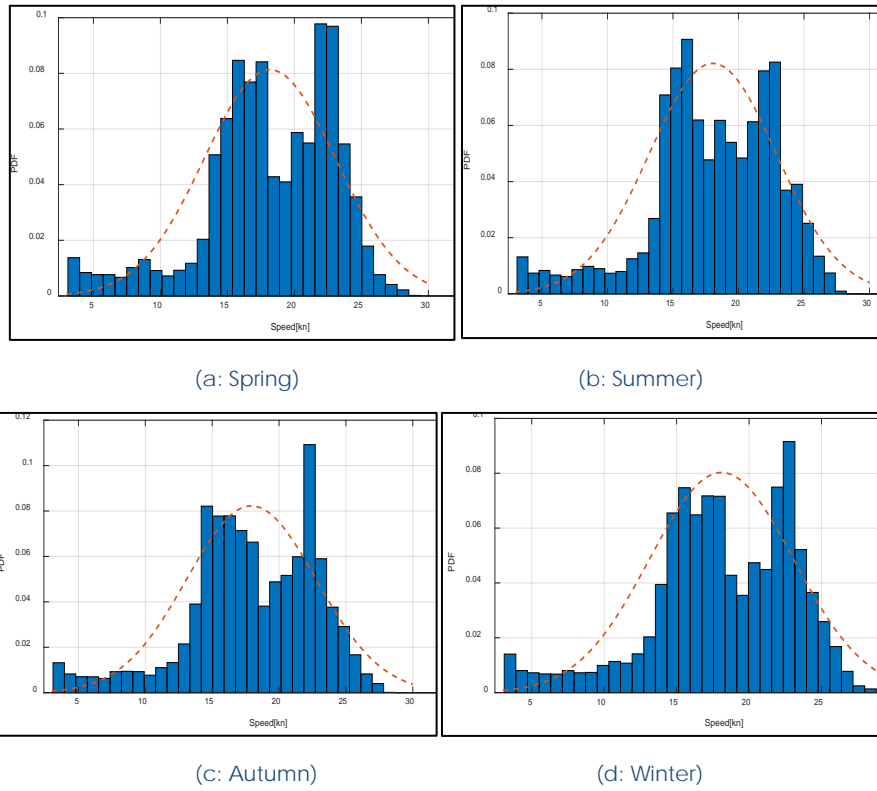


Figure 30. Seasonal speed distributions of Ropax ships in the Gulf of Finland.

## 5.2 Trends from sample ship weather data

The sample ship (Table 4) was analyzed in real operational and weather conditions of relevance to the Gulf of Finland over three years (2017 – 2019). Cumulative distributions of weather parameters and encounter angles are presented in Figures 31,32. Based on these results it appears that for most of the time the Ro-Pax navigated in less than 1.0 meter significant heights, except for the autumn season when wave heights were 2m or marginally more. During spring wave heights appeared to be the lowest and during summer the highest. In general, wind speed was of the order of less than 10 m/s, except for autumn when it was marginally higher. Most of the time, the sample ships navigated in 0.5 swell and currents with speed less than 0.2 m/s. For most of the time the sample ship has been influenced by lateral wind and waves.

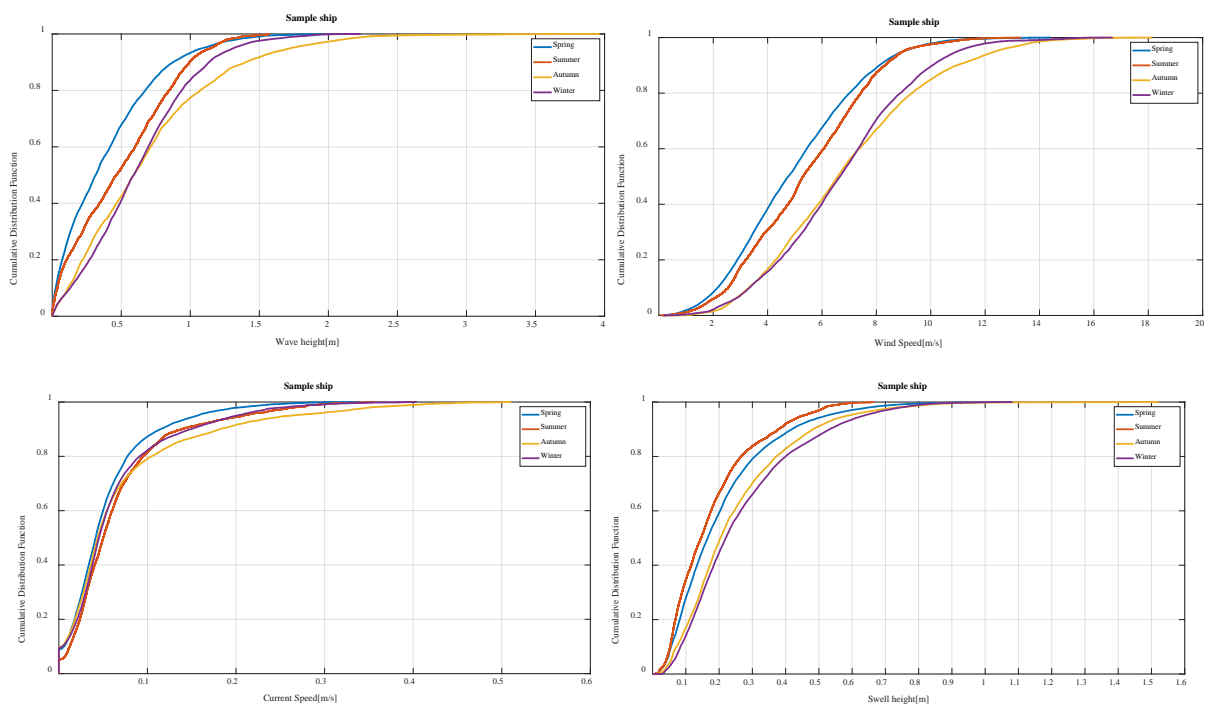


Figure 31. Weather parameters cumulative distributions for the 3-year operations (covering the three-year operational history of the sample ship).

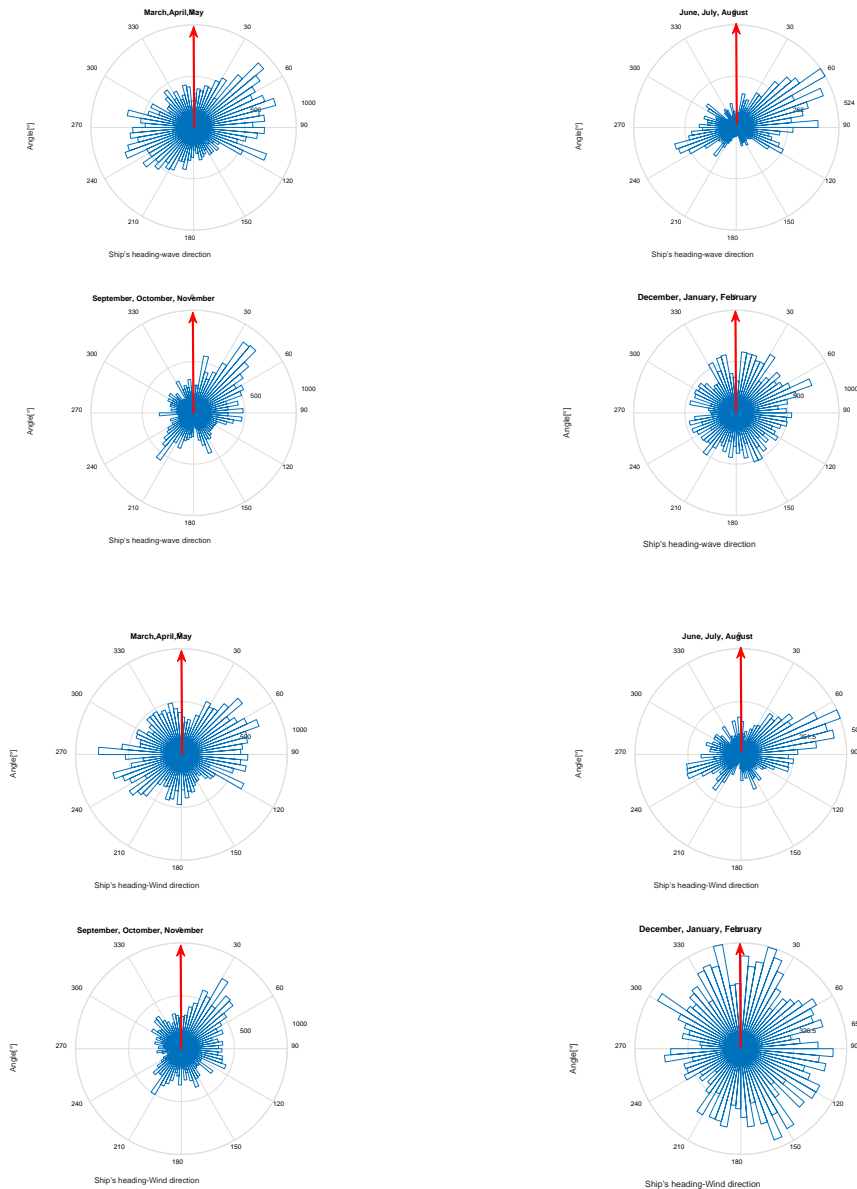


Figure 32. Encounter angles distribution (covering the three-year operational history of the sample ship).

### 5.3 Demonstration of collision encounters

Based on the procedure presented in Section 4.2 the minimum distance between the sample Ro-Pax ship and other ships in way of her proximity was determined (see Figure 33). The encounter scenarios considered for one year of operation (year 2019) are summarised in Table

6 for the locations shown in Figure 34. Collision events for the selected ship types are presented in Figure 35. Ships have been divided into 6 groups on the basis of which the mass and speed distribution of the striking ships was evaluated (see Table 7 and Figure 36). For FLARE, group 2 has been selected as the most relevant sample (See Table 7, Figure 37; for demonstration of collision encounters for all other ship groups see Annex B). Whereas group 2 presents a sample that is not in terms of ship numbers conveniently high (represents only 10% of the overall records) it is the most appropriate in terms of idealising collision encounters and associated risks for passenger and Ro-Pax ships that are relevant to this project. A summary of the distribution of speed and mass of the struck/striking ships, the distances between these ships and their relative bearing angles are shown in Figures 37-43. To analyze the encounters, collision energy was calculated based on the distributions of ship speed, mass, ship distances and the collision angles. In summary for the selected group 2 the speed of the struck ship was up to 25 Knots, and the average speed of striking ships was identified between 11 and 23 knots. The mass of the struck ship was more than  $2.7 \cdot 10^4$  tonnes and the masses of striking ships have been between  $1 \cdot 10^4$  and  $2.5 \cdot 10^4$  tones. Collision angles varied between  $[90^\circ - 120^\circ]$  and  $[210^\circ - 260^\circ]$ , and most of the striking ships appeared in way of the bow and stern areas of struck ship.

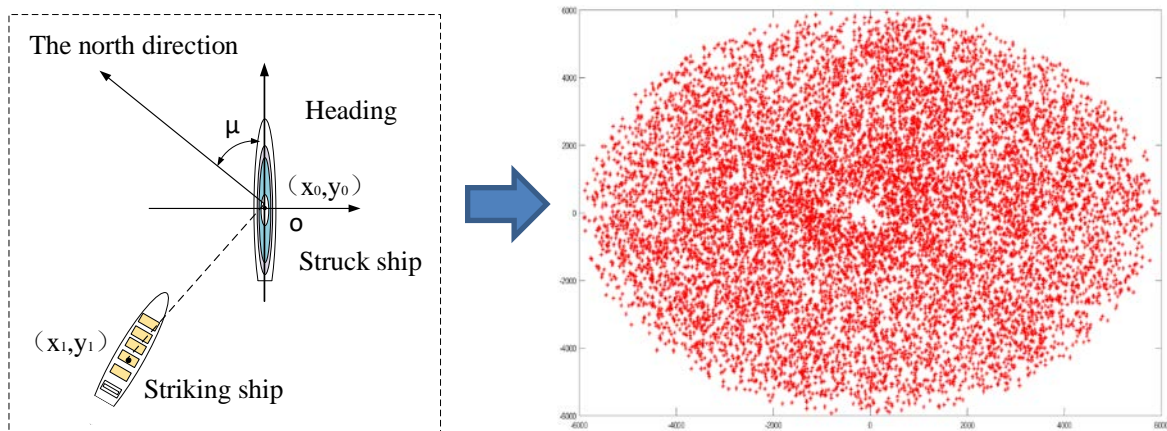


Figure 33. The minimum distance could between two ships.

Table 6. The encountered potential collision events of the selected ships.

Minimum dis.	Encounter Scenarios		
	Crossing	Overtaking	Head-On
13954	1174	27	419

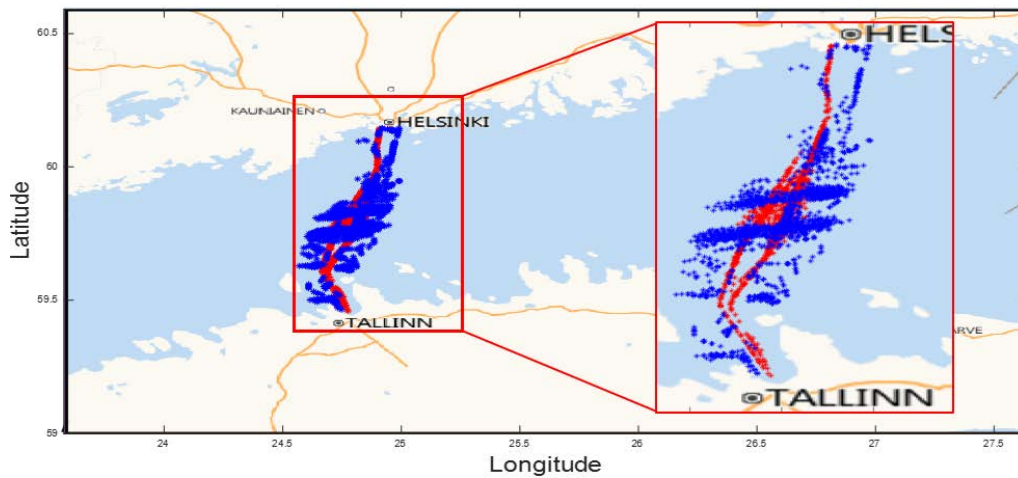


Figure 34. The locations of the mentioned encounter scenarios.

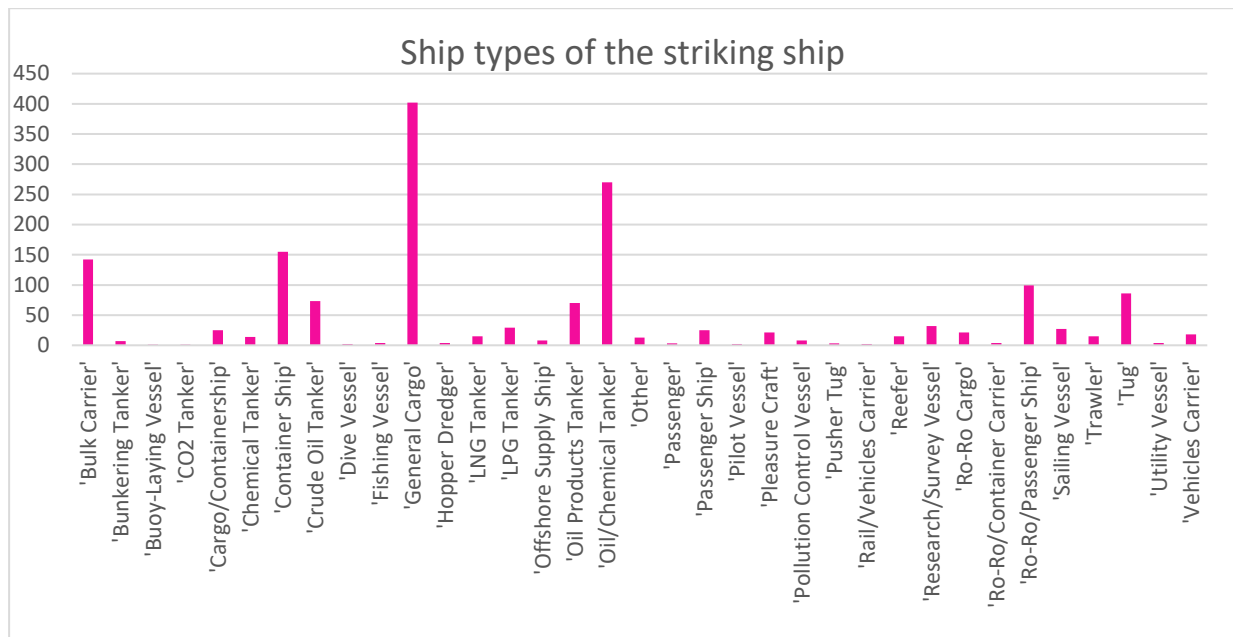


Figure 35. The number of ship types of the striking ship.



Table 7. The groups of the striking ship types

Grouping of the striking ship types						
Group 1	Group 2	Group 3	Group 4	Group 5	Group 6	
CO2 Tanker	Ro-Ro/Passenger Ship	Bulk Carrier	Container Carrier	General Cargo	Others	
Chemical Tanker	Ro-Ro Cargo	LNG Tanker	Reefer			
Crude Oil Tanker	Rail/Vehicles Carrier	LPG Tanker	Container Ship			
Oil Products Tanker	Passenger Ship		Cargo/Containership			
Chemical Tanker	Passenger		Ro-Ro/Container Carrier			
Oil/Chemical Tanker	Vehicles Carrier					

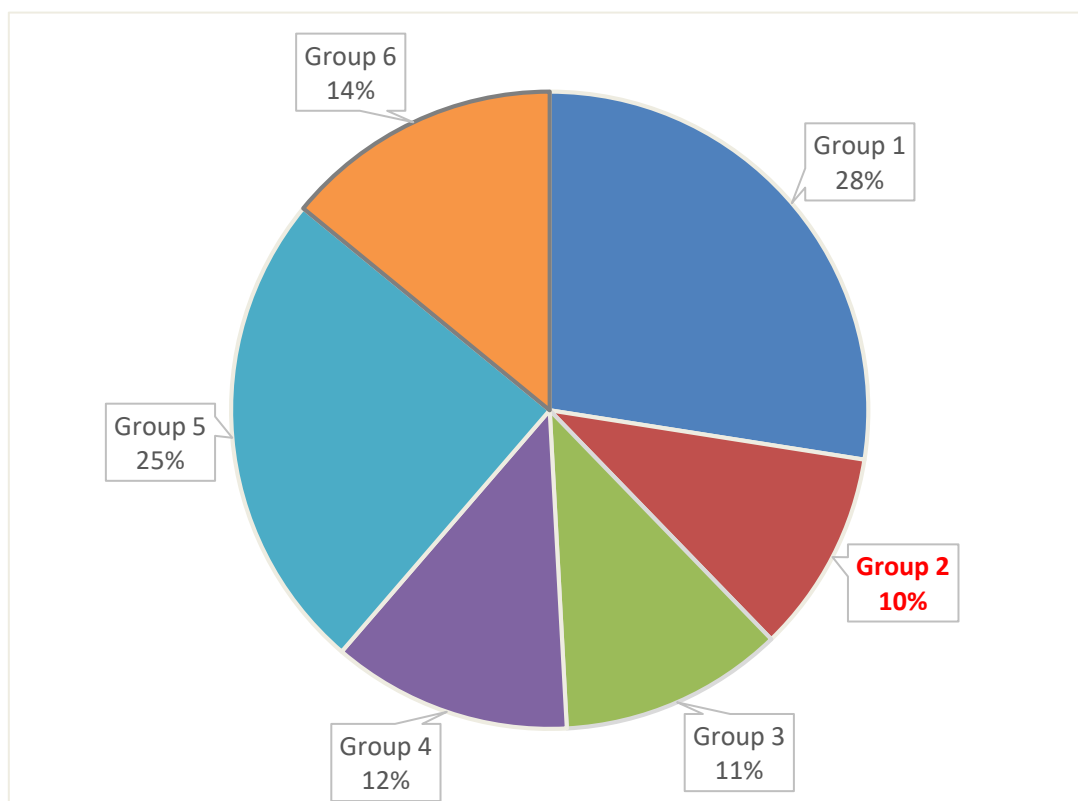


Figure 36. Types of striking ships of 6 groups.

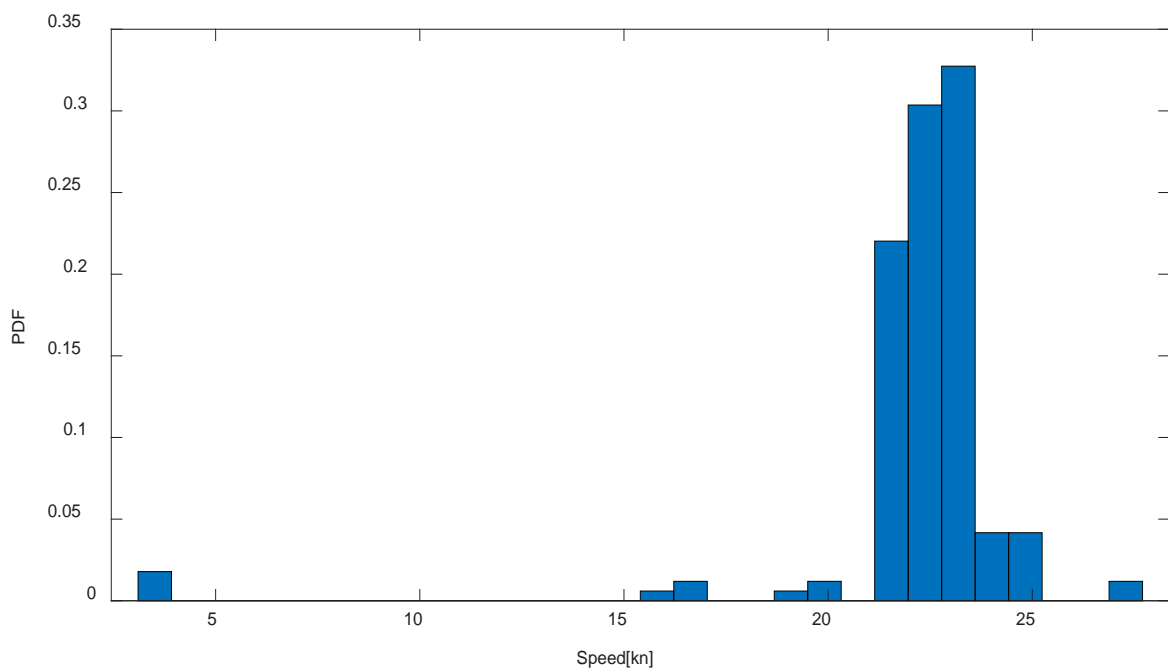


Figure 37. The speed distributions of the struck ship.

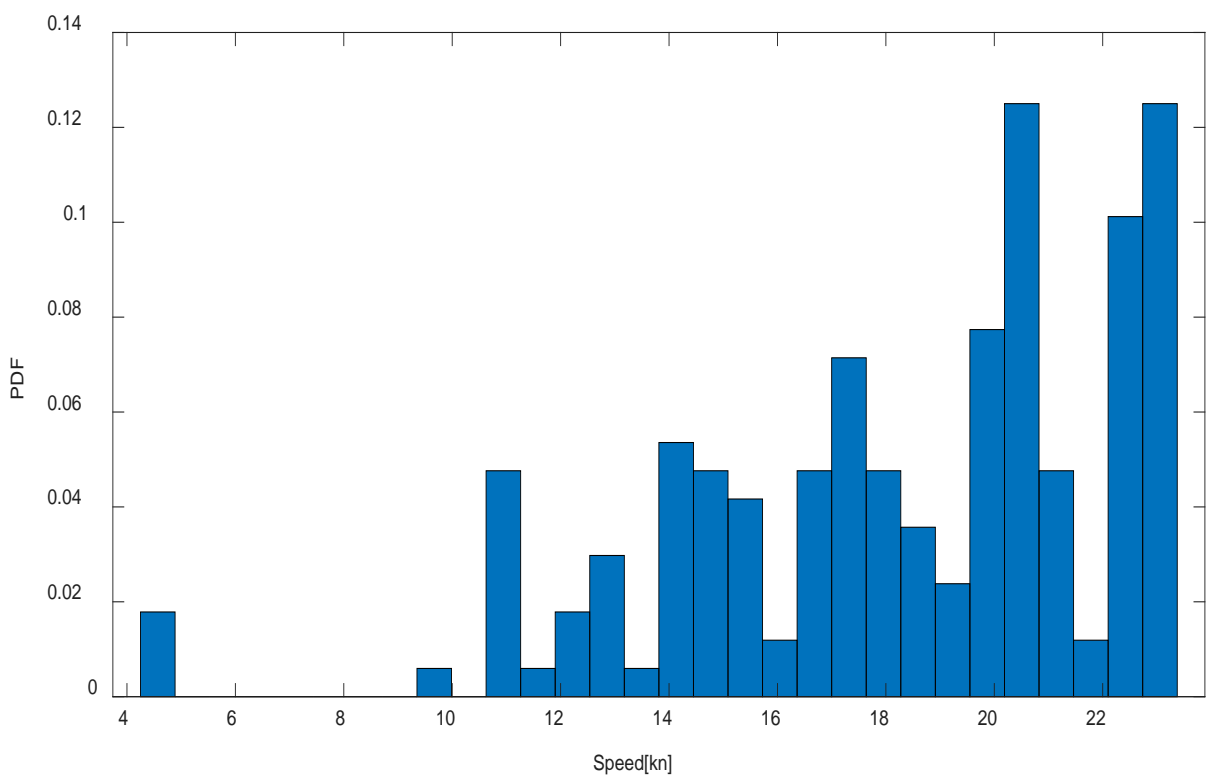


Figure 38. The speed distributions of the striking ships of group 2.

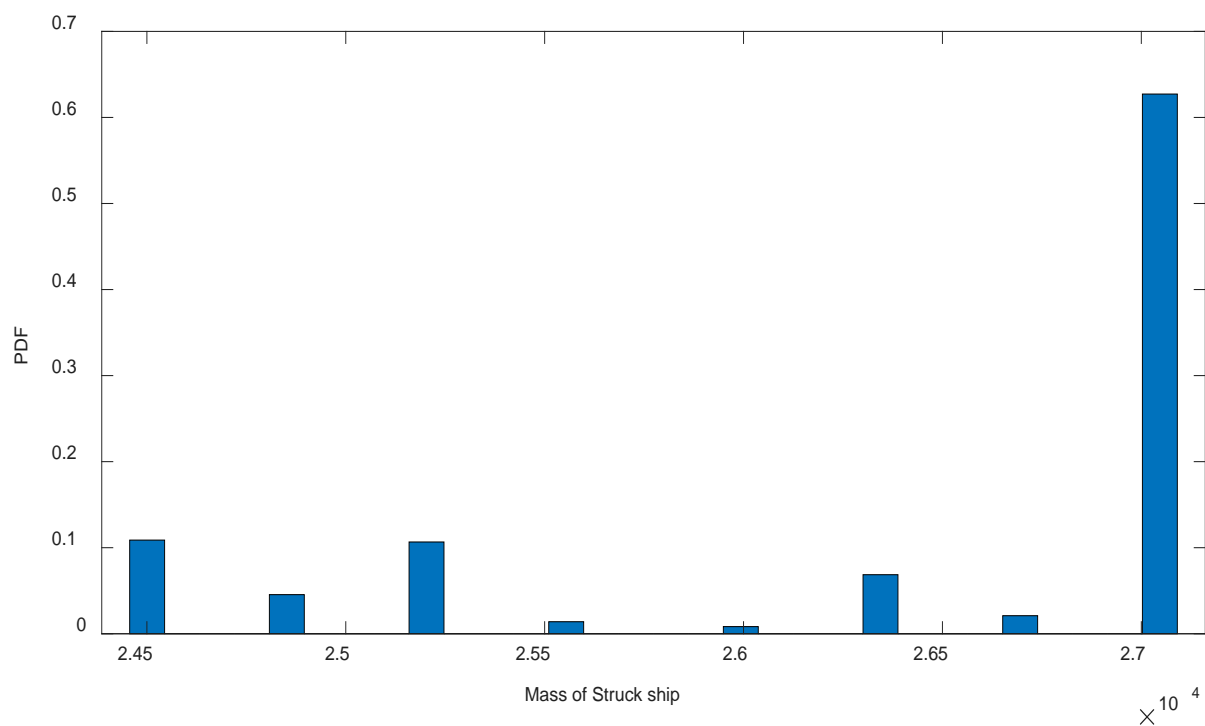


Figure 39. The mass of the struck ship for each voyage.

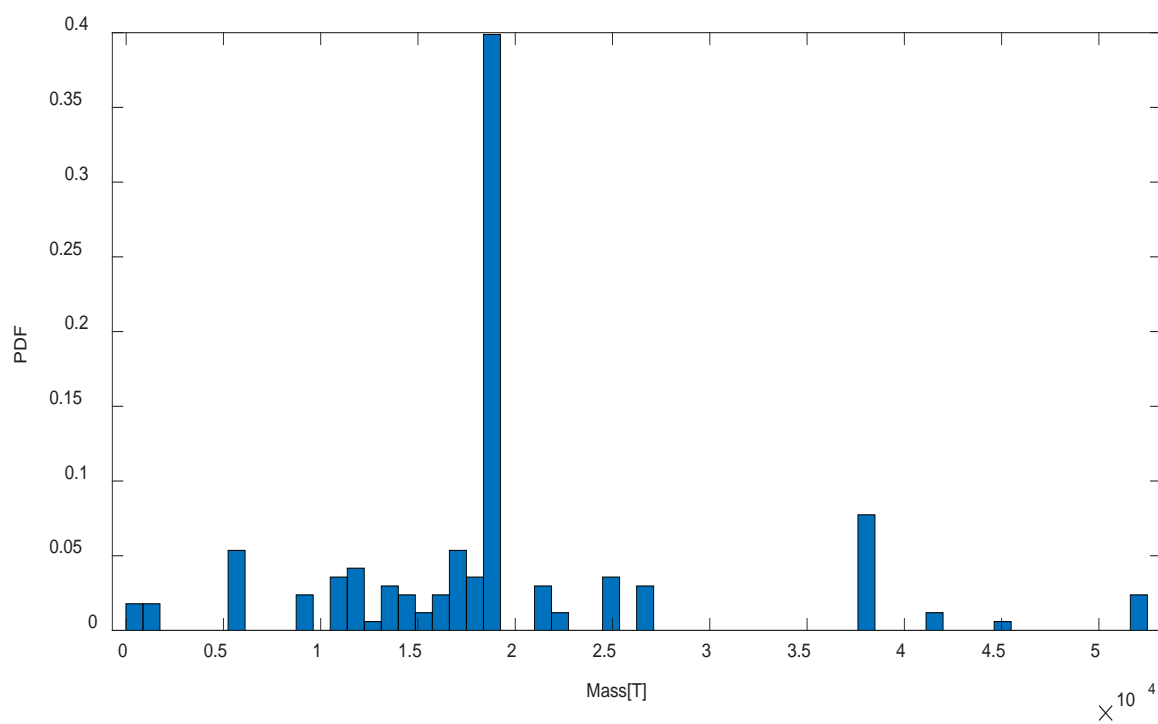


Figure 40. The mass of the striking ships of group 2.

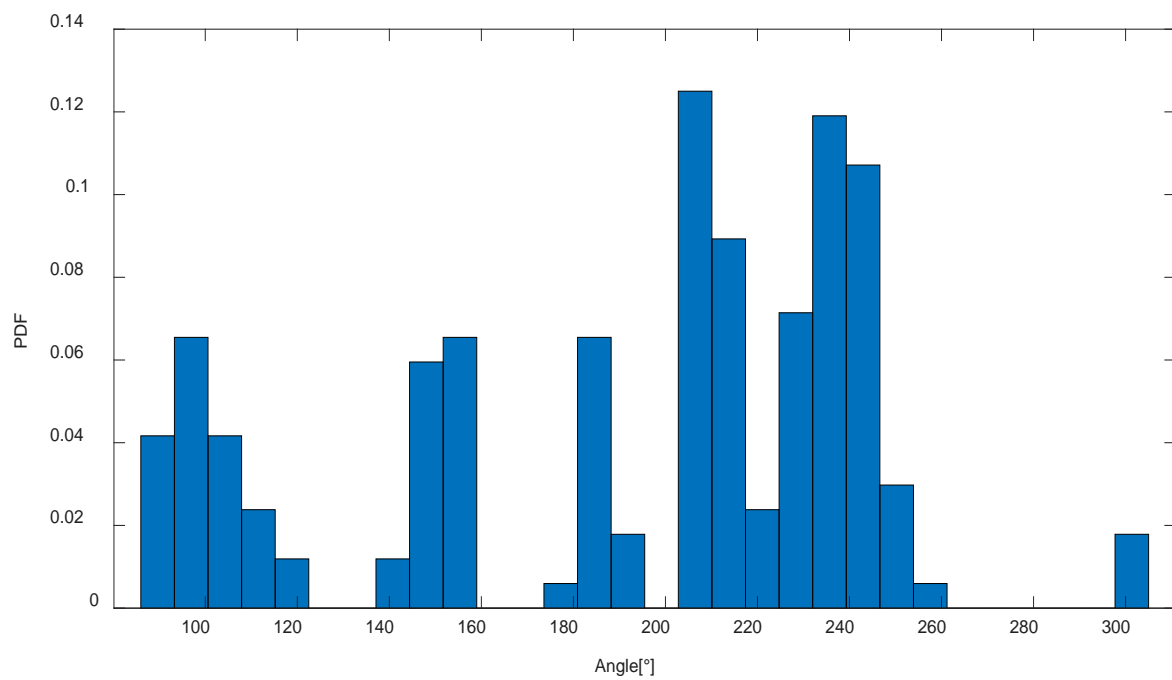


Figure 41. The distribution of collision angles.

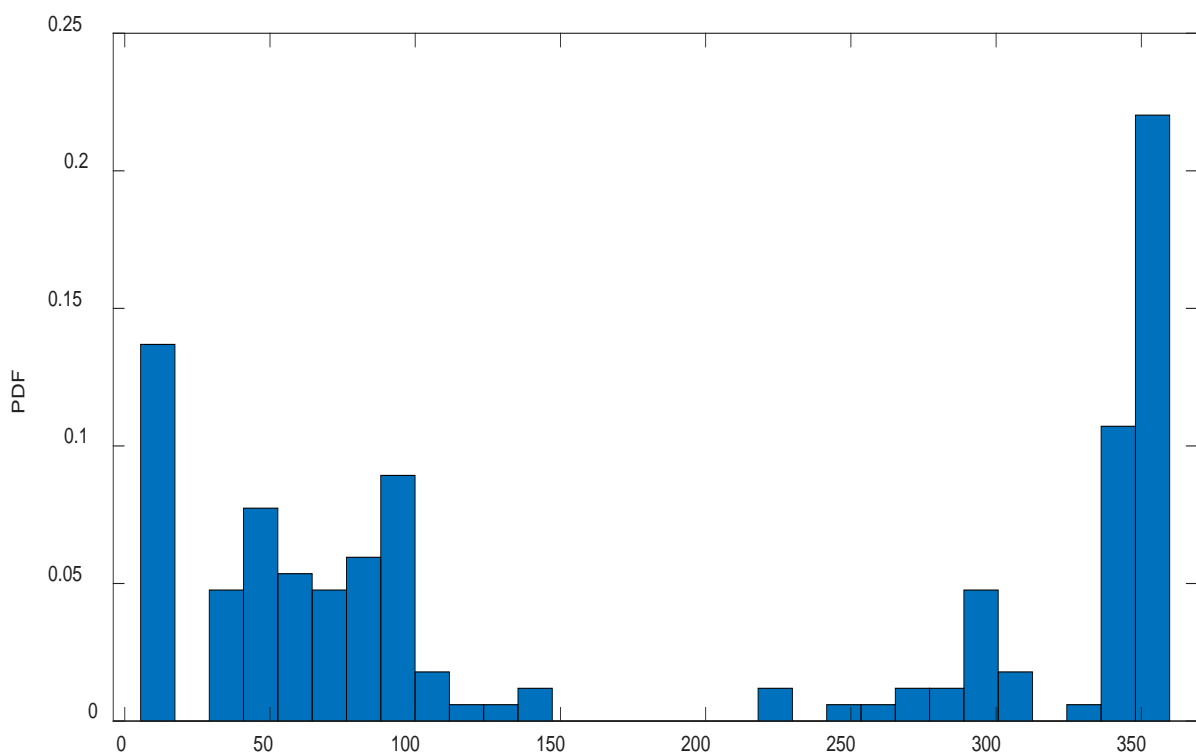


Figure 42. The distribution of relative bearing angles.

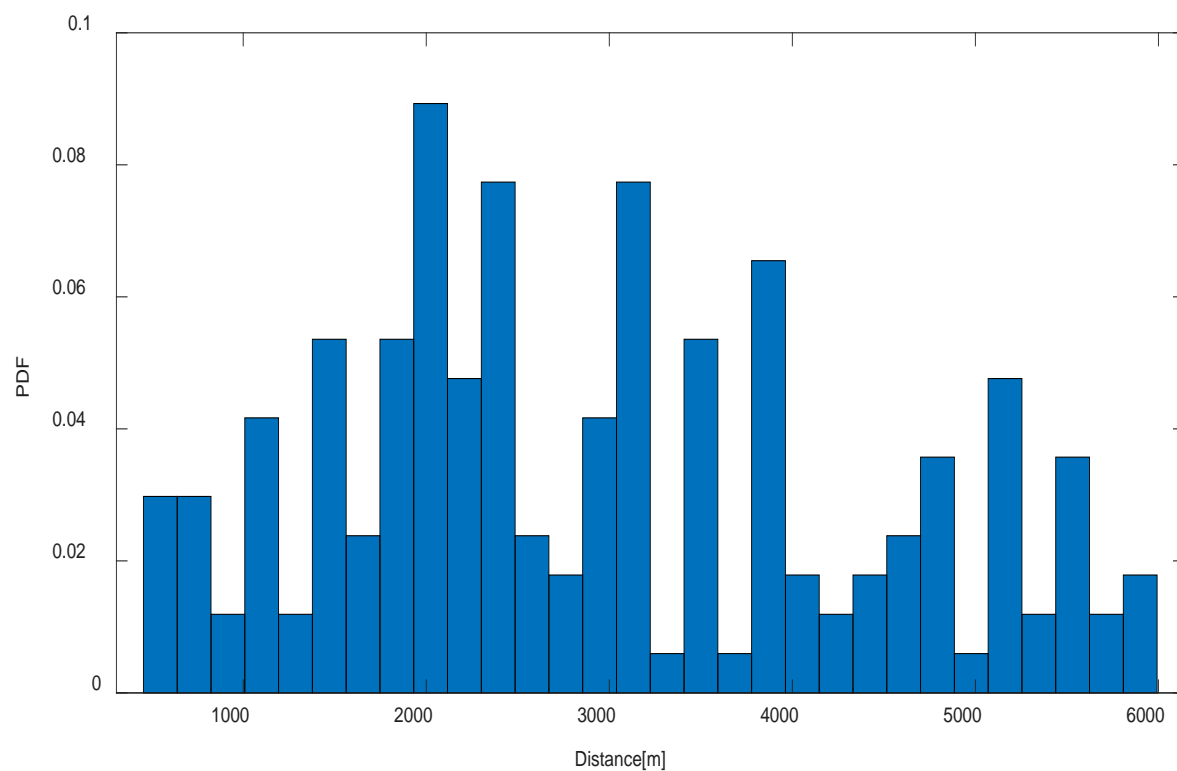


Figure 43. The distribution of the distance between two ships.

## 5.4 Demonstration of grounding encounters

Based on the procedure outlined in 4.3 an analysis of grounding scenarios is hereby presented. The bathymetry map and the ship trajectories for the selected Ro-Pax vessel (see Table 3) are shown in Figures 44, 45. GEBCO bathymetry data charts were used to identify shallow waters encounters in way of which the ship changed direction to avoid grounding. Processed data lead to the identification of two key grounding risk scenarios corresponding to power and drift grounding in open sea conditions (scenario 1) and during port operations (scenario 2) as shown in Figure 46. Based on these grounding scenarios, the probability density distributions of draft, mass, and speed were evaluated. A summary of the distributions of draft, mass, speed and distance in shallow waters corresponding to both drift and power grounding scenarios is presented in Figures 47 – 56. For the shake of completion a more detailed summary of grounding encounters is presented in Annex B.

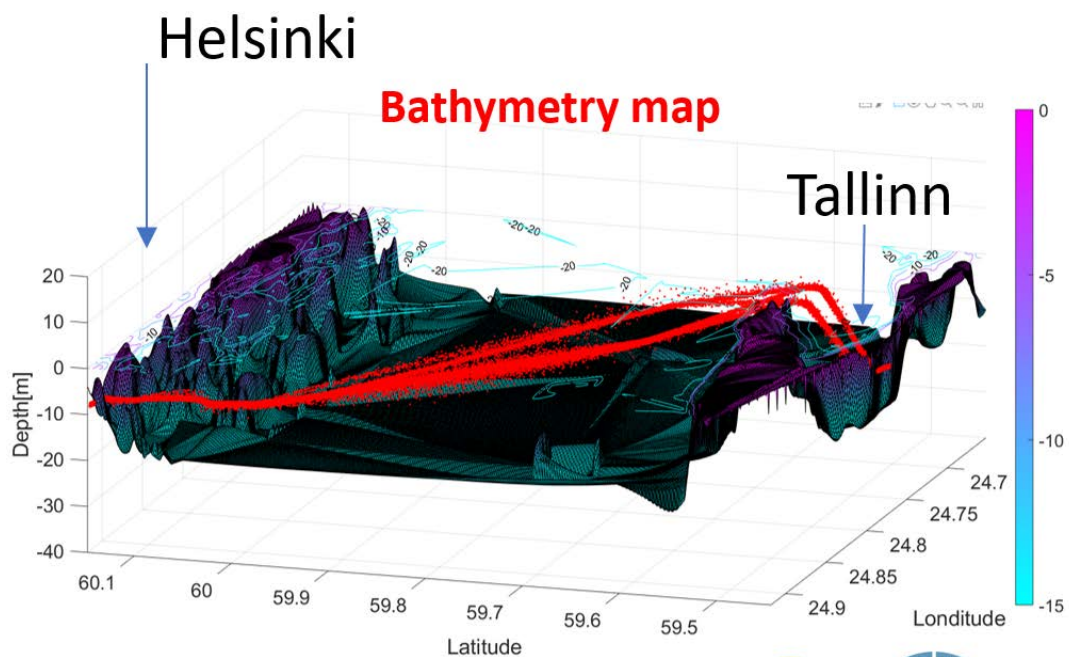


Figure 44. The bathymetry map with the recorded ship trajectories delivered from AIS data.

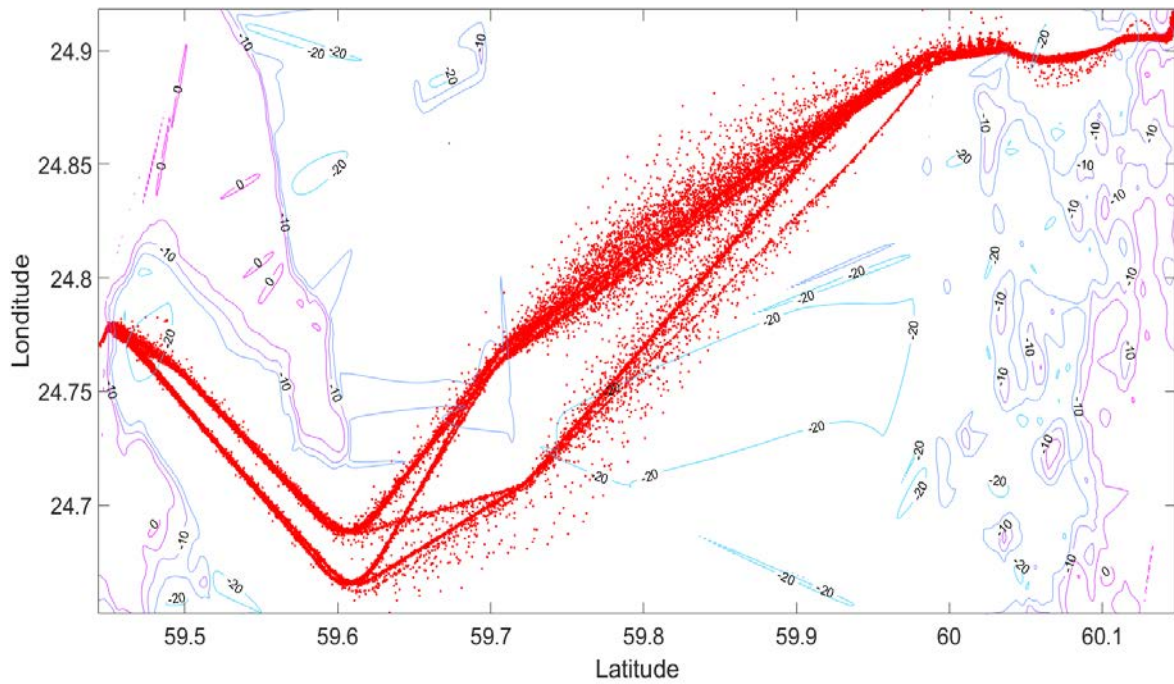
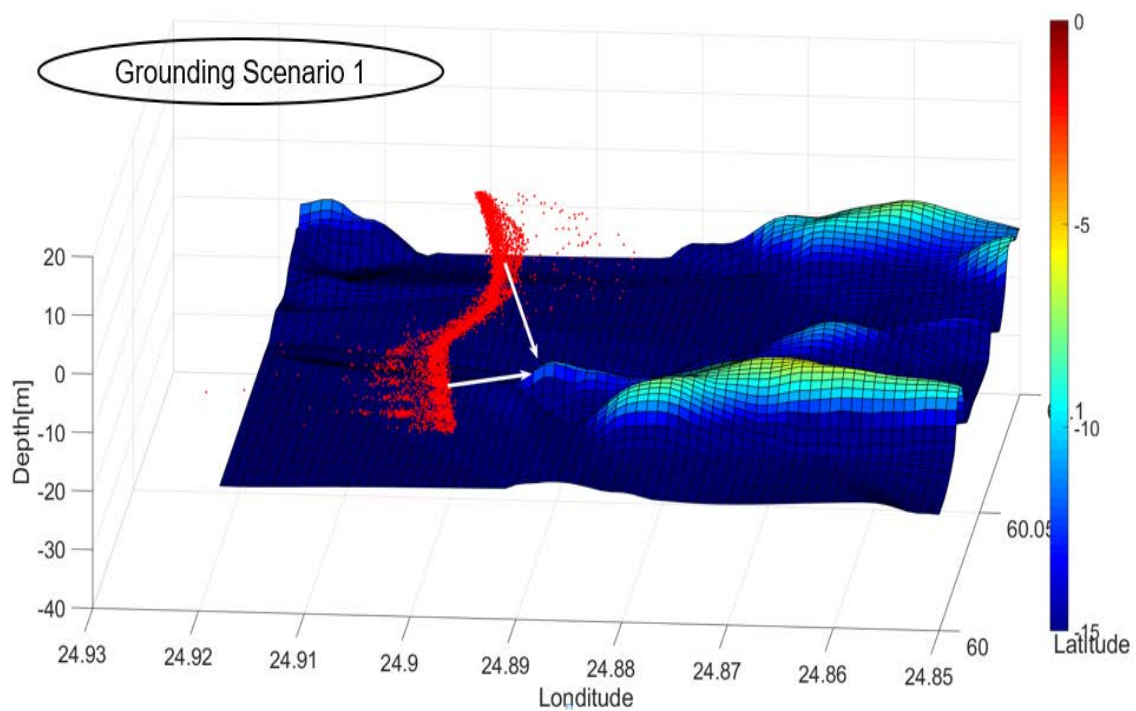
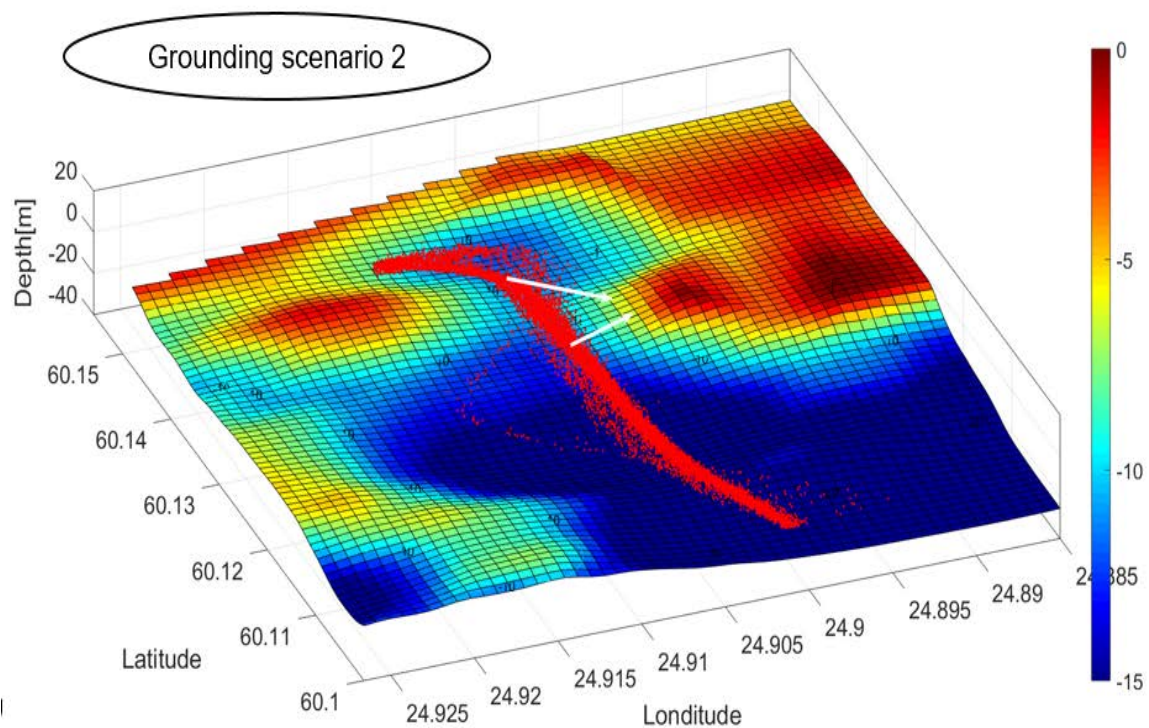


Figure 45. The relationship between isobaths and ship trajectories.



(a) Power grounding scenario



(b) Drift grounding scenario

Figure 46. The typical grounding scenarios in the Gulf of Finland.



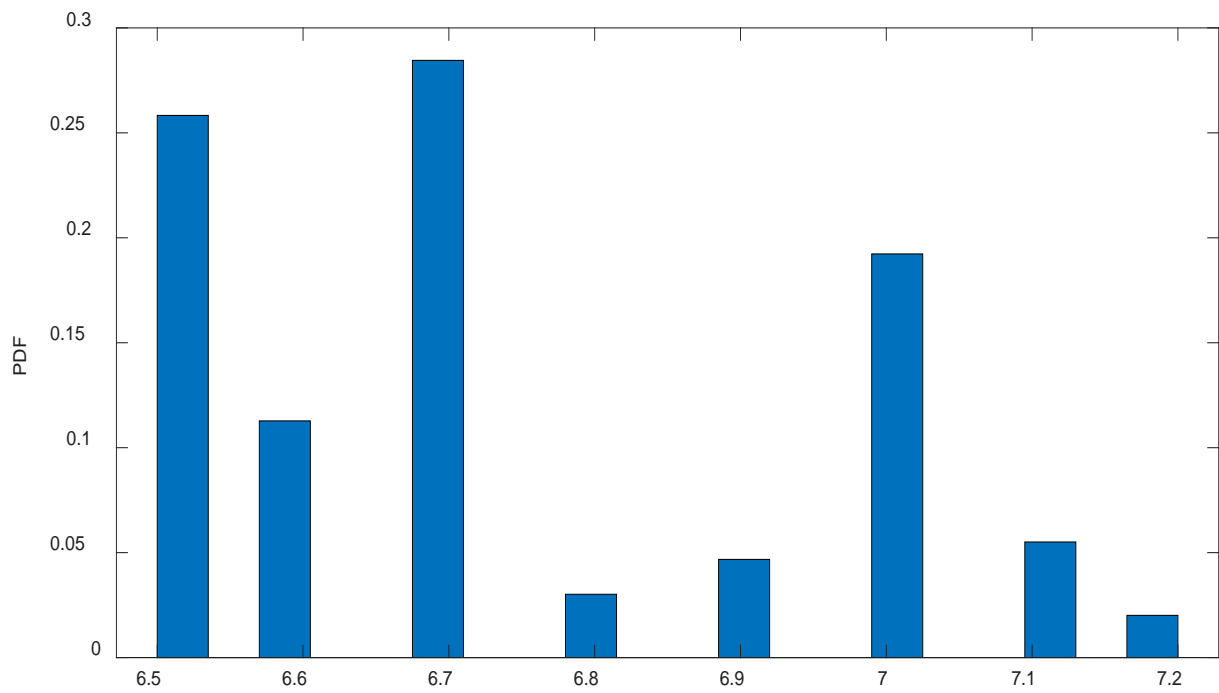


Figure 47. The distribution of the draught of the selected ship.

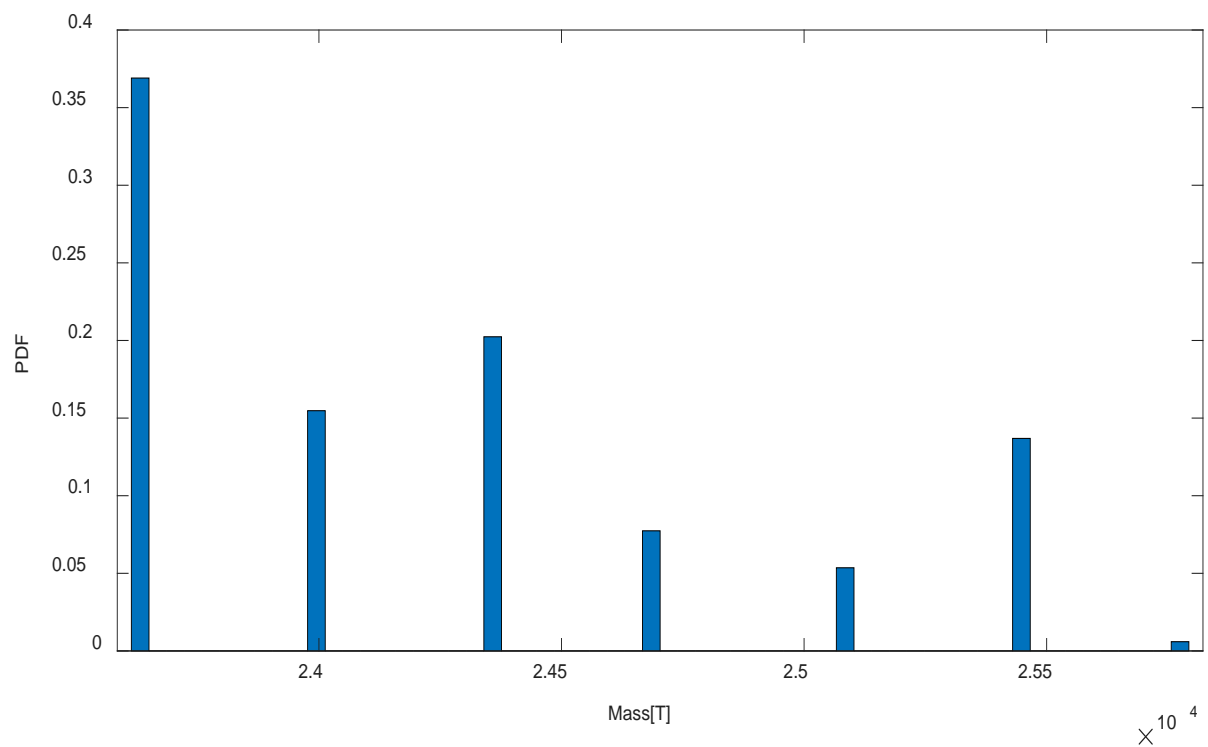


Figure 48. The distribution of the mass of the selected ship.

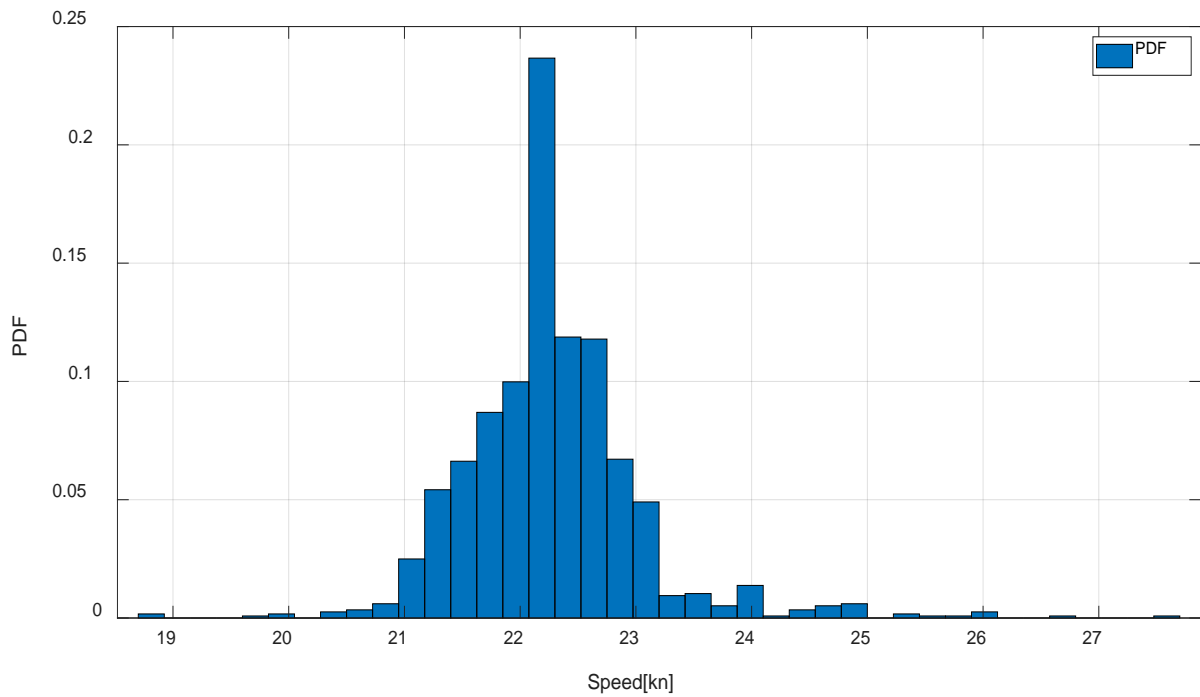


Figure 49. The speed distribution of the selected ship encountered for power grounding.

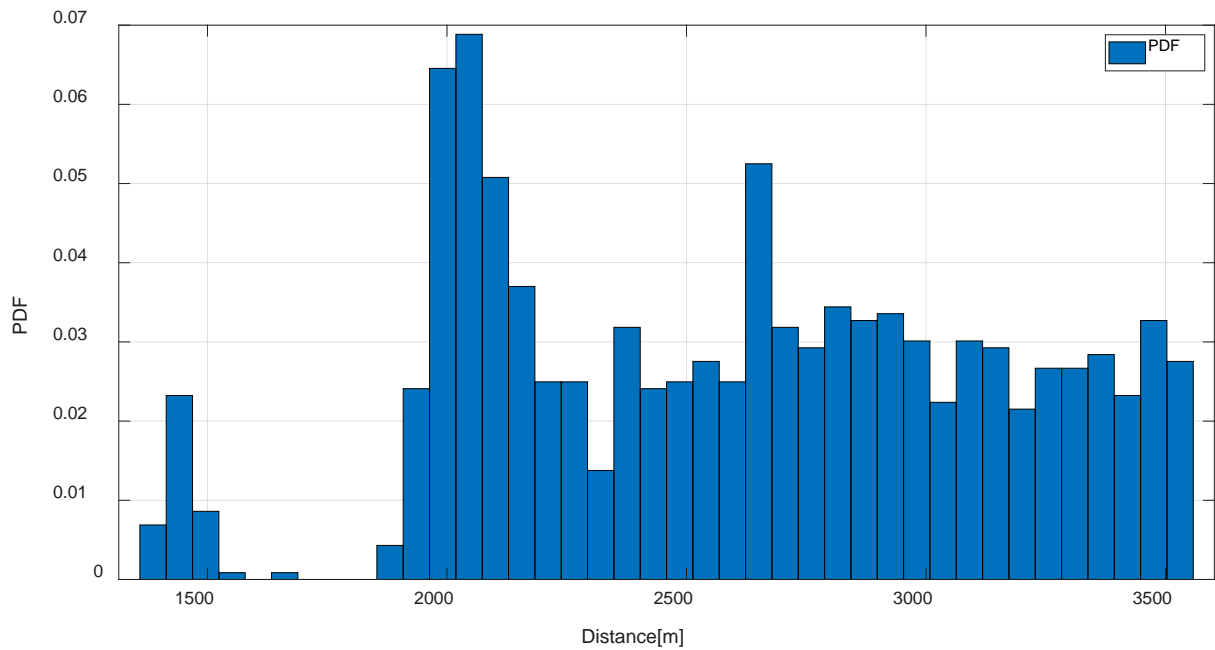


Figure 50. The distance distribution of the selected ship to the shallow water (forward to shallow waters) for power grounding.

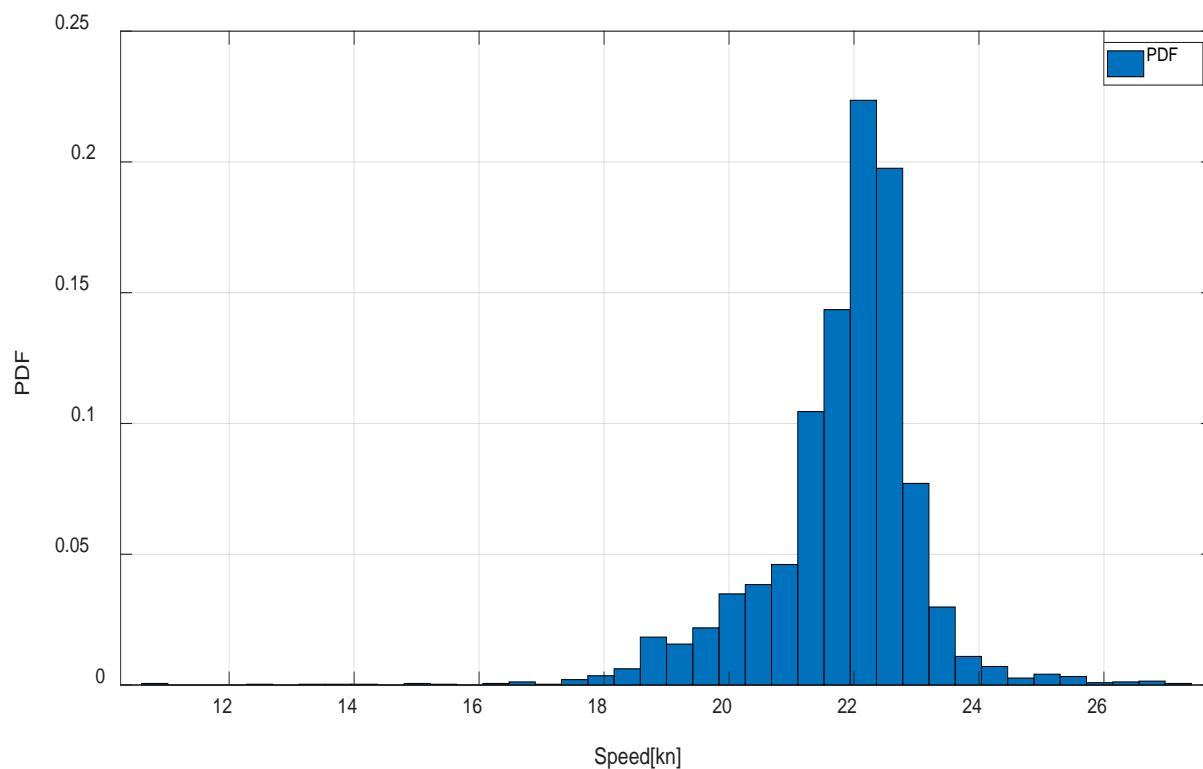


Figure 51. The speed distribution of the selected ship encountered for drift grounding.

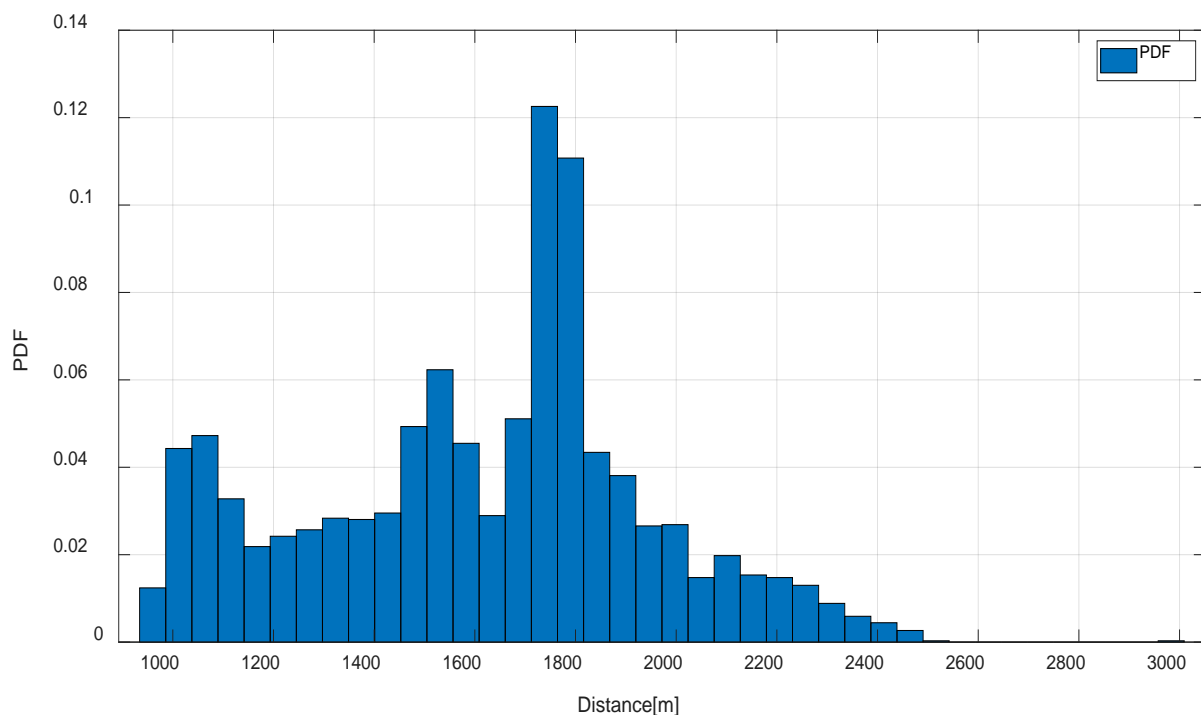


Figure 52. The distance distribution of the selected ship to the shallow water (lateral to shallow waters) for drift grounding.

## 5.5 Discussion

The methods presented in this section show that hydro-meteorological, AIS and GEBCO data may be useful in terms of mitigating risks for various ship segments globally. Notwithstanding, the results presented are of course of greater relevance to large passenger vessels (e.g. cruise ships) and Ro-Pax ships that are the subject matter of FLARE project. Some key information on patterns of hydro-meteorological data of relevance to passenger ships in the 8 key areas of operations investigated under FLARE are presented in Tables B.1 – B.5 (Annex B). Based on these data some key observations follow:

- From an overall perspective for 99% of the time passenger ships navigate in less than 6.4m significant wave heights, in swell height of less than 5.7 m, in wind speed conditions that are less than 24.8 m/s over ground and in currents that are less 1.7 m/s over-ground. However, the combination of these conditions do not reflect hydro-meteorological data encountered in one area of operation over the same time year period. They rather reflect extreme encounters in different areas of operation during different times of the year.
- The trends observed in hydro-meteorological data reflected in seasonal variations are similar to those expected by the global wave statistics. For example, ship operations in the Caribbean are subject to the highest average current speeds during autumn (1.8 m/s) and North Atlantic weather conditions represent the highest average wave heights / average wind speeds during spring (27.39 m/s); Maximum wave periods are experienced in North Pacific in Autumn (17.17 min).
- Tables B.1 – B.5 demonstrate the combinations of different hydro-meteorological conditions on the basis of which somebody could derive different combinations of parameters that may be used in designing experiments. As an example, the North Atlantic area during winter time seems to represent a convenient combination of demanding hydro-meteorological conditions<sup>9</sup>. A conclusion on the most representative combination of parameters is left to the reader.
- Most of the passenger and Ro-Pax ships are navigating in speed intervals between 12 and 20 knots. In general, the average sailing speed of passenger ships is higher than Ro-Pax ships.
- Based on available data for the three key risk areas investigated in this project all ships navigate at their highest average speed in Gibraltar straight. Very few passenger ships sail

---

<sup>9</sup> In the North Atlantic significant wave height = 6.4 m, Current speed = 0.81 m/s, Wind Speed = 20.45 m/s, Wave period = 12.84 min and swell height = 5.6 m



in the Gulf of Finland in winter. The variations of ship speed are not so markedly significant over different seasons or day/night time navigation.

- Differences in the geographical shape, weather, bathymetry and local shipping regulations may lead to differences in collision encounter scenarios. For example, in the Gulf of Finland, 72.5 % of the collision encounter scenarios are crossing and most of the striking locations are located laterally to the struck ships. On the other hand, in the English Channel, 63.1% of the collision encounter scenarios are crossing and 57.6% relate to head-on or overtaking encounters. In the same area most of the striking locations are located in way of the bow/ stern of the struck ship.
- With reference to the Ro-Pax sample ship encounters investigated in the Gulf of Finland in 2019 it was concluded that the speed of struck ship is between 22 and 26 knots in most of collision scenarios. The mass for 62% of the collision encounter scenarios varies between  $2.7 \cdot 10^4$  and  $2.8 \cdot 10^4$  tonnes. Most of collision angles vary between  $[200^\circ - 250^\circ]$  for ships under Group 1 (see Figure B.1 – Annex B);  $[90^\circ - 120^\circ]$  and  $[210^\circ - 260^\circ]$  for ships under Group 2 (see Figures 37 – 43) ;  $[220^\circ - 240^\circ]$  for ships under Group 3 (see Figure B.2 – Annex B);  $[210^\circ - 250^\circ]$  for ships under Group 4 (see Figure B.3 – Annex B);  $[220^\circ - 260^\circ]$  for ships under Group 5 (see Figure B.4 – Annex B);  $[100^\circ - 180^\circ]$  and  $[200^\circ - 260^\circ]$  for ships under Group 6 (see Figure B.5 – Annex B).
- Similarly to above for the Ro-Pax sample ship encounters investigated in the Gulf of Finland in 2019 it was concluded that striking ships could navigate in the speed interval between 8 and 14 knots in Group 1 (see Figure B.1 – Annex B); the speed interval 14 and 23 knots in Group 2 (see Figures 37 – 43); the speed interval 4 and 11 knots in Group 3 (see Figure B.2 – Annex B); the speed interval 10 and 18 knots in Group 4 (see Figure B.3 – Annex B); the speed interval 9 and 13 knots in Group 5 (see Figure B.4 – Annex B); the speed interval 4 and 12 knots in Group 6 (see Figure B.5 – Annex B).
- For the striking ship, most of the mass of the ships is more than  $1.0 \cdot 10^4$  and below  $4 \cdot 10^4$  tonnes in Group 1 (see Figure B.1 – Annex B); in the interval  $1.0 \cdot 10^4$  and  $2.5 \cdot 10^4$  tonnes in Group 2 (see Figures 37 – 43); in the interval  $1.5 \cdot 10^4$  and  $3.5 \cdot 10^4$  tonnes in Group 3 (see Figure B.2 – Annex B); in the interval  $1.5 \cdot 10^4$  and  $3.5 \cdot 10^4$  tonnes in Group 4 (see Figure B.3 – Annex B); below  $0.5 \cdot 10^4$  tonnes in Group 5 (see Figure B.4 – Annex B); below 1500 tonnes in Group 6 (see Figure B.5 – Annex B).
- Differences in the geographical shape, weather, bathymetry and local shipping regulations may lead to differences in speed distributions of grounding scenarios. Two scenarios were considered namely grounding in open seas (scenario 1) or grounding in port operations

(scenario 2). It may be concluded that the speed of the sample ships is between 21 and 23 knots encountered for power grounding in open seas (Figures 49); between 19 and 23 knots encountered for drift grounding in open seas (Figure 51); between 13 and 15 knots encountered for power grounding in port area (Figure B.9); between 15 and 17 knots encountered for drift grounding in port area (Figure B.11).

- During grounding the distance of ship to shallow waters depends on ship speed and area of operation with open seas grounding being prone to longer distances than port grounding (see Figures 50, 52 and Figures B.10, B.12). For example, the distance may vary between 2 and 3.5 Km for power grounding and 1 – 2 km for drift grounding in open seas while the corresponding numbers are 350– 550 m and 150 - 300m for power and drift grounding in port respectively.

## 6. CONCLUSIONS

This study presented big data analytics methods and results on the influence of key hydro-meteorological conditions on accidental (collision or grounding) encounters of particular relevance to large passenger ships and Ro-Pax vessels. Available AIS data, for cruise and Ro-Pax operations have been collected to develop procedures able to use big data analytics for the analysis of marine traffic risks also considering the influence of bathymetry and environmental conditions (global weather data). The results show that the area of operation is interlinked with geography (e.g. bathymetry conditions), hydro-meteorological conditions and traffic patterns that together or separately may have a significant impact on the probability to encounter serious flooding following collision or grounding encounters. The principles, methods and data presented may be used by WP3.1 and WP4 of project FLARE.

## 7. REFERENCES

- Aase, J. G., & Jabour, J. (2015). Can monitoring maritime activities in the European High Arctic by satellite-based Automatic Identification System enhance polar search and rescue? *The Polar Journal*, 5 (2), 386–402.
- Arguedas, V. F., Pallotta, G., & Vespe, M. (2018). Maritime traffic networks: From historical positioning data to unsupervised maritime traffic monitoring. *IEEE Transactions on Intelligent Transportation Systems*, 19(3), 722–732.
- Bidlot J.-R. (2017), Intercomparison of operational wave forecasting systems against buoys: data from ECMWF, MetOffice, FNMOC, MSC, NCEP, MeteoFrance, DWD, BoM, SHOM, JMA, KMA, Puerto del Estado, DMI, CNR-AM, METNO, SHN-SM January 2016 to



- December 2016, European Centre for Medium-range Weather Forecasts (ECMWF), [https://www.jcomm.info/index.php?option=com\\_oe&task=viewDocumentRecord&docID=18333](https://www.jcomm.info/index.php?option=com_oe&task=viewDocumentRecord&docID=18333)
- Campana, I., Angeletti, D., Crosti, R., Luperini, C., Ruvolo, A., Alessandrini, A., & Arcangeli, A. (2017). Seasonal characterisation of maritime traffic and the relationship with cetacean presence in the Western Mediterranean Sea. *Marine Pollution Bulletin*, 115(1-2), 282–291.
- Goerlandt F, Kujala P. On the reliability and validity of ship–ship collision risk analysis in light of different perspectives on risk. *Safety Science*. 2014;62:348-65.
- Goerlandt F, Montewka J, Zhang W, Kujala P. An analysis of ship escort and convoy operations in ice conditions. *Safety Science*. 2017;95:198-209.
- Hansen, M. G., Jensen, T. K., Lehn-Schiøler, T., Melchior, K., Rasmussen, F. M., & Ennemark, F. (2013). Empirical ship domain based on AIS data. *Journal of Navigation*, 66(6), 931–940.
- Haranen, M.; Myöhänen, S.; Cristea, D.S. 2017 – The Role of Accurate Now-Cast Data in Ship Efficiency Analysis, 2nd Hull Performance & Insight Conference (HullPIC), Ulrichshusen, pp.25-38, [http://data.hullpic.info/hullpic2017\\_ulrichshusen.pdf](http://data.hullpic.info/hullpic2017_ulrichshusen.pdf)
- Huang, Y., Chen, L., & van Gelder, P. H. A. J. M. (2019). Generalized velocity obstacle algorithm for preventing ship collisions at sea. *Ocean Engineering*, 173, 142-156.
- Hulkkonen, T., Manderbacka, T., Sugimoto, K., 2019 – Digital Twin for Monitoring Remaining Fatigue Life of Critical Hull Structures, 18th Conference on Computer Applications and Information Technology in the Maritime Industries (COMPIT2019), 25-27 March 2019, Tullamore, Ireland. [http://data.hiper-conf.info/compit2019\\_tullamore.pdf](http://data.hiper-conf.info/compit2019_tullamore.pdf) ISBN 978-3-89220-709-2
- IALA. (2004). IALA guideline no. 1028 on the Automatic Identification System (AIS) volume 1, part I operational issues edition 1.3. Retrieved from <https://www.e-navigation.nl/sites/default/files/universal-automatic-identification-system-ais-volume-1-part-2-technical-issues-1029.pdf>
- IALA. (2016). IALA guideline no. 1082 on an overview of AIS. Retrieved from
- IMO – AIS transponders. <http://www.imo.org/en/ourwork/safety/navigation/pages/ais.aspx> accessed on 24 Oct 2019.
- IMO, (2014). SOLAS Consolidated edition. ISBN 978-92-801-1549
- IMO, Safety of Navigation SN/Circ.277 (2003). Guidelines for the installation of a shipborne automatic identification system (AIS). <http://www.imo.org/en/OurWork/Safety/Navigation/Documents/227.pdf>
- Johansen TA, Perez T, Cristofaro A. Ship Collision Avoidance and COLREGS Compliance Using Simulation-Based Control Behavior Selection With Predictive Hazard Assessment. *IEEE Transactions on Intelligent Transportation Systems*. 2016;17(12):3407-22.



- Kang L, Meng Q, Zhou C, Gao S. How do ships pass through L-shaped turnings in the Singapore strait? *Ocean Engineering*. 2019;182:329-42.
- Kim, D., Hirayama, K., & Okimoto, T. (2017). Distributed stochastic search algorithm for multi-ship encounter situations. *Journal of Navigation*, 70(4), 699–718.
- Kite-Powell, H. L., Jin, D., Jebesen, J., Papakonstantinou, V., & Patrikalakis, N. (1999). Investigation of potential risk factors for groundings of commercial vessels in US ports. *International Journal of Offshore and Polar Engineering*, 9(01).
- Kivekäs, N., Massling, A., Grythe, H., Lange, R., Rusnak, V., Carreno, S.,...Kristensson, A. (2014). Contribution of ship traffic to aerosol particle concentrations downwind of a major shipping lane. *Atmospheric Chemistry and Physics*, 14(16), 8255–8267.
- Kujala P, Hänninen M, Arola T, Ylitalo JJRE, Safety S. Analysis of the marine traffic safety in the Gulf of Finland. 2009;94(8):1349-57.
- Li, L., Lu, W., Niu, J., Liu, J., & Liu, D. (2018). AIS data-based decision model for navigation risk in sea areas. *The Journal of Navigation*, 71(3), 664–678.
- Liu K, Xin X, Ma J, Zhang J, Yu Q. Sensitivity analysis of ship traffic in restricted two-way waterways considering the impact of LNG carriers. *Ocean Engineering*. 2019;192.
- Longépé, N., Mouche, A. A., Goacolou, M., Granier, N., Carrere, L., Lebras, J. Y.,...Besnard, S. (2015). Polluter identification with spaceborne radar imagery, AIS and forward drift modeling. *Marine Pollution Bulletin*, 101(2), 826–833.
- Manderbacka, T. 2019 – On the uncertainties of the weather routing and support system against dangerous conditions. *Proceedings of the 17th International Ship Stability Workshop (ISSW2019)*, 10-12 June 2019, Helsinki, Finland.
- Mazaheri, A., J. Montewka & P. Kujala (2014) Modeling the risk of ship grounding—a literature review from a risk management perspective. *WMU Journal of Maritime Affairs*, 13, 269-297.
- Mazaheri, A., Montewka, J., Kotilainen, P., et al., 2015. Assessing Grounding Frequency using Ship Traffic and Waterway Complexity. *Journal of Navigation*, 68(1): 89-106.
- Montewka J, Ehlers S, Goerlandt F, Hinz T, Tabri K, Kujala P. A framework for risk assessment for maritime transportation systems—A case study for open sea collisions involving RoPax vessels. *Reliab Eng Syst Safe*. 2014;124:142-57.
- Montewka J, Krata P, Goerlandt F, Mazaheri A, Kujala P. Marine traffic risk modelling - an innovative approach and a case study. *Proceedings of the Institution of Mechanical Engineers Part O-Journal of Risk and Reliability*. 2011;225(O3):307-22.
- Montewka, J., Hinz, T., Kujala, P., et al., 2010. Probability modelling of vessel collisions. *Reliability Engineering & System Safety*, 95(5): 573-589.





- Mou JM, van der Tak C, Ligteringen H. Study on collision avoidance in busy waterways by using AIS data. *Ocean Engineering*. 2010;37(5-6):483-90.
- Otto, S., Pedersen, P. T., Samuelides, M., & Sames, P. C. (2002). Elements of risk analysis for collision and grounding of a RoRo passenger ferry. *Marine Structures*, 15(4-5), 461-474.
- Pallotta, G., Horn, S., Braca, P., & Bryan, K. (2014). Context-enhanced vessel prediction based on Ornstein-Uhlenbeck processes using historical AIS traffic patterns: Real-world experimental results. In *Information Fusion (Fusion)*, 2015 18th International Conference on (pp. 1152–1159). IEEE.
- Qu X, Meng Q, Suyi L. Ship collision risk assessment for the Singapore Strait. *Accid Anal Prev*. 2011;43(6):2030-6.
- Qu, X., Meng, Q., and Suyi, L. (2011). Ship collision risk assessment for the Singapore Strait. *Accident Analysis & Prevention*, 43(6), 2030-2036.
- Sidibé, A., & Shu, G. (2017). Study of automatic anomalous behaviour detection techniques for maritime vessels. *Journal of Navigation*, 70(4), 847–858.
- Sormunen, O. V. E., Castrén, A., Romanoff, J., & Kujala, P. (2016). Estimating sea bottom shapes for grounding damage calculations. *Marine Structures*, 45, 86-109.
- Sormunen, O. V., Hänninen, M., Häkkinen, J., & Posti, A. (2015). Tanker grounding frequency and spills in the Finnish Gulf of Finland. *Zeszyty Naukowe Akademii Morskiej w Szczecinie*.
- Szlapczynski, R., Krata, P., & Szlapczynska, J. (2018). Ship domain applied to determining distances for collision avoidance manoeuvres in give-way situations. *Ocean Engineering*, 165, 43-54.
- Tu, E., Zhang, G., Rachmawati, L., Rajabally, E., & Huang, G. B. (2018). Exploiting AIS data for intelligent maritime navigation: A comprehensive survey from data to methodology. *IEEE Transactions on Intelligent Transportation Systems*, 19, 1559–1582.
- Wang, J., Zhu, C., Zhou, Y., & Zhang, W. (2017). Vessel spatio-temporal knowledge discovery with AIS trajectories using co-clustering. *Journal of Navigation*, 70(6), 1383–1400.
- Watson, R. T., Holm, H., & Lind, M. (2015). Green steaming: A methodology for estimating carbon emissions avoided. *Thirty Sixth International Conference on Information Systems*, Fort Worth, the U.S.A.
- Weng JX, Meng Q, Qu XB. Vessel Collision Frequency Estimation in the Singapore Strait. *Journal of Navigation*. 2012;65(2):207-21.
- Winther, M., Christensen, J. H., Plejdrup, M. S., Ravn, E. S., Eriksson, Ó. F., & Kristensen, H. O. (2014). Emission inventories for ships in the Arctic based on satellite sampled AIS data. *Atmospheric Environment*, 91, 1–14.

- Yang D, Wu L, Wang S, Jia H, Li KX. How big data enriches maritime research – a critical review of Automatic Identification System (AIS) data applications. *Transport Reviews*. 2019;1-19.
- Zhang WB, Goerlandt F, Kujala P, Wang YH. An advanced method for detecting possible near miss ship collisions from AIS data. *Ocean Engineering*. 2016;124:141-56.
- Zhang WB, Goerlandt F, Montewka J, Kujala P. A method for detecting possible near miss ship collisions from AIS data. *Ocean Engineering*. 2015;107:60-9.
- Zhao, J., Xie, P., Zhang, M., Sang, Y. F., Chen, J., & Wu, Z. (2018). Nonstationary statistical approach for designing LNWLs in inland waterways: a case study in the downstream of the Lancang River. *Stochastic environmental research and risk assessment*, 32(11), 3273-3286.
- Zhou Y, Daamen W, Vellinga T, Hoogendoorn SP. Ship classification based on ship behavior clustering from AIS data. *Ocean Engineering*. 2019;175:176-87.

## ANNEX A

### Guidelines on AIS pre-processing method

Big data analytics resulting from AIS records used the following pre-processing methods :

Search algorithm for wrong AIS data timestamps

In practice AIS data are transmitted by a Type A transceiver every 10 seconds or at least every 30 seconds by a Type B transceiver. The environment and the state of the ship influence data transmission. The time stamp for a particular ship  $i$  should be estimated by:

$$t_{(j,j+1)}^i = T_{(j+1)}^i - T_j^i \quad (\text{A.1})$$

where  $T_j^i$  stands for the timestamp of ship  $i$  at instant  $j$ , and  $T_{(j+1)}^i$  stands for the time stamp for ship  $i$  at an instant  $(j+1)$ . Note that the timestamp is in UTC (Universal Time Coordinated), using units in terms of seconds. According to the function of the AIS transceiver, reasonable and reliable information should satisfy the following :

$$2 \text{ s} \leq t_{(j,j+1)}^i \leq 30 \text{ s} \quad (\text{A.2})$$

When  $t_{(j,j+1)}^i$  is less than two seconds, the timestamp  $T_{(j+1)}^i$  or  $T_j^i$  should be deleted, according to the  $t_{(j+1,j+2)}^i (T_{j+2}^i - T_{j+1}^i)$  and  $t_{(j-1,j+1)}^i (T_{j+1}^i - T_{j-1}^i)$ ; When  $t_{(j,j+1)}^i$  is greater than 30 seconds, the timestamp should be inserted between  $T_{(j+1)}^i$  and  $T_j^i$ , based on a cubic spline interpolation method.

Identification of irrational speed data from the AIS database

Ship speed data is key in terms of elaborating traffic patterns. Based on ship navigational standards and rules, the average speed of a ship can be calculated as the distance between the position (longitude  $x_j$  and latitude  $y_j$ ) at a time stamp  $T_j$ . The position (longitude  $x_{(j+2)}$  and latitude  $y_{(j+2)}$ ) at a time stamp  $T_{(j+2)}$  and the sailing time of a ship is defined as  $i$ . As such, speed data can be checked by the formulae :

$$\left\{ \begin{array}{l} C = \sin(x_{j,T_j}) \times \sin(x_{(j+2),T_{(j+2)}}) + \cos(y_{j,T_j}) \times \cos(y_{(j+2),T_{(j+2)}}) \times \cos D\lambda \\ D = \frac{R \times \arccos(C) \times \frac{\pi}{180}}{1852} \\ \bar{V}_{i,t_{(j,j+2)}} = 3600 \times \frac{D}{T_{(j+2)} - T_j} \end{array} \right. \quad (A.3)$$

where  $\bar{V}_{i,t_{(j,j+2)}}$  is the average speed of ship  $i$  at time interval  $[T_j, T_{(j+2)}]$ ;  $R$  is the radius of the earth. In addition, the longitude  $x_j$  and latitude  $y_j$  at the timestamp  $T_j$  and the longitude  $x_{(j+2)}$  and latitude  $y_{(j+2)}$  at time stamp  $T_{(j+2)}$  denote the position of ship  $i$ ;  $D\lambda$  denotes the difference between the position (longitude  $x_j$  and latitude  $y_j$ ) at time  $T_j$  and the position (longitude  $x_{(j+2)}$  and latitude  $y_{(j+2)}$ ) in longitude. Note that the position of a ship in Gulf of Finland is located in both the northern hemisphere and the eastern hemisphere. Hence, the longitude and latitude are positive values in Formula A.3. Also, the longitude and latitude coordinates are in the WGS-84 coordinate system, with units of degree.

Based on the statistics reviewed for the purposes of this project for only one ship sailing in the Gulf of Finland, the speed has been less than three knots. This would indicate normal birthing conditions in port. On the other hand speed of more than 30 knots have been impossible to track. Therefore, the AIS speed data should satisfy :

$$\left\{ \begin{array}{l} 3 \leq |SOG_{i,T_j}| \leq 30 \\ \left| \bar{V}_{i,t_{(j,j+1)}} - |SOG_{i,T_{(j+1)}}| \right| \leq 5 \\ \left| \bar{V}_{i,t_{(j,j+1)}} - |SOG_{i,T_{(j)}}| \right| \leq 5 \end{array} \right. \quad (A.4)$$

where  $SOG_{i,T_{(j)}}$  is the speed over ground (SOG) of ship  $i$  at the time  $T_j$ , using units of knots and seconds, and  $\bar{V}_{i,t_{(j,j+1)}}$  is the average speed of ship  $i$  at time interval  $[T_j, T_{(j+1)}]$ . In conclusion, to update incorrect speed data the following algorithm may be used :

$$SOG_{i,T_{(j)}} = \begin{cases} Delete & \text{If the speed is less than 3 knots} \\ \bar{V}_{i,t_{(j,j+1)}} & \text{If the speed is out of range} \\ |SOG_{i,T_{(j)}}| & \text{Others} \end{cases} \quad (A.5)$$

Identify irrationally position data in the AIS database

Even if the time stamp and speed data included in AIS data base are appropriately defined or corrected some irrationally positioned data may need to be cleaned. However, longitude

$x_j$  and latitude  $y_j$  should also satisfy Formula (6) with the units of degrees as follows:

$$\left\{ \begin{array}{l} D' = \frac{1}{3600} \sqrt{\left( \frac{SOG_{i,T_j,x} + SOG_{i,T(j+1),x}}{2} \times t_{(j,j+1)} \right)^2 + \left( \frac{SOG_{i,T_j,y} + SOG_{i,T(j+1),y}}{2} \times t_{(j,j+1)} \right)^2} \\ \frac{R \times \arccos(\sin(x_{j,T_j}) \times \sin(x_{(j+2),T(j+2)}) + \cos(y_{j,T_j}) \times \cos(y_{(j+2),T(j+2)}) \times \cos D\lambda) \times \frac{\pi}{180}}{1852} \leq D' + \Delta D \end{array} \right. \quad (A.6)$$

where  $D'$  stands for the distance that ship  $i$  sails during the time interval  $[T_j, T_{(j+1)}]$ ;  $D\lambda$  denotes the difference between the position (longitude  $x_j$  and latitude  $y_j$ ) at the time  $T_j$  and the location (longitude  $x_{(j+2)}$  and latitude  $y_{(j+2)}$ ) in longitude;  $\Delta D$  is the threshold value, which is defined according to the speed and the length of ship  $i$  and the cleaning efficacy. Moreover, we will update the incorrect speed data as follows:

$$\left\{ \begin{array}{l} \hat{x}_{i,T(j+1)} = \begin{cases} x_{i,T(j+1)} & \text{If the longitude is within range} \\ x_{i,T(j)} \pm \frac{1}{60} \times \frac{SOG_{i,T_j,x} + SOG_{i,T(j+1),x}}{2} \times \frac{t_{(j,j+1)}^i}{3600} & \text{If the longitude is out of range} \end{cases} \\ \hat{y}_{i,T(j+1)} = \begin{cases} y_{i,T(j+1)} & \text{If the latitude is within range} \\ y_{i,T(j)} \pm \frac{1}{60} \times \frac{SOG_{i,T_j,y} + SOG_{i,T(j+1),y}}{2} \times \frac{t_{(j,j+1)}^i}{3600} & \text{If the latitude is out of range} \end{cases} \end{array} \right. \quad (A.7)$$

The following sign conventions hold:

if the longitude is out of range, the ship course ranges from  $0^\circ$  to  $180^\circ$  and the plus sign is used;

if the longitude is out of range and the ship course ranges from  $180^\circ$  to  $360^\circ$ , the minus sign is used;

if the latitude is out of range and the ship course ranges from  $270^\circ$  and  $090^\circ$  and the plus sign is used;

if the ship course ranges from  $90^\circ$  to  $270^\circ$ , the minus sign is used.

Additionally, the static AIS data (such as ship length) could be updated according to the MMSI number, because some AIS records may be inaccurate in terms of ship length information.

## ANNEX B - Supplementary Material

### Collision Scenarios for other ship Groups in the Gulf of Finland

#### Group 1 - Tankers

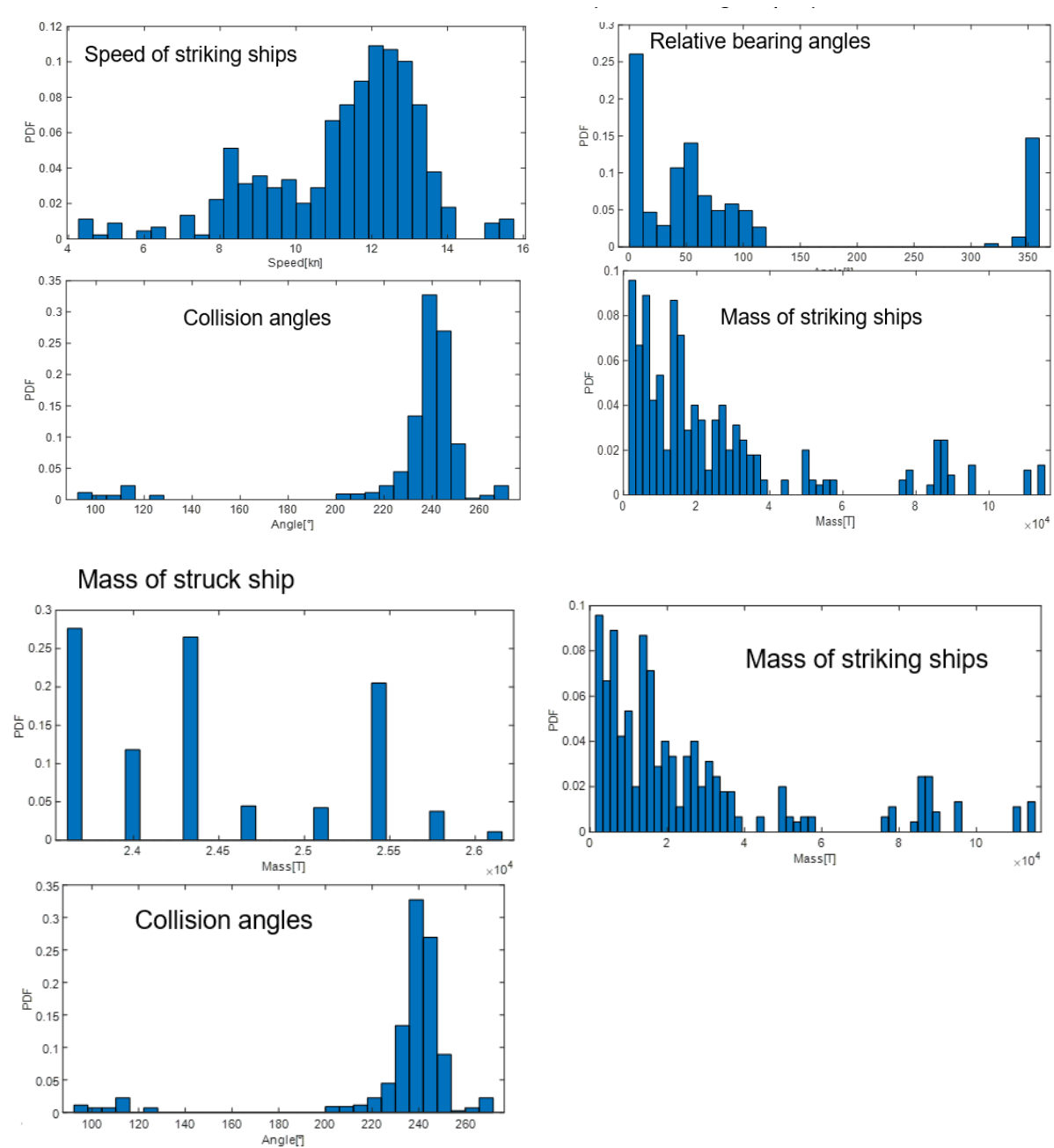


Figure B. 1. The collision encounter analysis for Group 1.

- Group 3 – Bulk and Gas Carriers

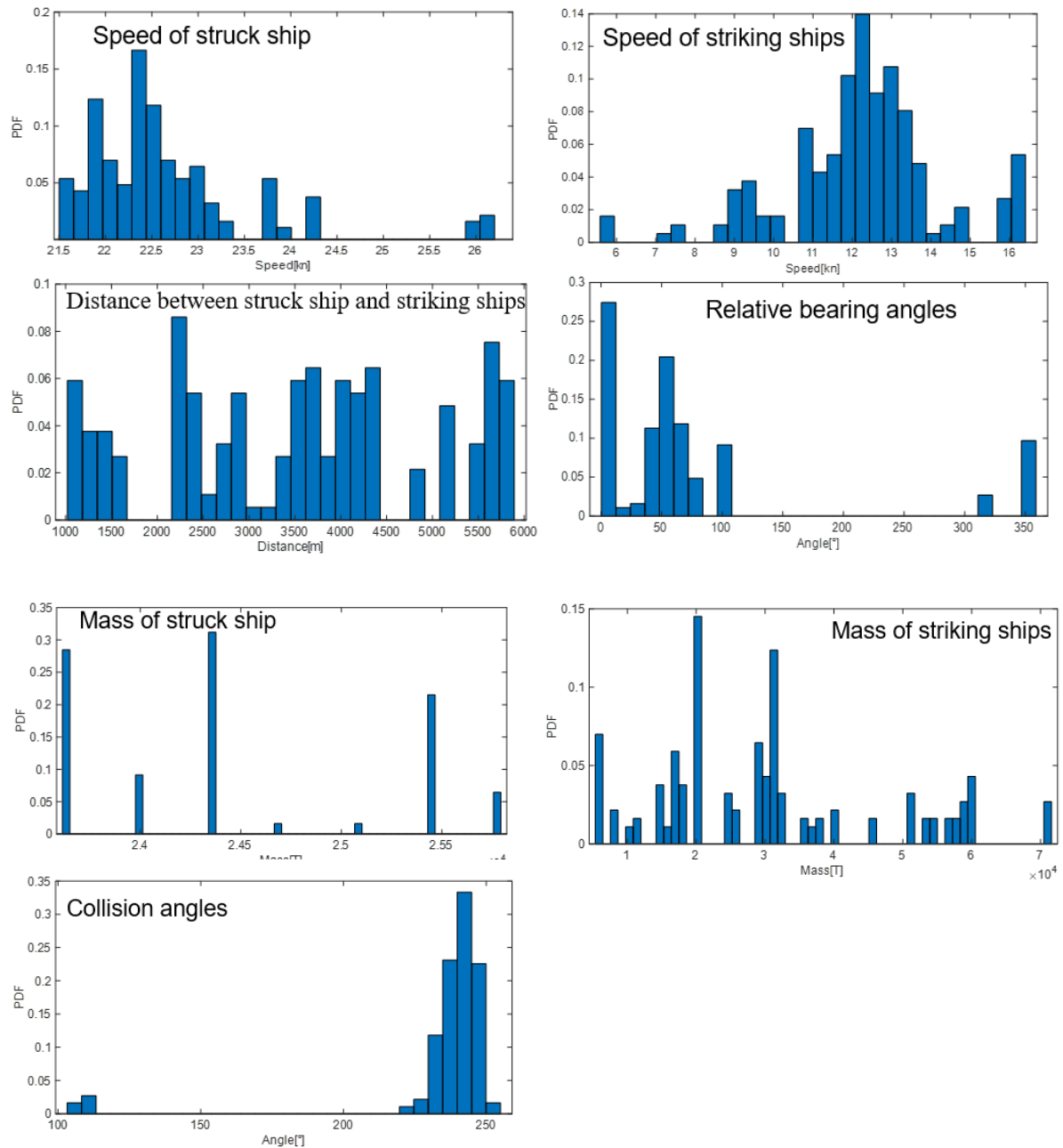


Figure B. 2. The collision encounter analysis for Group 2.

- Group 4 – Container ships

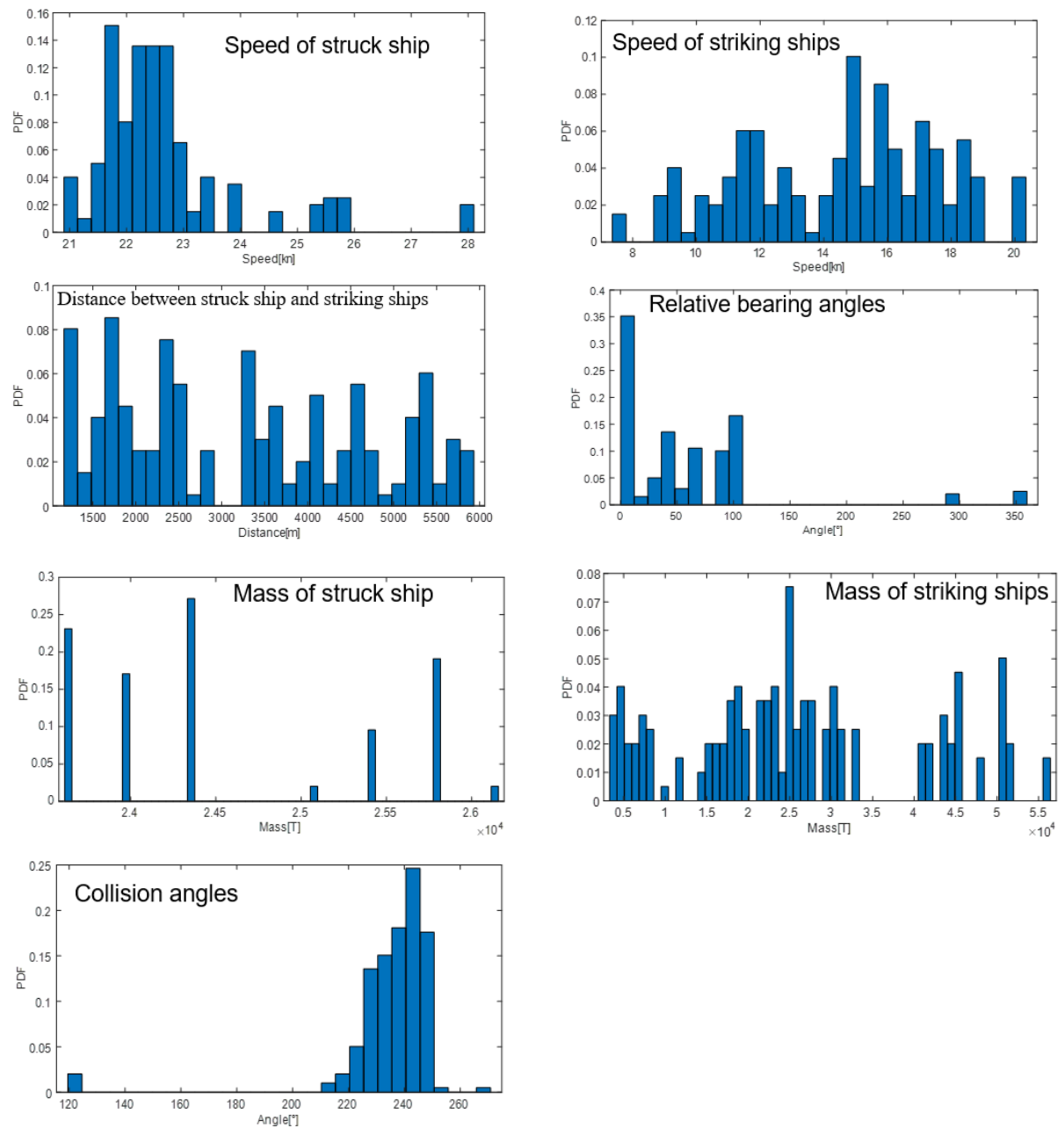


Figure B. 3. The collision encounter analysis for Group 4.



- Group 5 – General Cargo ships

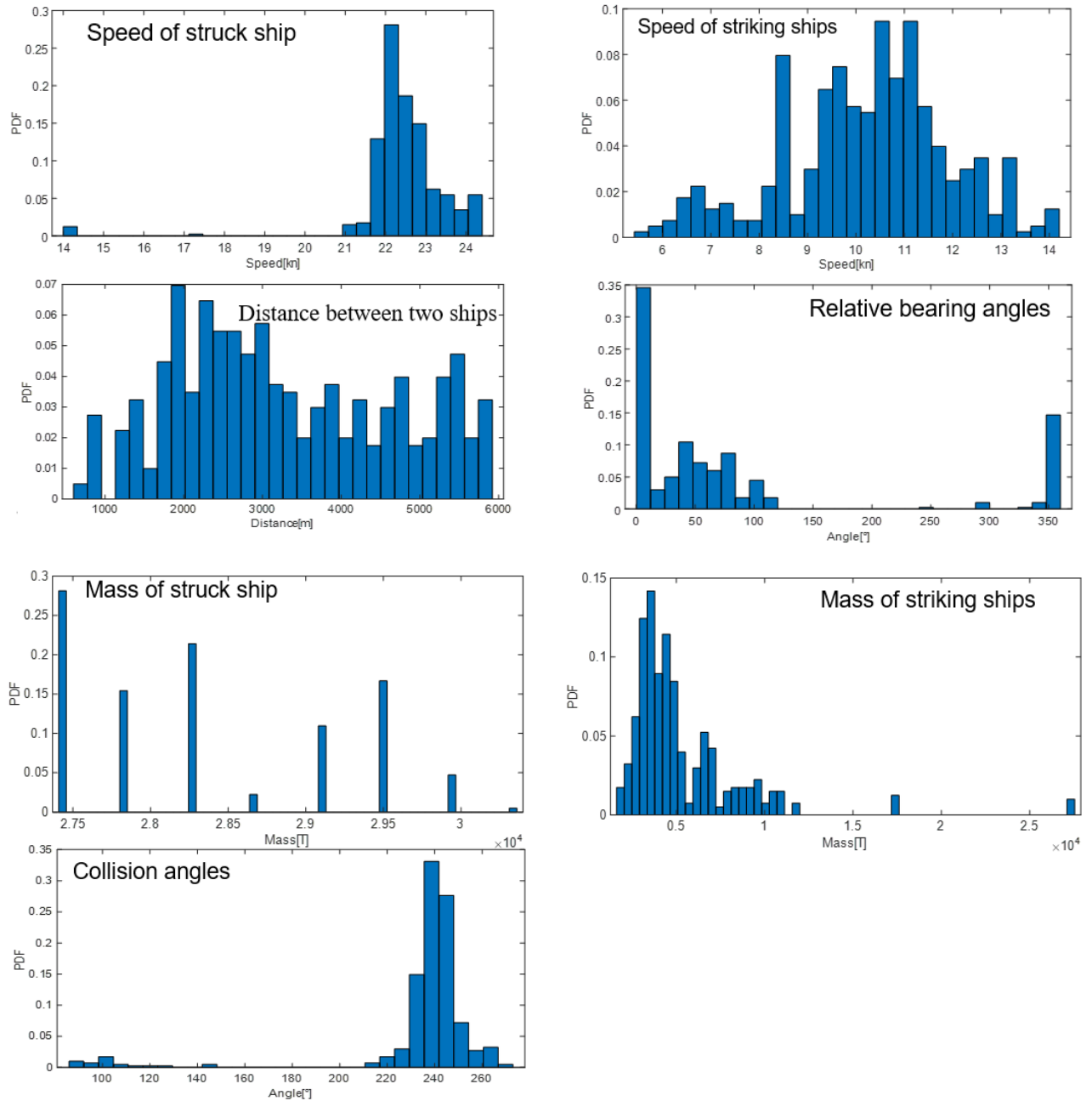


Figure B. 4. The collision encounter analysis for Group 5.

- Group 6 – Other ships

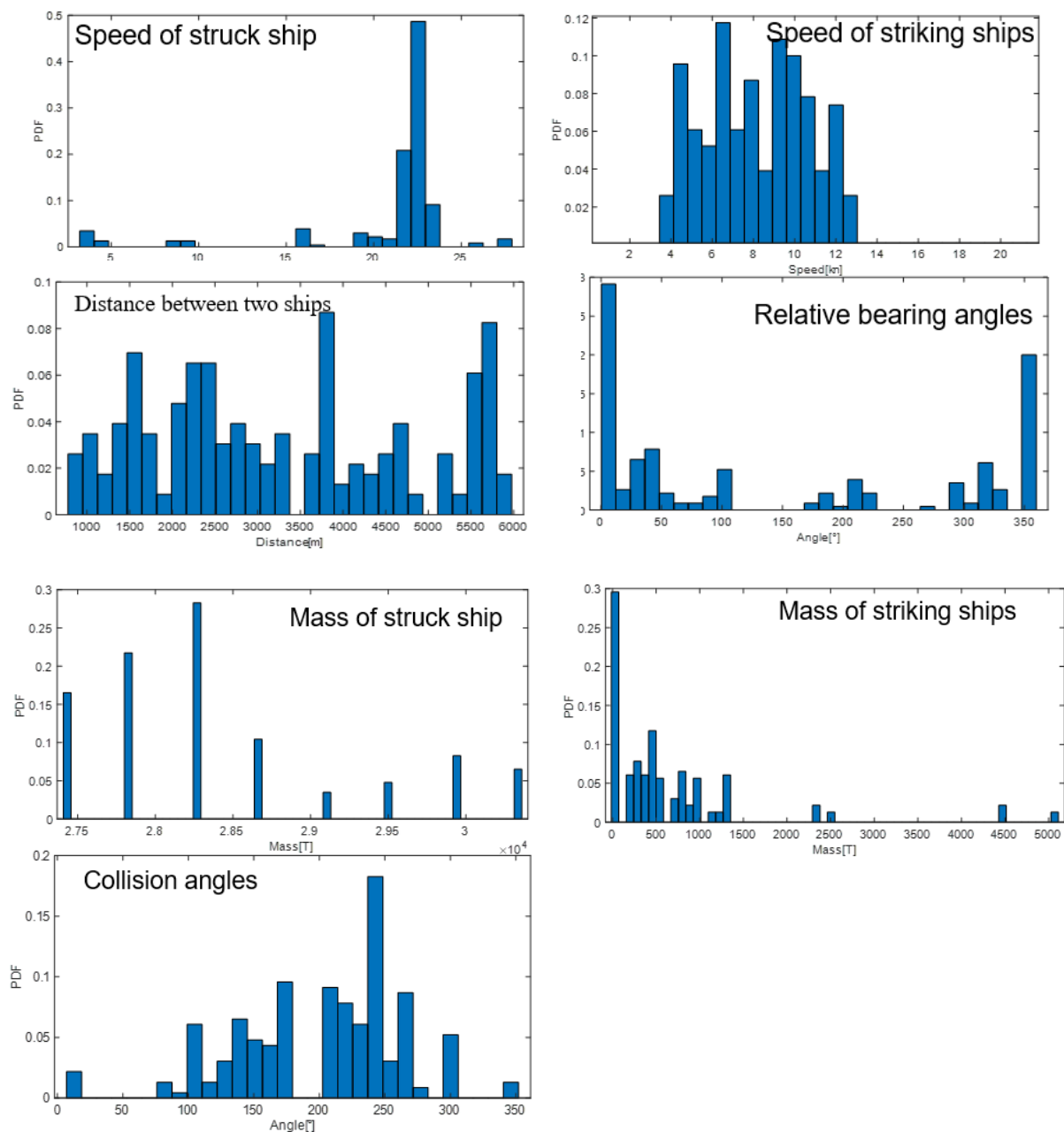
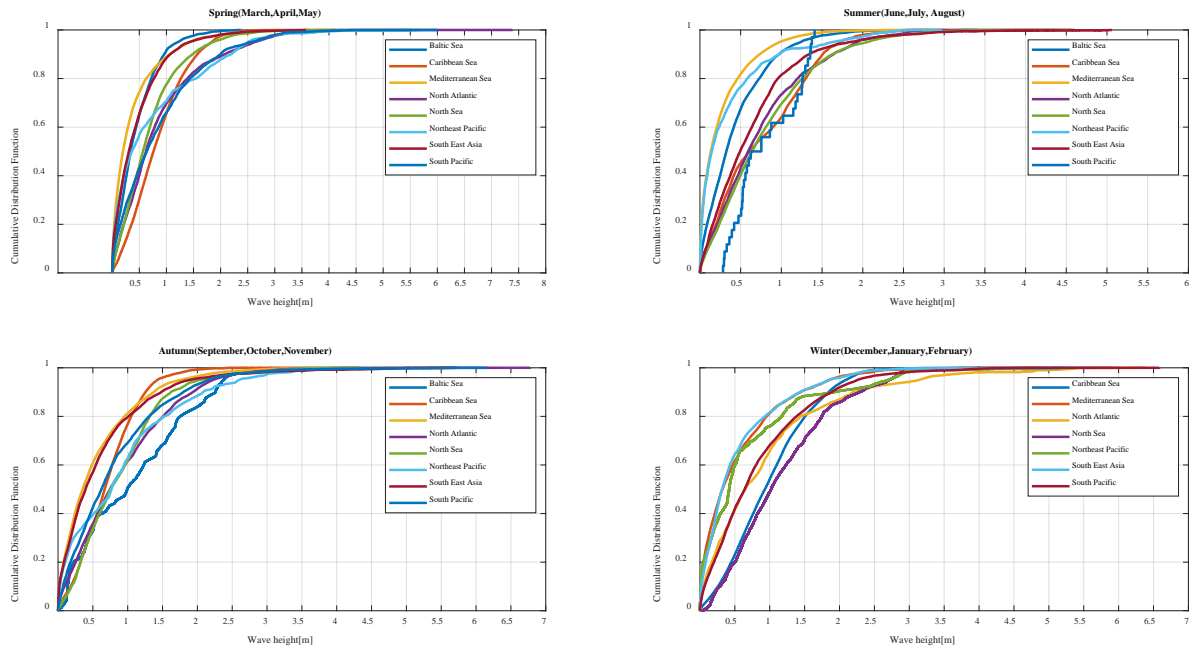
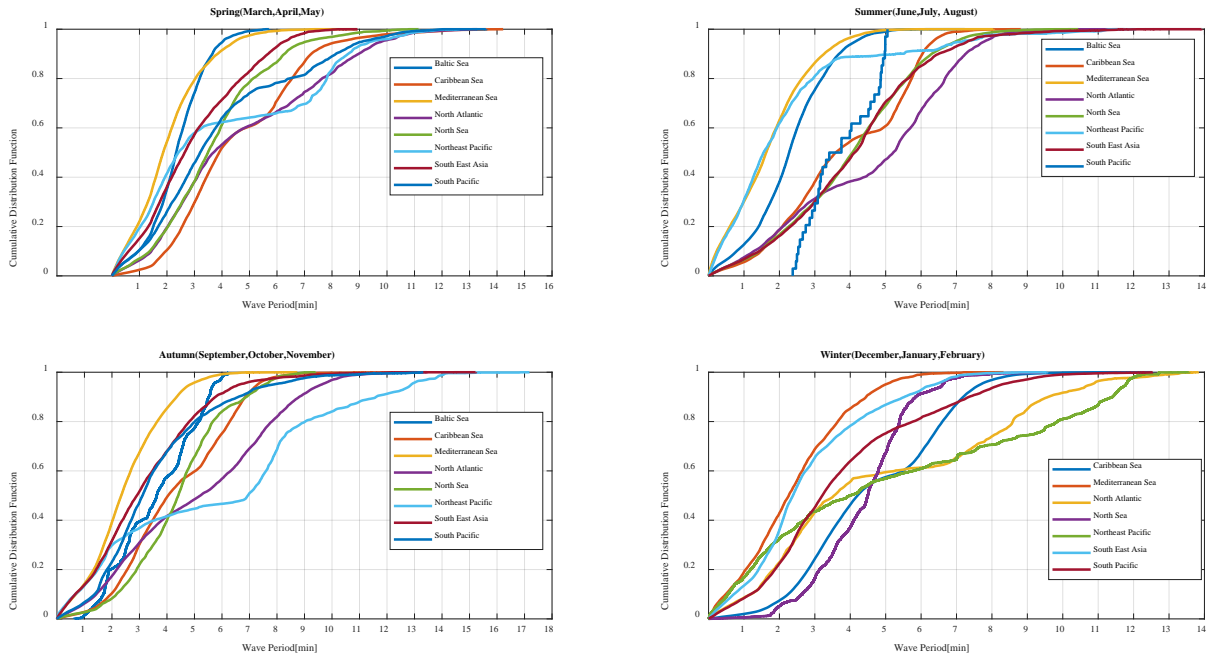


Figure B. 5. The collision encounter analysis for Group 6.

## Weather data distributions – passenger ships

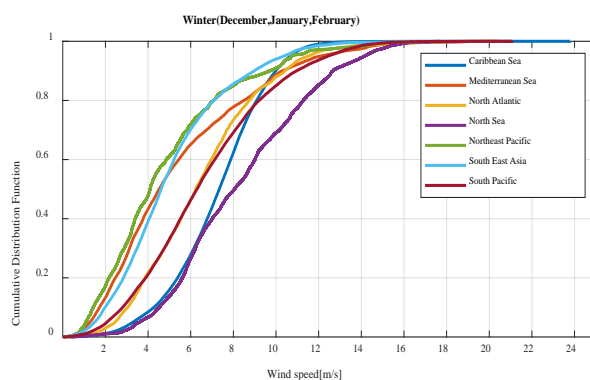
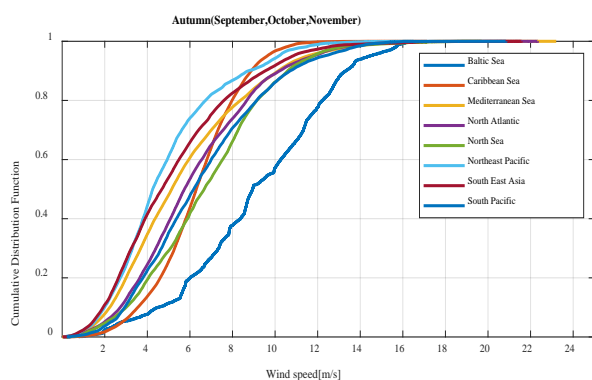
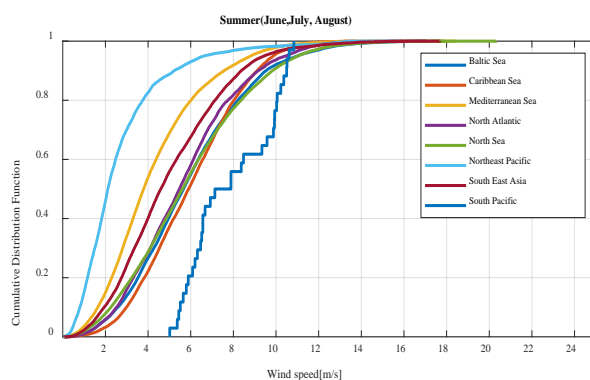
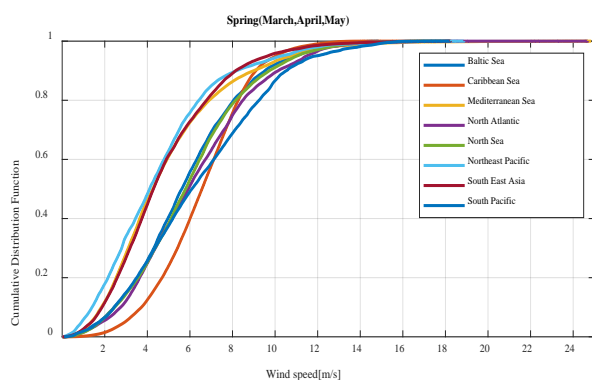


(A: Wave Height)

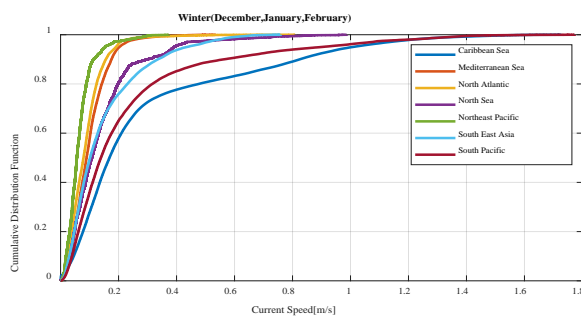
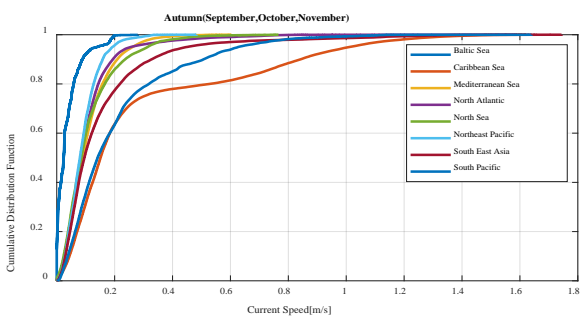
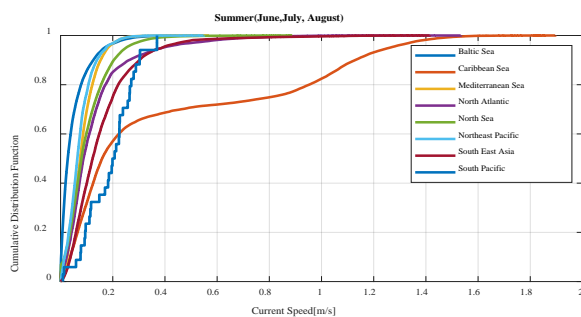
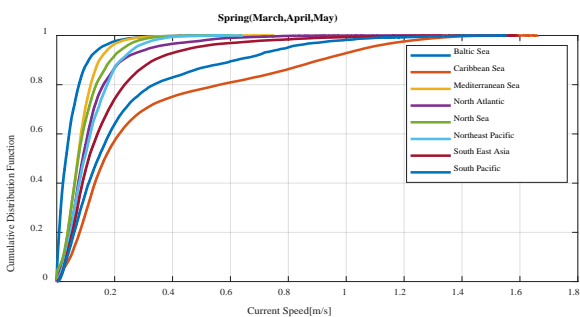


(B: Wave Period)

Figure B. 6 - A. Key Weather parameters cumulative distributions for Passenger ships.

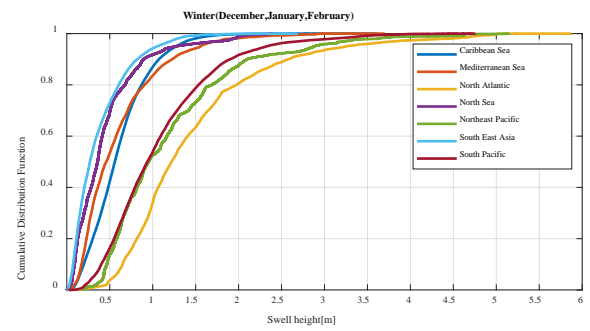
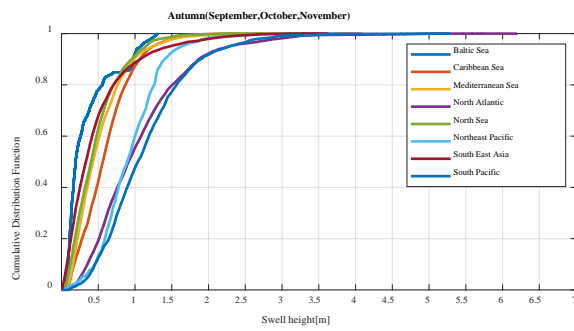
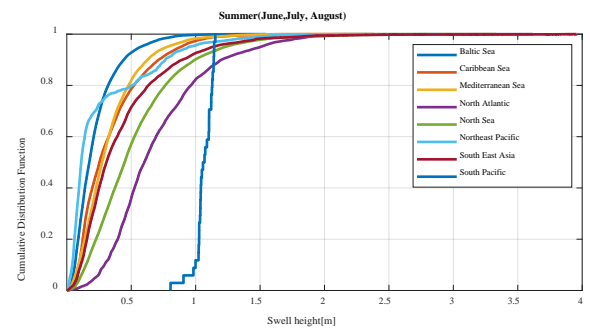
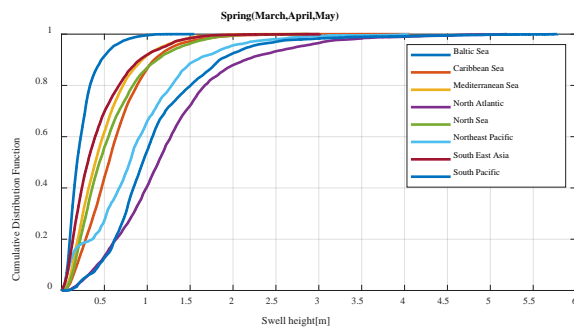


### (C: Wind Speed)



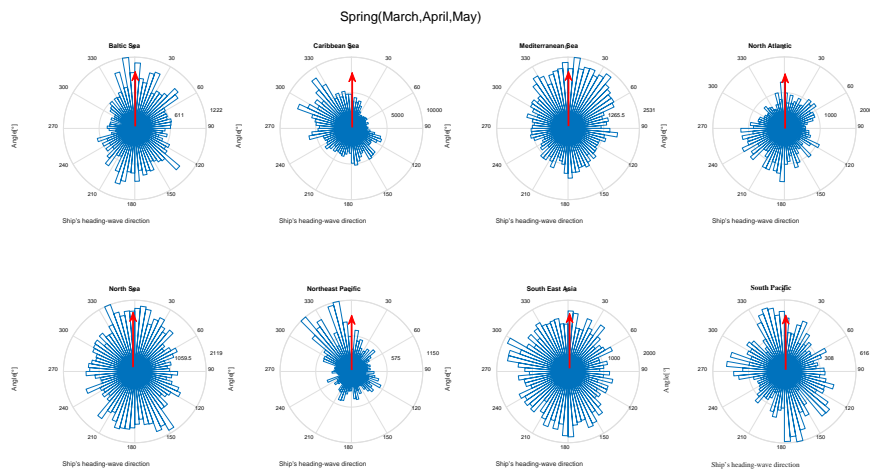
### (D: Current Speed)

Figure B.6 - B. Key Weather parameters cumulative distributions for Passenger ships

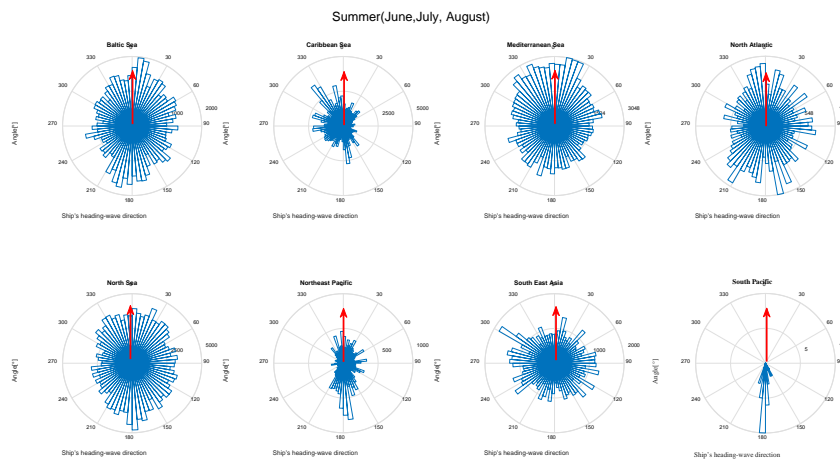


### (E: Swell Height)

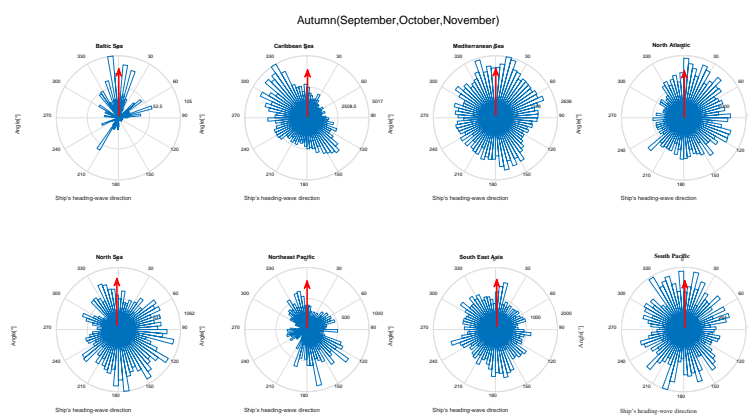
Figure B.6 - C. Key Weather parameters cumulative distributions for Passenger ships.



**(A: Wave direction vs ship heading in Spring)**

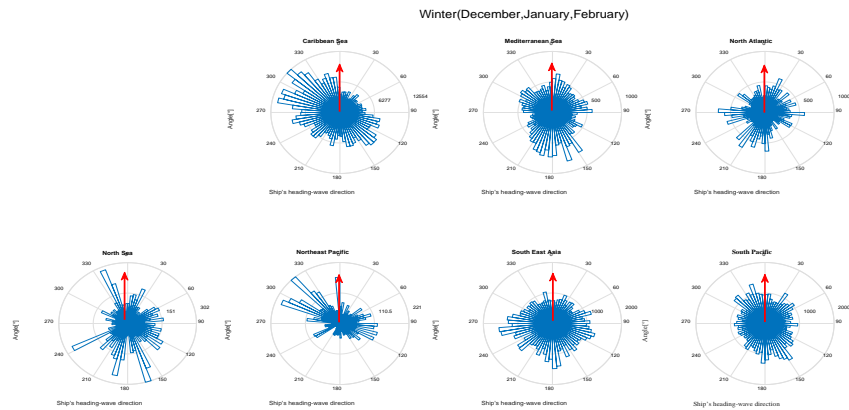


**(B: Wave direction vs ship heading in Summer)**

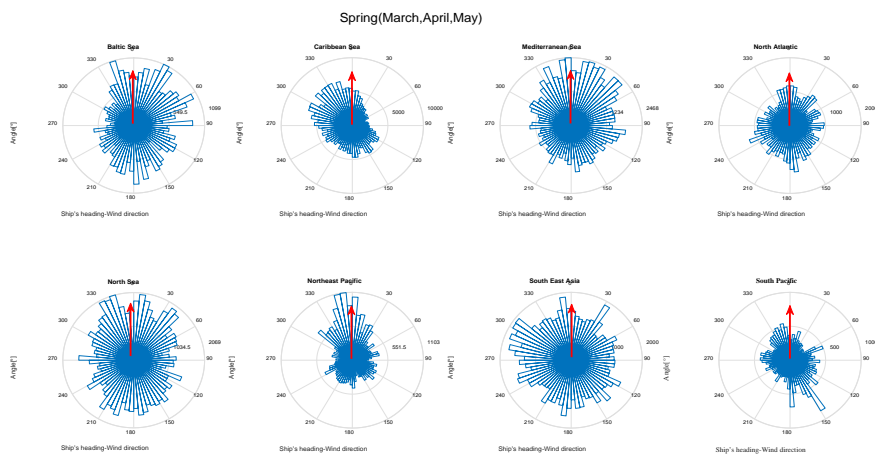


**(C: Wave direction vs ship heading in Autumn)**

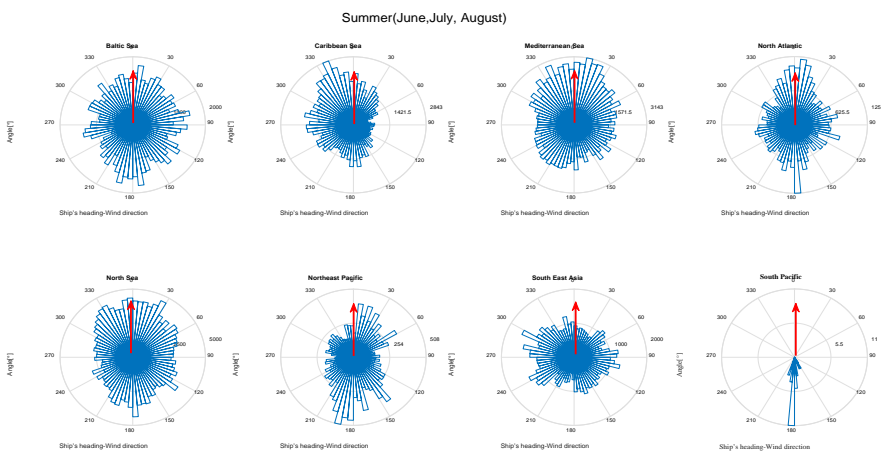
Figure B. 7. - A Wave or Wind direction with respect to ship heading each season.



(D: Wave direction vs ship heading in Winter)



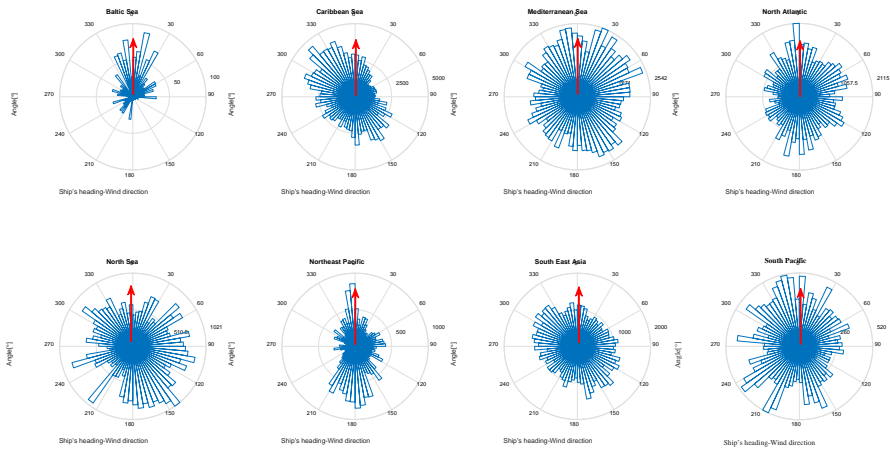
(E: Wind direction vs ship heading in Spring)



(F: Wind direction vs ship heading in Summer)

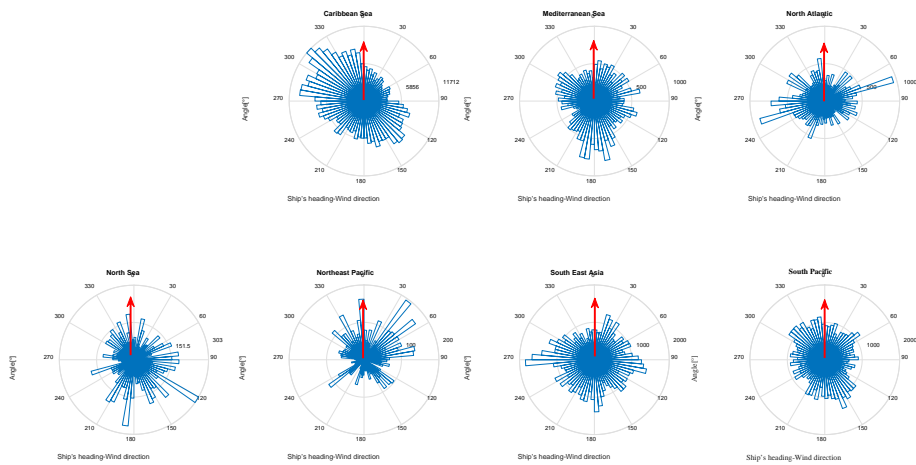
Figure B.7.-B Wave or Wind direction with respect to ship is heading each season.

Autumn(September,October,November)



(G: Wind direction vs ship heading in Autumn)

Winter(December,January,February)

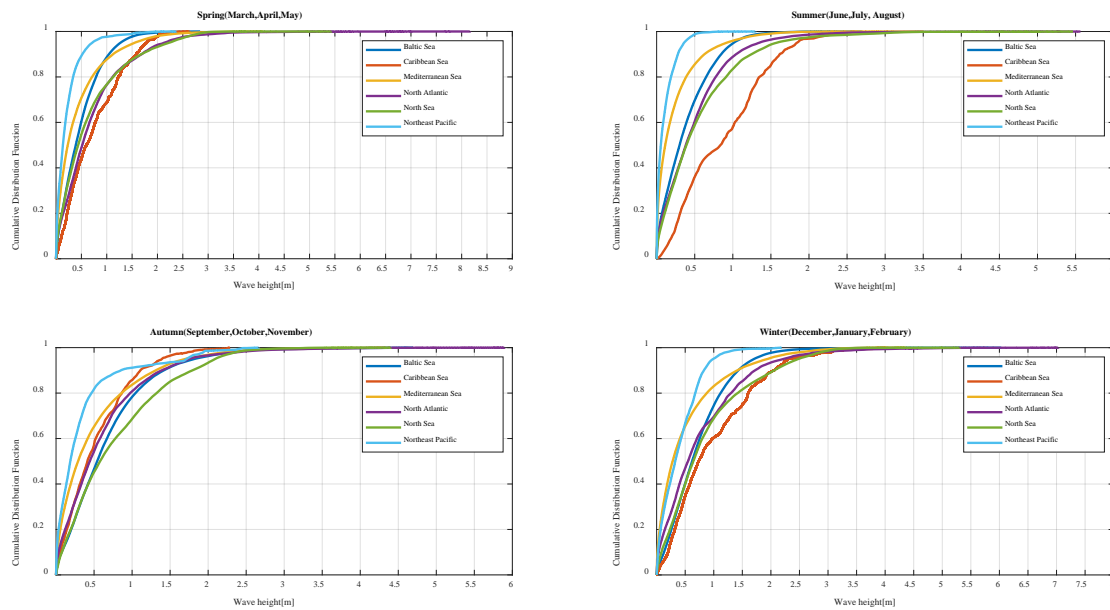


(H: Wind direction vs ship heading in Winter)

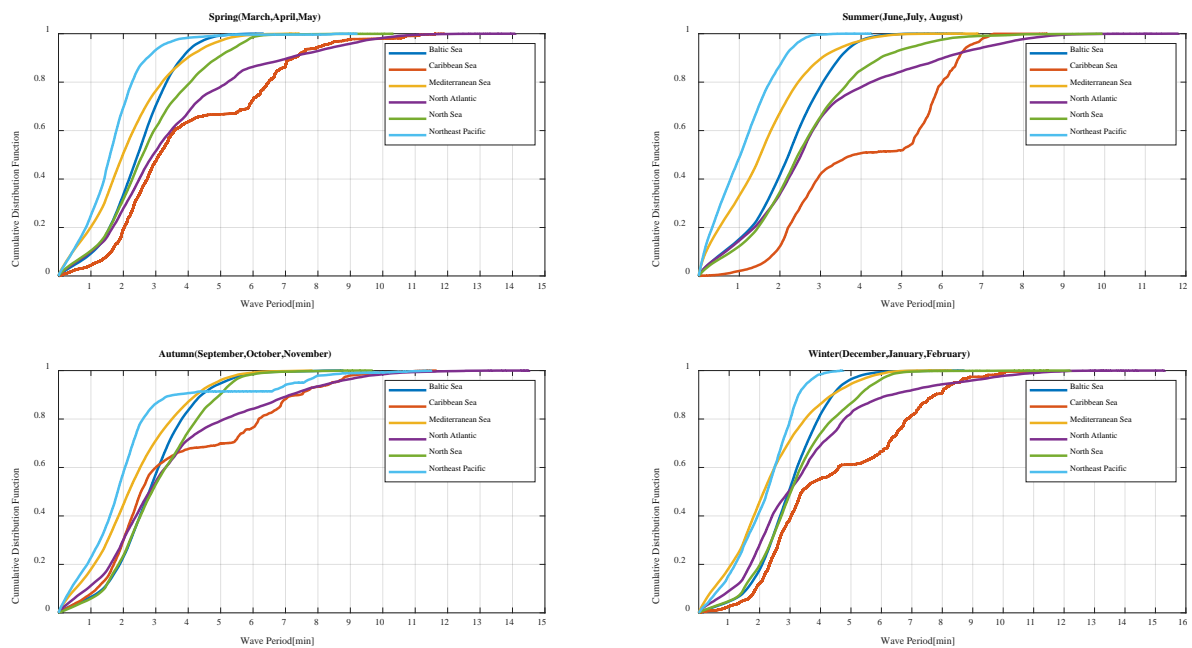
Figure B.7.-C Wave or Wind direction with respect to ship is heading each season.



## Weather data distributions – RoPax ships

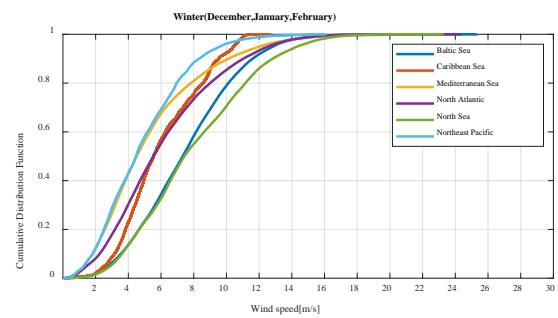
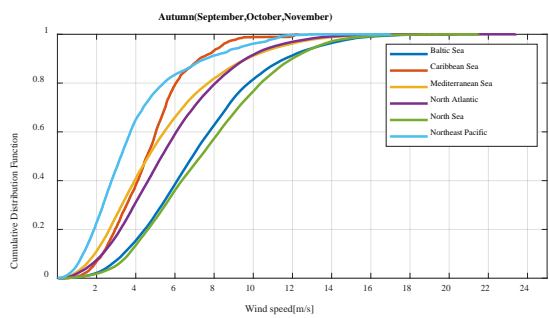
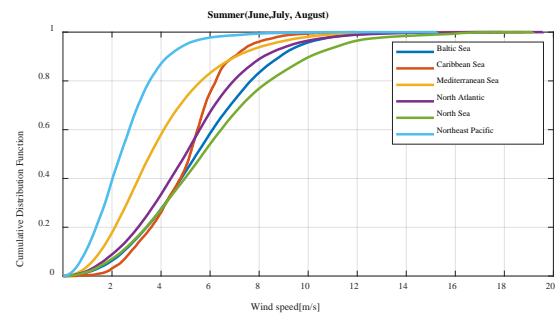
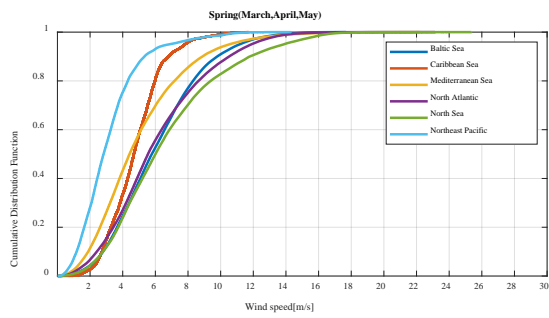


(A: Wave Height)

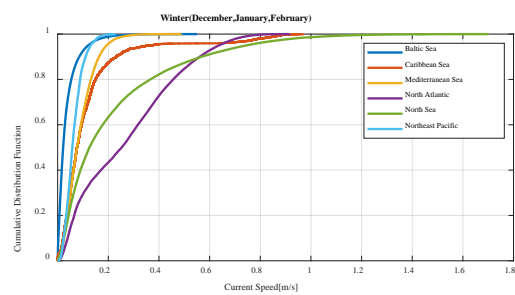
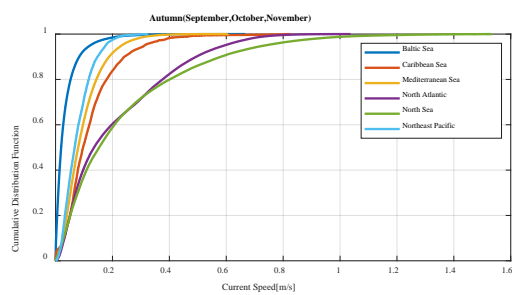
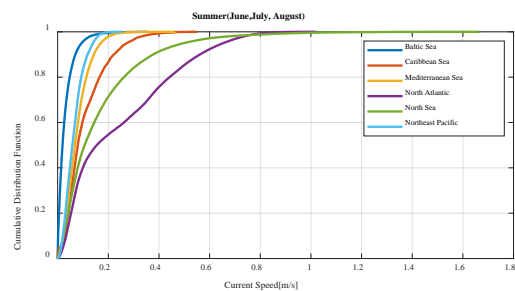
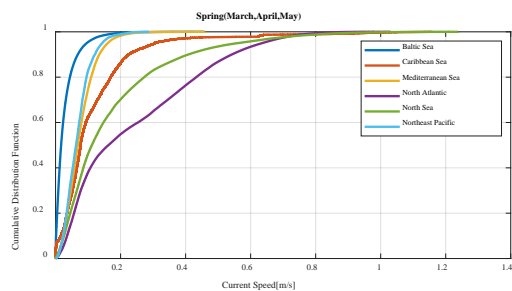


(B: Wave Period)

Figure B. 8. -A Key Weather parameters cumulative distributions for RoPax ships.

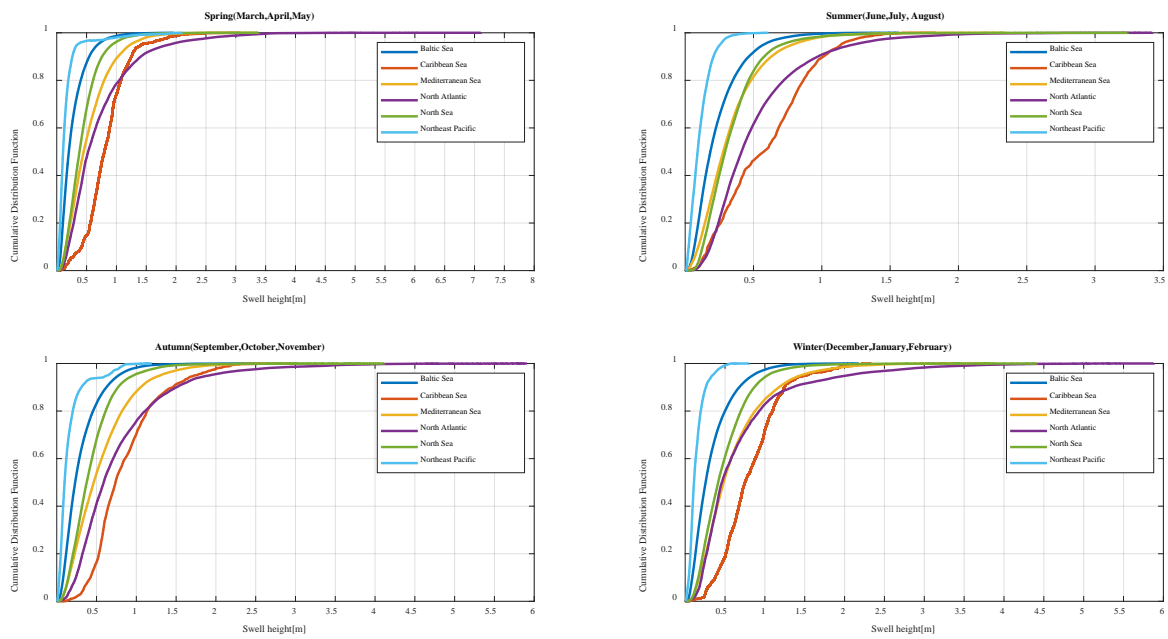


(C: Wind Speed)



(D: Current Speed)

Figure B.8.-B Key Weather parameters cumulative distributions for RoPax ships.



### (E: Swell Height)

Figure B.8. – C Key Weather parameters cumulative distributions for RoPax ships.

## Weather data statistics in 8 Areas

Table B. 1. Wave height variations – Passenger ships

	Areas	Spring				Summer				Autumn				Winter			
		25%	50%	75%	99%	25%	50%	75%	99%	25%	50%	75%	99%	25%	50%	75%	99%
Wave height (m)	Baltic Sea	0.1485	0.341	0.6446	2.318	0.1259	0.3243	0.6256	3.241	0.3843	0.9912	1.662	2.899	None			
	Caribbean Sea	0.4284	0.7615	1.162	3.59	0.246	0.6056	1.204	2.77	0.3824	0.6689	0.9707	3.137	0.5307	0.9301	1.382	4.054
	Mediterranean Sea	0.055	0.198	0.514	4.601	0.0273	0.1339	0.3694	2.657	0.1185	0.3534	0.8017	5.646	0.081	0.3214	0.8258	4.747
	North Atlantic	0.2862	0.6237	1.179	5.45	0.2738	0.5923	1.048	3.286	0.3257	0.7447	1.342	6.291	0.2382	0.6489	1.238	6.371
	North Sea	0.2707	0.5665	0.9395	4.248	0.3009	0.6417	1.127	4.509	0.3843	0.7503	1.222	4.328	0.5824	1.02	1.63	4.014
	Northeast Pacific	0.080	0.3624	1.125	5.65	0.0331	0.1447	0.4582	2.979	0.155	0.7683	1.291	4.986	0.1124	0.4181	0.9371	5.2
	South East Asia	0.100	0.3067	0.6624	3.577	0.207	0.4925	0.8661	5.057	0.1354	0.3945	0.8346	5.699	0.1206	0.3165	0.7478	5.339
	South Pacific	0.218	0.6383	1.239	6.003	0.5062	0.6241	0.7353	1.409	0.2509	0.623	1.157	6.011	0.2723	0.6408	1.209	6.248

Table B. 2. Current speed variations – Passenger ships.

		Spring				Summer				Autumn				Winter			
		25%	50%	75%	99%	25%	50%	75%	99%	25%	50%	75%	99%	25%	50%	75%	99%
Current Speed (m/s)	Baltic Sea	0.011	0.03161	0.06654	0.5047	0.0098	0.0274	0.06502	0.5236	0.003747	0.02388	0.05094	0.2809				
	Caribbean Sea	0.09255	0.1659	0.3966	1.604	0.0791	0.1592	0.8063	1.847	0.08372	0.1511	0.3014	1.613	0.0913	0.1686	0.3381	1.704
	Mediterranean Sea	0.04395	0.0727	0.1072	0.7433	0.0447	0.0751	0.1105	0.5639	0.05003	0.08915	0.1409	0.5872	0.05506	0.08954	0.1302	0.5253
	North Atlantic	0.0537	0.08959	0.1415	1.166	0.0510	0.0876	0.1516	1.373	0.04943	0.08319	0.13	1.189	0.04458	0.07905	0.1141	0.8072
	North Sea	0.044	0.0741	0.1215	0.5675	0.0438	0.08	0.1381	0.8639	0.04612	0.0848	0.1441	0.7644	0.0538	0.1083	0.1813	0.9876
	Northeast Pacific	0.05495	0.0958	0.1568	0.6423	0.0383	0.0642	0.096	0.5499	0.04883	0.0801	0.117	0.481	0.03654	0.05622	0.08106	0.374
	South East Asia	0.06297	0.1105	0.2043	1.566	0.0687	0.1226	0.1997	1.375	0.0534	0.0954	0.1851	1.692	0.05495	0.1016	0.1934	0.7525
	South Pacific	0.07226	0.1433	0.2755	1.553	0.1106	0.1989	0.2643	0.3695	0.07534	0.1411	0.261	1.63	0.07293	0.1391	0.267	1.758

Table B. 3. Wind speed variations – Passenger ships.

		Spring				Summer				Autumn				Winter			
		25%	50%	75%	99%	25%	50%	75%	99%	25%	50%	75%	99%	25%	50%	75%	99%
Wind Speed (m/s)	Baltic Sea	3.94	5.617	7.561	14.85	3.871	5.657	7.656	17.91	6.756	8.95	11.69	16.21				
	Caribbean Sea	5.073	6.566	7.962	14.81	4.198	5.9	7.626	13.51	4.968	6.302	7.625	14.84	5.784	7.341	8.723	16.9
	Mediterranean Sea	2.821	4.254	6.276	24.8	2.57	3.792	5.504	16.25	3.344	5.145	7.611	19.98	2.85	4.517	7.557	20.17
	North Atlantic	4.008	5.928	8.004	22.39	3.706	5.47	7.227	16.33	4.038	5.742	8.138	21.86	4.313	6.231	8.177	20.45
	North Sea	3.99	5.797	7.617	17.34	3.679	5.608	7.76	18.28	4.572	6.672	8.646	18.82	5.904	8.053	10.7	17.69
	Northeast Pacific	2.468	4.104	5.914	18.43	1.325	2.114	3.343	15.76	3.044	4.251	6.128	16.24	2.573	4.099	6.393	20.41
	South East Asia	2.9	4.286	6.229	18.18	3.048	4.597	6.644	16.77	2.943	4.683	6.971	21.34	3.18	4.61	6.476	20.32
	South Pacific	3.956	6.091	8.675	17.77	6.202	7.132	9.936	10.84	4.24	6.179	8.525	18.58	4.341	6.296	8.6	20.83

Table B. 4. Wave period variations – Passenger ships.

		Spring				Summer				Autumn				Winter			
		25%	50%	75%	99%	25%	50%	75%	99%	25%	50%	75%	99%	25%	50%	75%	99%
Wave period (min)	Baltic Sea	1.689	2.334	3.029	5.688	1.581	2.274	2.983	6.237	2.431	3.628	4.777	6.232				
	Caribbean Sea	2.789	3.898	6.219	14.19	2.379	3.59	5.559	8.528	2.8	4.041	5.987	12.7	3.027	4.205	6.363	12.19
	Mediterranean Sea	1.114	1.861	2.757	7.368	0.8059	1.625	2.403	6.458	1.541	2.337	3.352	8.736	1.315	2.264	3.37	8.18
	North Atlantic	2.298	3.69	7.082	13.15	2.478	5.214	6.435	11.59	2.517	5.212	7.433	13.35	2.104	3.541	8.128	12.84
	North Sea	2.307	3.488	4.678	10.79	2.624	4.06	5.306	10.16	3.202	4.412	5.438	9.395	3.447	4.494	5.234	9.434
	Northeast Pacific	1.317	2.42	7.525	12.63	0.8344	1.551	2.577	12.05	1.755	6.938	8.33	17.17	1.443	3.995	9.209	13.57
	South East Asia	1.536	2.644	4.279	8.916	2.68	4.125	5.287	12.56	1.687	2.905	4.446	14.47	1.614	2.382	3.718	9.562
	South Pacific	1.955	3.205	5.132	13.53	2.924	3.407	4.813	5.05	2.095	3.113	4.598	13.32	2.134	3.211	4.964	12.54

Table B. 5. Swell height variations – Passenger ships.

		Spring				Summer				Autumn				Winter			
		25%	50%	75%	99%	25%	50%	75%	99%	25%	50%	75%	99%	25%	50%	75%	99%
Swell height (m)	Baltic Sea	0.1097	0.1815	0.2991	1.516	0.101	0.1746	0.2829	1.379	0.1226	0.1909	0.4469	1.306				
	Caribbean Sea	0.3331	0.5527	0.8024	3.484	0.1373	0.2538	0.4558	1.733	0.3439	0.5623	0.7964	3.126	0.3526	0.5593	0.7961	2.803
	Mediterranean Sea	0.2209	0.3943	0.646	2.483	0.163	0.2743	0.4294	2.157	0.2491	0.4271	0.6965	2.966	0.2559	0.4598	0.7815	3.318
	North Atlantic	0.7424	1.129	1.556	5.192	0.4255	0.6013	0.8922	3.576	0.5705	0.9116	1.368	5.591	0.8985	1.22	1.765	5.557
	North Sea	0.2538	0.4427	0.7529	2.854	0.2654	0.4485	0.6905	3.258	0.2142	0.4027	0.6299	2.656	0.1613	0.3591	0.5546	2.4
	Northeast Pacific	0.4629	0.7958	1.163	4.049	0.068	0.1121	0.2951	2.875	0.6387	0.894	1.185	3.314	0.6312	0.954	1.55	5.157
	South East Asia	0.1565	0.3079	0.5812	2.961	0.1768	0.3077	0.5496	3.94	0.1575	0.3313	0.6167	3.519	0.1312	0.2691	0.527	2.688
	South Pacific	0.6894	0.9468	1.348	5.743	1.027	1.057	1.121	1.153	0.7074	1.039	1.441	5.253	0.6115	0.9379	1.402	4.667



## Grounding data for scenario 2

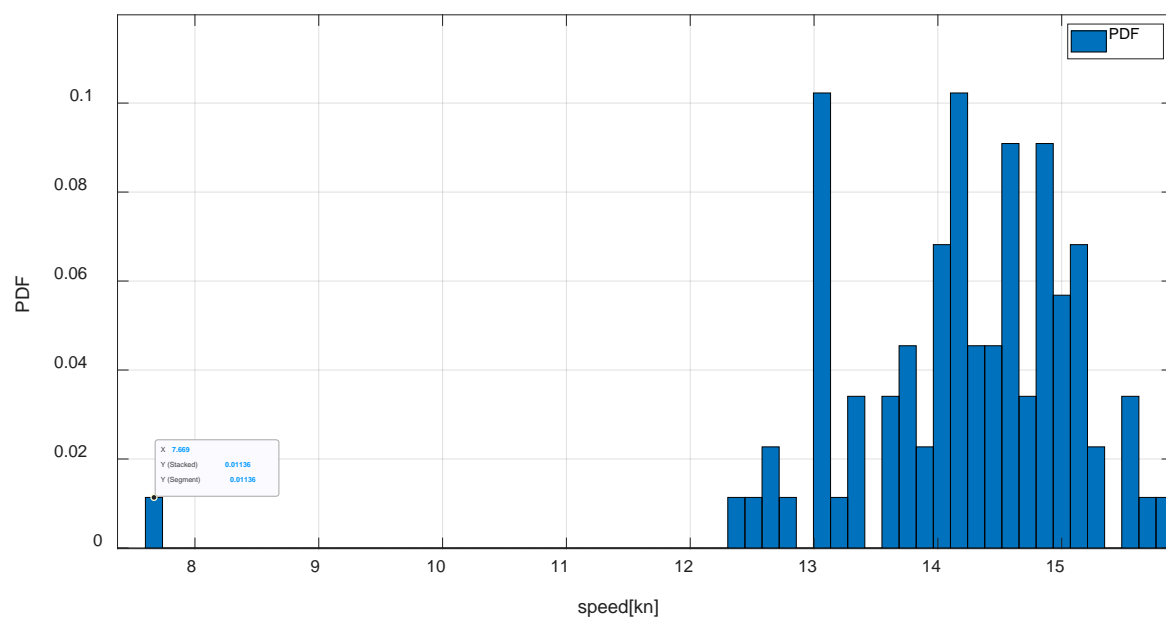


Figure B. 9. The speed distribution of the selected ship encountered during power grounding

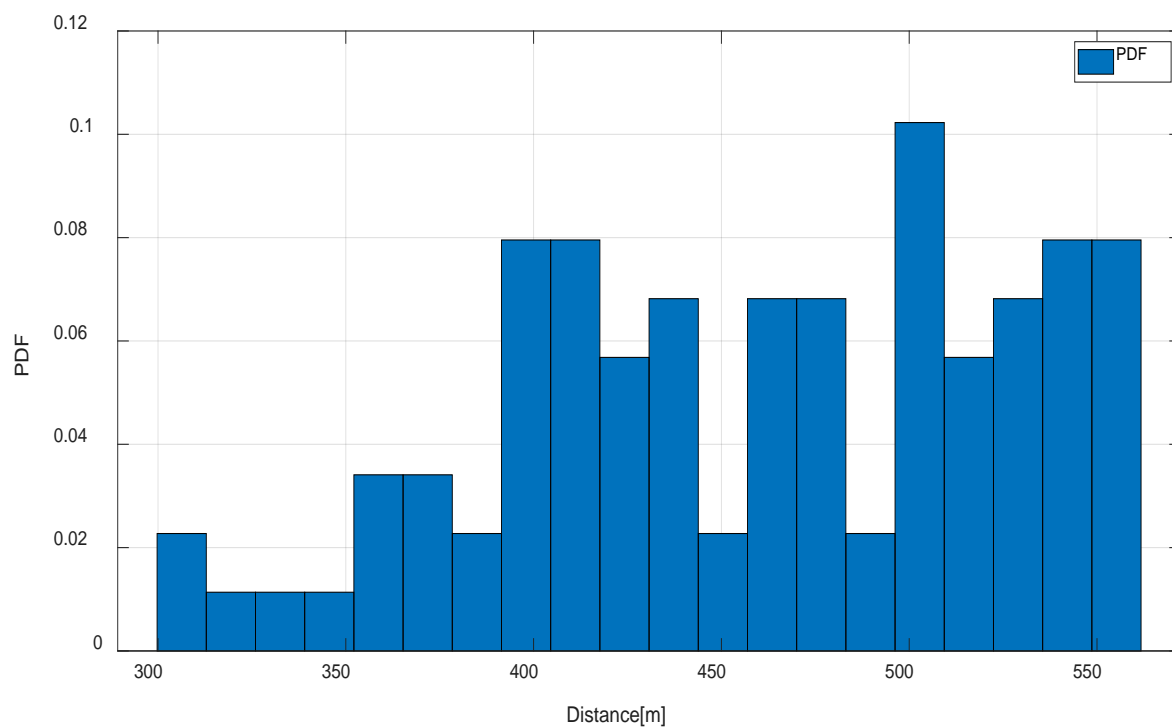


Figure B. 10. The distance distribution of the selected ship to the shallow water (Forward to shallow waters) during power grounding.

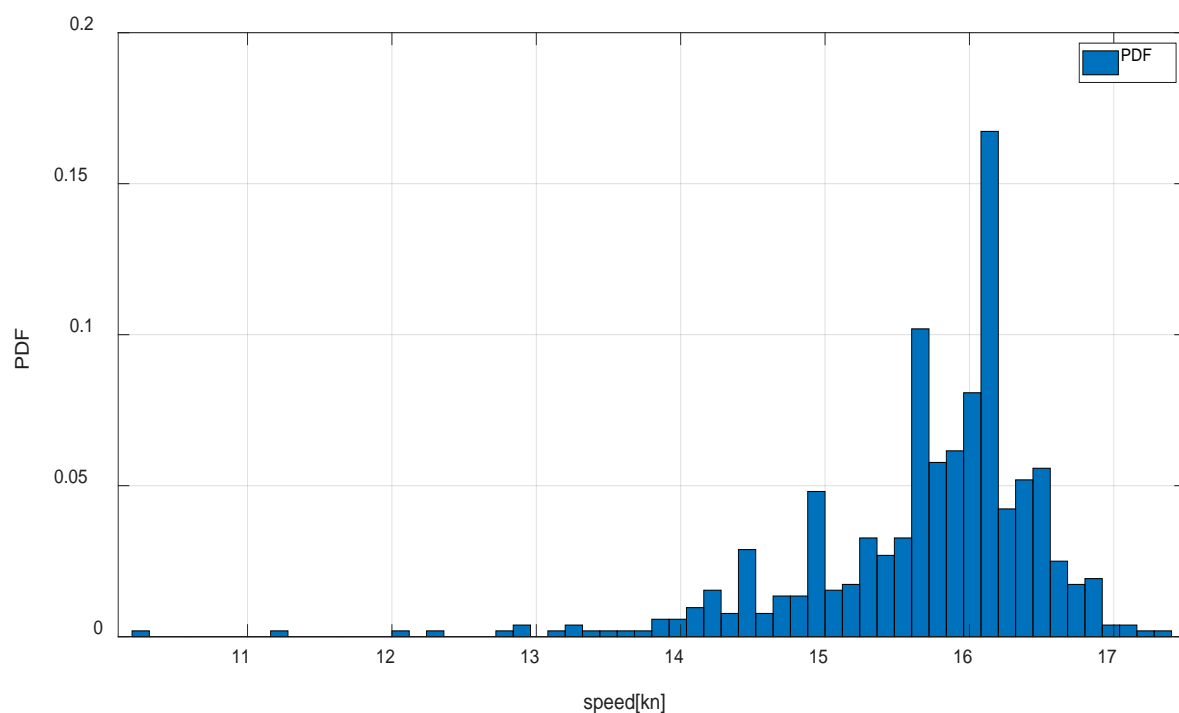


Figure B. 11. The speed distribution of the selected ship encountered during drift grounding

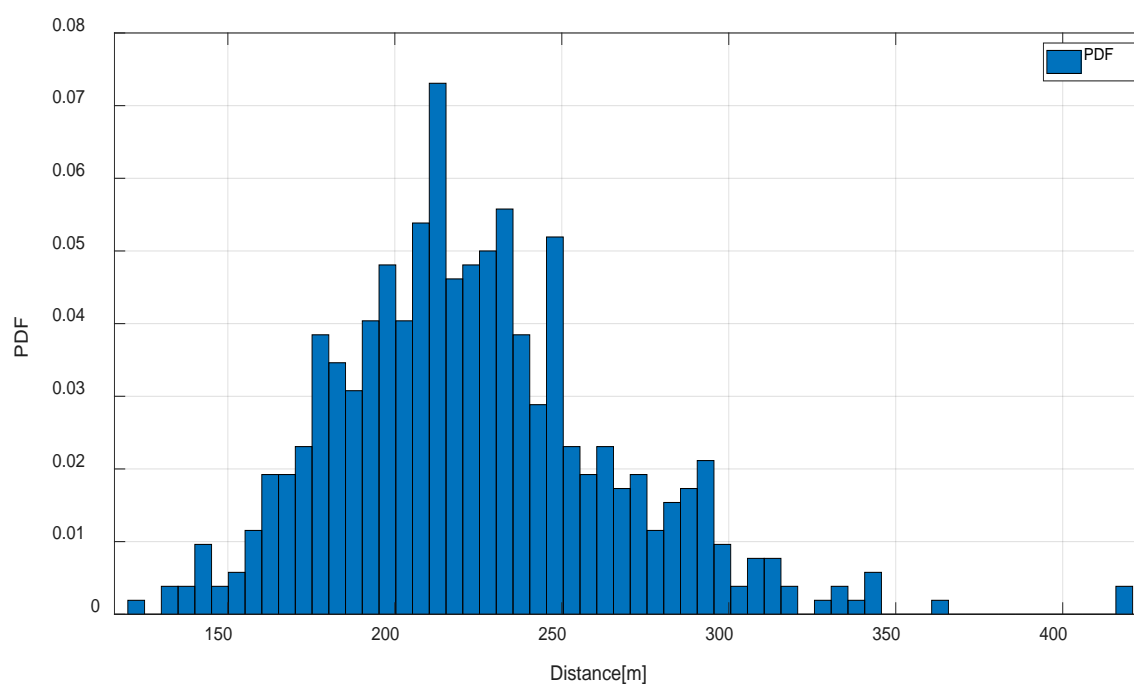


Figure B. 12. The distance distribution of the selected ship to the shallow water (lateral to shallow waters) during drift grounding.

## Public summary

This report presents state of the art methods for the collection and processing of big data analytics combining trends of passenger vessels and RoPax ship operations under global hydro-meteorological conditions and vessel encounters in three key risk areas (Gulf of Finland, English Channel and Gibraltar Straight). Weather mapping accounted for environmental conditions (e.g. sea states, currents, wind, swell etc.) for which real time hydro-meteorological data were made available by commercial providers at frequent intervals on a grid. Vessel positioning data were made available by AIS (Automatic Identification System) messages within 2 minutes interval sampling from all cruise and Ro-Pax vessels in three key risk areas of interest from 2017-2019. GEBCO bathymetry data and weather data were interpolated for each AIS data point location and time and the information was statistically analysed. It was concluded that for the selected areas of operation and the ship samples considered big data analytics could help identify key encounters and environmental conditions leading to serious flooding.

Name of responsible partner: Aalto University, Finland

Name of responsible person: Eur.Ing Assoc. Prof. Spyros Hirdaris PhD

Contact info (e-mail address etc.): [spyridon.cheirdaris@aalto.fi](mailto:spyridon.cheirdaris@aalto.fi)

